Multi-protein chimeric antigens, a novel combined approach for efficiently targeting and blocking the blood stage of *Plasmodium falciparum*

विद्या वाचस्पति की

उपाधि की अपेक्षाओं की आंशिक पूर्ति में प्रस्तुत शोध प्रबंध

A thesis

Submitted in partial fulfillment of the requirements of the degree of

Doctor of Philosophy

द्वारा / By

भाग्यश्री देशमुख / Bhagyashree Deshmukh

पंजीकरण सं. / Registration No.: 20172012

शोध प्रबंध पर्यवेक्षक / Thesis Supervisor:

डॉ. कृष्णपाल कर्मोदिया / Dr. Krishanpal Karmodiya

At

IISER PUNE

भारतीय विज्ञान शिक्षा एवं अनुसंधान संस्थान पुणे

INDIAN INSTITUTE OF SCIENCE EDUCATION AND RESEARCH PUNE

2024

This thesis is dedicated to my mother….

For inspiration, support & Love!

To my father and brother…..

For strength & courage!

CERTIFICATE

I certify that the work contained in the thesis titled "**Multi-protein chimeric antigens, a novel combined approach for efficiently targeting and blocking the blood stage of *Plasmodium falciparum***" submitted by Bhagyashree Deshmukh was carried out by her, under my supervision. The work presented in this thesis or any part of it has not been included in any other dissertation submitted previously for the award of any degree or diploma from any university or institution.

Dr. Krishanpal Karmodiya
(Supervisor)

Date: 03-08-24

Declaration by Student

Name of Student: Bhagyashree Dhanaji Deshmukh

Reg. No.: 20172012

Thesis Supervisor(s): Dr. Krishanpal Karmodiya

Department: Biology

Date of joining program: August 2017

Date of Pre-Synopsis Seminar : 26 October 2023

Title of Thesis : Multi-protein chimeric antigens, a novel combined approach for efficiently targeting and blocking the blood stage of *Plasmodium falciparum*

I declare that this written submission represents my idea in my own words and where others' ideas have been included; I have adequately cited and referenced the original sources. I declare that I have acknowledged collaborative work and discussions wherever such work has been included. I also declare that I have adhered to all principles of academic honesty and integrity and have not misrepresented or fabricated or falsified any idea/data/fact/source in my submission. I understand that violation of the above will be cause for disciplinary action by the Institute and can also evoke penal action from the sources which have thus not been properly cited or from whom proper permission has not been taken when needed.

The work reported in this thesis is the original work done by me under the guidance of Dr. Krishanpal Karmodiya.



Date: 03 August 2024

ACKNOWLEDGEMENTS

A long journey like that of a Ph.D. is impossible without inspiration, guidance, and support. On the concluding note of my thesis, I would like to present my sincere gratitude to all the people who have made this possible! I am immensely grateful to IISER Pune and the Int.Ph.D. program for its unique research platform, student-oriented culture, and support. This work would be impossible without the support of IISER Pune folks.

I would like to express my heartfelt gratitude to my supervisor, Dr. Krishanpal Karmodiya, for his consistent and dedicated guidance, support, and patience. I am incredibly privileged to receive his mentorship through scientific temperament, knowledge, ideas, resourcefulness, and care. I am thankful for all the scientific discussions and the learning opportunities that have shaped my research skills. He allowed me the complete liberty of pursuing this project, and I am thankful for his every suggestion and encouragement. I will always remember him for his kindness and consideration and for being a well-balanced boss.

A big thanks to Dr. Anamika Krishanpal for all the exciting discussions and fun times during the trips, hosting parties, and lovely homemade meals. Special thanks to Ankrisha and Kiyaan for the lovely company.

I would also like to acknowledge my Research Advisory Committee members, Prof. Richa Rikhy, Dr. Siddhesh Kamat, and Dr. Dhanasekaran Shanmugam, for their valuable suggestions, encouragement, and support. I am grateful to Prof. Satyajit Rath for his valuable suggestions for this project.

A huge thanks to Prof. Chaitanya Athale and Dhruv Khatri for their help in quantifying and analyzing microfluidic experiments. I am also thankful to Dr. Sanjay Kumar Kochar and Prof. Somenath Roy for providing us with patient samples. A big thanks to Dr. Hem Chandra Jha for kindly gifting us the HBEC-5i cells and for the memorable hospitality at IIT Indore. Thanks to Prof. Carole Long and Dr. Kazutoyo Miura for sharing their GIA protocol.

No institute is managed without its dedicated staff—thanks to Piyush and Kalpesh for always helping with biostore materials, reagents, and orders. Thanks to Mrinalini and Rupali, Hariprasad and Sachin sir for their help. I am grateful for the timely support from the academic office, and thanks to Swapnil sir for his help with the documentation. Thanks to Tushar sir as well for his timely help. I am grateful to the IISER Animal House facility and Mr. Suraj Ingle for his help with the antibody generation. I am also grateful to the IISER NGS facility for its support with sequencing on the Illumina platform. Thanks to the IISER Microscopy facility and Mr. Vijay for his technical help. I am grateful to the IISER Mass-spectrometry facility, library, purchase, and Revvity-IISER Center for Excellence for their support in my work. Thanks to the support of the IISER Science Activity Center, Science Media Center, and the DISHA-Prerna group.

I sincerely acknowledge IISER Pune for being my principal source of funding for my Int.Ph.D. duration. I thank the DBT-CTEP and Infosys Travel Award for funding my trip to the GRS/GRC 2023 conference. A special thanks to the MAM Travel Award for making my attendance at MAM2024 possible.

I am eternally grateful to my two outstanding seniors, Dr. Mukul Rawat and Dr. Abhishek Kanyal, for their mentorship, timely guidance, and belief in me. I am privileged to have them watch over me and guide me professionally and personally (and occasionally keep up with my silly behavior). I am fortunate to have found a friend in Anjani Gopal Rao; her presence in my life has helped me fight countless battles and comforted me in the darkest times. I am thankful to her for the unconditional love she shared. A special thanks to Dr. Tanwee Das De for her support, intellectual discussions, and homemade meals. I will always cherish the time I spent with her in the lab and during GRC. Another special thanks to soon-to-be Dr. Deepak Choubey for his timely help and support.

A big thanks to one and only Krish Lab members– for making my PhD the best time of my life. The company, the journey, the support, the trust, the comfort, and the love shared by my labmates is incomparable. I am incredibly grateful to Mamatharani for being there for me. A big thanks to Disha, Trisha, and Saptarshi for making my time here memorable. I would also like to

thank Kushankur and Nirav for their help and support. I thank all the past rotation students, Lakshmi, Kalyan, Shantanu, Bhuwan, Sakshi, and Nikkita, for their help.

Thanks to our neighbors AKB and SG lab for being ever-ready to help me in several ways. Thanks to Nilam, Amey, Shirsa, Mohit, Ankita, Greg, Ayush. A special thanks to Nikita Patil for being a friend who always helped, for all the chai discussions, and for lending an ear whenever I needed someone to hear me. I am also grateful to Dr. Shanmugam's lab at NCL for always helping us in various ways, and thanks to Dr. Parag Maru for teaching me mass-spec analysis.

I am grateful to my high school and college teachers, who have sparked my curiosity about research. Thanks to the grooming of my high school teachers, Mr. Kiran Bhamre, Mrs. Anuradha Ambekar, and Mr. Gangadhar Waghmare, and my college teachers, Mrs. Vidula Bindu, Mrs. Meghana Kulkarni, and Mrs. Gauri Anekar. A special thanks to Dr. Mayur Jain and Dr. Vijayalakshmi Rajendran for their unconditional love and guidance throughout my Ph.D.

All my friends – Shreya, Shraddha, Nikhil, Akhin, Aishwarya, Vaishnavi, and Prajakta- thank you for your support. Especially thanks to Shreya for the precious friendship, care, and love.

My eternal, most incomparable gratitude goes to my mother for believing in me, motivating me, always looking after me in every way possible, and encouraging me for my independence. I am extremely fortunate to have my brother Ganesh– a perfect elder sibling who always looked after the family responsibility (hence I was free to chase my dreams), shielded me from every harm, and cared unconditionally. Thanks to my father for his worldly pearls of wisdom and for pointing me in the right direction. A special thanks to my sis-in-law Vedantika for being a friend, helping me, and caring for me. My gratitude extends to every person who has helped, encouraged, and supported me through this journey!
Lots of love, good health, and a life full of mischief for my two lovelies, Coffee and Caramel!

Yours Sincerely,
Bhagyashree

CONTENTS

CERTIFICATE……..……3
DECLARATION……..4
ACKNOWLEDGEMENTS…….……5
CONTENTS…….……8
ABSTRACT……13
SYNOPSIS……...……14
ABBREVIATION……16

Chapter 1: Introduction

1.1 History of Malaria……...…18
1.2 The burden of malaria……19
1.3 Malaria symptoms……..21
1.4 Malaria prevention and control……..……...….22
1.5 Emergence of drug resistance against malaria……..….22
1.6 *Plasmodium* genus……...……..….24
1.7 The life cycle of *Plasmodium falciparum*……25
1.8 Host immunity against malaria……...…...…….26
1.8.1 Host immune response against sporozoite stage……..……...…...26
1.8.2 Host immune response during hepatocytic invasion……...……..27
1.8.3 Host immune response against blood stage of infection……...28
1.9 Vaccines…….……..……..29
1.9.1 The anti-infection vaccine (Pre-erythrocytic stage).....….....31
1.9.2 Transmission Blocking Vaccine (Mosquito Stage).....….....….....32
1.9.3 Blood stage vaccine (Erythrocytic stage).....….....33
1.10 The var gene family…….……...…….34
1.11 The var genes and tissue tropism…….…….35
1.12 Cerebral Malaria……..……..38
1.13 Merozoite reinvasion…….……39
1.13.1 Initial attachment of the merozoites…….……..…40

1.13.2 Reorientation to face apical surface…….……40
1.13.3 Formation of Invasion Bridge between parasite and host RBC…….……..41
1.14 Immunodominancy and redundancy in malaria infection……..……...41
1.15 The strategy of chimera generation in infectious diseases……...42

Chapter 2: Design and construction of chimeric antigens targeting the blood stage of *P. falciparum*

2.1 Introduction…….……..43
2.2 Materials & Methods……..……..44
2.2.1 *In sillico* prediction of antigenic peptides……..……..44
2.2.2 Chimeric protein expression…….……...45
2.2.3 Western blotting of chimeric antigens……..…...45
2.2.4 Purification of chimeric antigens……..……...……46
2.2.5 Confirmation of chimeric antigens using Mass-spectrometry……..……...46
2.3 Results……..……46
2.3.1 Selection of proteins for generating chimeric antigens……..……..46
2.3.2 Generation of antigenic peptidome library……...49
2.3.3 Selection of antigenic peptides……...……...50
2.3.4 Expression and purification of chimeric constructs……..…….53
2.3.5 Mass-spectrometry validation of chimeric antigens…….……55
2.3.6 Additional confirmation of chimeric constructs using linker sequences……....56
2.4 Discussion…….……...57

Chapter 3: Assessment of human immune responses against chimeric antigens

3.1 Introduction……..……..60
3.2 Materials & Methods……...……..61
3.2.1 Sample Collection…….……....61
3.2.2 ELISA Assay……...…….62
3.2.3 Epitope Mapping Assay……..……..62

3.2.4 Epitope Mapping Assay Analysis……..63
3.2.5 Immunoprecipitation using malaria-infected human serum……..63
3.2.6 Mass-spectrometry……...…….64
3.3 Results…….64
3.3.1 The chimeric antigens show the presence of naturally circulating antibodies……...…64
3.3.2 Individual peptides show the heterogeneity of immune response……..…66
3.3.3 Proteins selected for chimeric antigens are exposed to the Indian malaria-exposed cohort……...72
3.4 Discussion……..…….…73

Chapter 4: Anti-chimeric varB antibodies can inhibit cytoadhesion

4.1 Introduction……..…...76
4.2 Materials & Methods…….…..78
4.2.1 Generation of polyclonal antibodies……..78
4.2.2 Purification of varB IgG fraction……..…….79
4.2.3 *Plasmodium falciparum* culturing……..79
4.2.4 Endothelial cell culture……...……80
4.2.5 Western blotting……...……...80
4.2.6 Static cytoadhesion assay……..…….80
4.2.7 RNA-sequencing……...…….81
4.2.8 RNA sequencing data analysis……..…….…81
4.2.9 Rosetting assay……82
4.3 Results……..……..…….82
4.3.1 HBEC-5i cells express the ICAM-1 receptor upon inflammatory conditions…….…...82
4.3.2 Standardization of cytoadhesion assay……..…..…84
4.3.3 RNA sequencing shows enrichment of chimeric varB-specific PfEMP1 genes……84
4.3.4 Anti-varB antibodies show inhibition of cytoadhesion……..……87
4.3.5 Anti-varB antibodies show inhibition of rosette formation……...…….87
4.3.6 Rabbit IgG fraction is specific to chimeric varB peptides……..89
4.4 Discussion……..……..90

Chapter 5: Anti-chimeric varB antibodies significantly inhibit cytoadhesion under physiological conditions

5.1 Introduction……..……..…92
5.2 Materials & Methods……...……..93
5.2.1 Seeding of HBEC-5i cells for generation of the capillary structure……...……..93
5.2.2 Preparation of iRBCs for the dynamic cytoadherence assay……...…..……94
5.2.3 Microfluidic Setup……...…….94
5.2.4 Quantification of the adhered RBCs…….……96
5.3 Result……..…..……..97
5.3.1 Standardization of dynamic microfluidic cytoadherence assay……97
5.3.2 Detection of adhered iRBCs……..97
5.3.3 Anti-varB antibodies inhibit the cytoadhesion significantly in dynamic condition…..98
5.4 Discussion……..….99

Chapter 6: Anti-chimeric MSP and InvP antibodies show growth inhibition of *P. falciparum*

6.1 Introduction……...…101
6.2 Materials & Methods…….103
6.2.1 Generation of polyclonal antibodies against chimeric MSP and InvP antigens……...103
6.2.2 Purification of anti-MSP and anti-InvP antibodies……..…….103
6.2.3 Peptide blocking assay……..……103
6.2.4 Immunofluorescence assay…….…...……104
6.2.5 Growth Inhibition Assay……..…….104
6.3 Result…….....105
6.3.1 Rabbit-generated antibodies recognize the parasite antigens……...……105
6.3.2 Anti-MSP and InvP antibodies inhibit the parasite growth……..106
6.4 Discussion…….……..…107

Chapter 7: Conclusion and Prospects……..……109

Appendix…….112

Publications……...…..123

References……...……124

Abstract

Plasmodium falciparum-induced malaria remains a fatal disease affecting millions of people worldwide. Mainly, the blood stage of malaria is highly pathogenic and symptomatic, rapidly damaging the host organs and occasionally leading to death. Currently, no vaccines are approved for use against the blood stage of malaria. In the past, canonical vaccines have selected the most immunodominant or essential protein to block the parasite's growth. This strategy works efficiently for low-complexity organisms such as viruses and a few bacteria but has not shown promising results for a malaria vaccine. *Plasmodium* has a complex life cycle, and vaccine candidates, especially during the blood stage, are ineffective due to multiple gene families showing redundancy, immune evasion, and insufficient antibody titer. Herein, we demonstrate a novel strategy of combining multiple antigens from the blood stage of *Plasmodium falciparum* using only the most immunodominant peptide sequences to tackle polymorphism and redundancy. We created three chimeric antigens targeting eight PfEMP1 proteins (chimeric varB) and eight merozoite surface proteins (chimeric MSP and InvP) by selecting and stitching B-cell epitopes. Our chimeric constructs show naturally circulating antibodies against individual peptides using epitope-mapping microarray and entire proteins in malaria-infected patients. We demonstrate that anti-varB antibodies are neutralizing in nature and significantly reduce the cytoadhesion on an organ-on-chip system with a microfluidic device mimicking physiological conditions. We have applied a Deep learning-based method to quantify the number of adhered RBCs under fluidic conditions used to study cytoadhesion. Furthermore, the anti-MSP and InvP antibodies show complete growth inhibition in a single cycle at a combined concentration of 0.13 mg/ml. Our results show that combining antigenic peptides from multiple antigens can function as a next-generation vaccine and effectively block the blood stage by reducing cytoadhesion and inhibiting parasite growth.

Synopsis

Chapter 1 details the malaria disease and its causative agents, focusing on *Plasmodium falciparum*. This chapter highlights the malaria burden, the role of vector control and antimalarials, parasite biology, host immune response to malaria infection, and possible interventions through vaccination. It focuses on different stages of vaccine development, previously considered antigens, and the possibility of next-generation vaccines.

Chapter 2 gives an in-detail overview of how chimeric antigens were generated. We show a detailed analysis for B cell epitope prediction and generation of peptidome library per protein. We further selected the highest antigenic peptide stretches from multiple proteins and stitched them to generate three chimeric antigens– varB, MSP, and InvP targeting the entire blood stage of *Plasmodium falciparum.* These antigens were cloned and expressed in the bacterial expression system and further purified and validated using Mass-spectrometry.

Chapter 3 shows the human immune response towards the designed chimeric antigens. We show that naturally circulating IgG antibodies present in malaria-infected individuals recognize the chimeric constructs, and the patients suffering from a severe form of malaria have significantly higher IgG titers. Through peptide-mapping microarray, we observed the presence of IgG and IgM response against each peptide taken to design the chimeric antigen. This IgG and IgM titer also showed heterogeneity of host immune response and further emphasized the need for a multi-protein vaccine target.

Chapter 4 explores the potential of anti-chimeric varB antibodies in inhibiting the parasite cytoadhesion. This chapter shows the standardization of primed HBEC-5i cells as a model system for studying cytoadhesion. We observed the enrichment of var genes upon bonding to primed HBEC-5i cells. This binding was significantly reduced when the anti-chimeric varB antibodies were co-incubated with the cytoadhesion assay settings.

Chapter 5 points to the importance of physiological conditions in determining sequestration outcomes. Here, we have designed, standardized, and quantified parasite cytoadhesion under dynamic fluidic conditions. We visualized the classic firm adhesion, weak adhesion, and rolling phenotypes of parasite affinities for primed HBEC-5i cell networks. When anti-chimeric varB antibodies were pre-incubated with the parasite culture, we observed a significant reduction in the parasite firm adhesion phenotype. In collaboration, we have also developed a machine-learning-based approach for identifying and quantifying the iRBC sequestration in real-time. Thus, this chapter shows the design of a new tool and its potential use in quantifying parasite cytoadhesion.

Chapter 6 highlights the action of anti-chimeric MSP and InvP antibodies in inhibiting the parasite growth. These antibodies were purified and validated using peptide blocking assay and immunofluorescence of the mature schizont stage. We observe an additive effect of these antibodies in inhibiting the parasite growth in GIA. The final concentration of 100% inhibition in a single cycle for both these antigens was calculated to be 0.13 mg/ml.

Chapter 7 concludes the thesis work and points to the prospects for the design of next-generation chimeric-based multi-component vaccines.

ABBREVIATIONS

WHO	World Health Organization
RBC	Red Blood Cell
PAMP	Pathogen-Associated Molecular Patterns
DC	Dendritic Cells
CD	Cluster of Differentiation
MHC	Major Histocompatibility Complex
IFN	Interferon
TNF	Tumor Necrosis Factor
IgG	Immunoglubulin G
IgM	Immunoglobulin M
iRBC	Infected Red Blood Cell
GPI	Glycosylphosphatidylinositol
DNA	Deoxyribonucleic Acid
RNA	Ribonucleic Acid
PfEMP1	*Plasmodium falciparum* Erythrocyte Membrane Protein 1
CHMI	Controlled Human Malaria Infection
PfSPZ	*Plasmodium falciparum* sporozoites
RH-5	Reticulocyte binding protein Homolog 5
AMA-1	Apical Membrane Antigen 1
MSP	Merozoite Surface Protein
EBA	Erythrocyte Binding Antigen
SERA-5	Serine Repeat Antigen 5
DBL	Duffy Binding Like
CIDR	Cysteine-rich Interdomain Region
ICAM-1	Intercellular Adhesion Molecule 1

EPCR	Endothelial Protein C Receptor
CSA	Chondroitin Sulfate A
RON	Rhoptry Neck Proteins
MTRAP	Merozoite TRAP
HPV	Human Papilloma Virus
GLURP	Glutamate Rich Proteins
RAMA	Rhoptry Associated Membrane Antigen
cyRPA	Cysteine-Rich Protective Antigen
BSA	Bovine Serum Albumin
PBST	Phosphate Buffer Saline with Triton X-100
HRP	Horse Radish Peroxidase
TMB	3,3',5,5'-Tetramethylbenzidine
ELISA	Enzyme-Linked Immunosorbent Assay
OD	Optical Density
PVDF	Polyvinylidene Fluoride
RPM	Revolutions per Minute
EDTA	Ethylenediamine Tetraacetic Acid
FACS	Fluorescence-Activated Cell Sorting
DAPI	4',6-diamidino-2-phenylindole
HEK293T	Human Embryonic Kidney 293 T
HBEC	Human Brain Endothelial Cells
uRBC	Uninfected Red Blood Cell
fps	frames per second
RiPR	merozoite Rh5 Interacting Protein
SDS-PAGE	Sodium Dodecyl Sulfate - Polyacrylamide Gel Electrophoresis
TCEP	tris(2-carboxyethyl)phosphine
TBST	Tris-Buffered Saline (TBS) with Tween 20
RT	Room Temperature

Chapter 1: Introduction

1.1 History of Malaria

Malaria is regarded as one of the most ancient diseases, appearing in Hindu scripture (sixth century BC), Egyptian Papyri (1570 BC), Mesopotamia (2000 BC), and Chinese texts (2700 BC). Although the disease and causative agent were unknown back then, people often identified it through symptoms such as high fever, spleen enlargement, and prevalence in marshy areas. In fact, the word malaria comes from the Italian word Mal'aria (Bad air), which is associated with this disease's prevalence in marshy lands (*1, 2*). The quest for the causative agent of the disease gained interest after Antoni Van Leeuwenhoek discovered micro-organisms in 1676, and a new belief was established that a bacterial infection might cause malaria. Two prominent scientists, Tommasi-Crudeli and Klebs, claimed to have isolated a malaria agent from the marsh waters, *Bacillus malariae*, that caused febrile fevers and enlarged spleens in rabbits upon injection (*3, 4*). This belief was challenged by Charles Louis Alphonse Laveran, a French army officer working in Algeria in 1880. He systematically studied the malaria-infected patient samples with the philosophy of 'follow the pigment' as it was established that pigment formation in the spleen is observed in malaria-infected individuals. The meticulous study of unstained blood samples from 200 infected patients blood showed the presence of several different forms of the organism, including a motionless spherical body with pigment, spherical bodies that move, and crescent shapes outside the corpuscles. He also observed that these organisms grew with time, formed pigments, and burst out from the corpuscles that had coincided with fever. One of the prominent observations by Laveran was that quinine removes these organisms from blood. Based on his observations, he named the causative agent *Oscillaria malariae*, which later was changed to *Plasmodium (2, 5)*. Charles Louis Alphonse Laveran was awarded the Nobel Prize in 1907 for his discovery.

It was fascinating as *Plasmodium* was the first protozoan parasite discovered to cause infection to the blood cells. During the same timeline, a Russian physiologist, Vassily Danilewsky, was studying infections in reptiles and birds and had identified three types of parasite families, namely, *Plasmodium*, *Haemoproteus*, and *Leucocytozoon* in their blood. Later, his work was

recognized in 1889, and the hunt for the *Plasmodium* genus began (*6*). Marchiafava, Bignami, Golgi, and Romanowsky also significantly contributed to the field of malaria in identifying spring (benign tertian) vs summer-autumn (malignant tertian) malaria (*2, 7, 8*).

Despite discovering the causative agent, the question of transmission to humans was still unanswered. In 1898, the significant discovery of malaria transmission was made by Ronald Ross, an army officer in India who began to look at transmissions of infections through vectors. His experiments of feeding three different types of mosquitoes on infected individuals and later in zoonotic infection established that mosquitoes were the intermittent hosts for malaria infections (*9*). Subsequently, many Italian scientists, specifically Grassi, showed that only female Anopheline mosquitoes transmit malaria. Within a century, the life cycle of malaria was well established (*10*).

1.2 The burden of malaria

Five known species of *Plasmodium* infect humans, namely, *P. falciparum, P. vivax, P. malariae, P. ovale, and P. knowlesi.* This disease remains a major public health threat despite centuries of discoveries and efforts. In 2022, 249 million incidences and 608,000 deaths were a result of malaria infection in 85 countries. Four countries, Nigeria, the Democratic Republic of the Congo, Niger, and the United Republic of Tanzania, reported almost half the malaria-related deaths. The African nations bear the most malaria cases, with 90% infection incidences, followed by Southeast Asian (SEA) countries (Figure 1.1) (*11*).

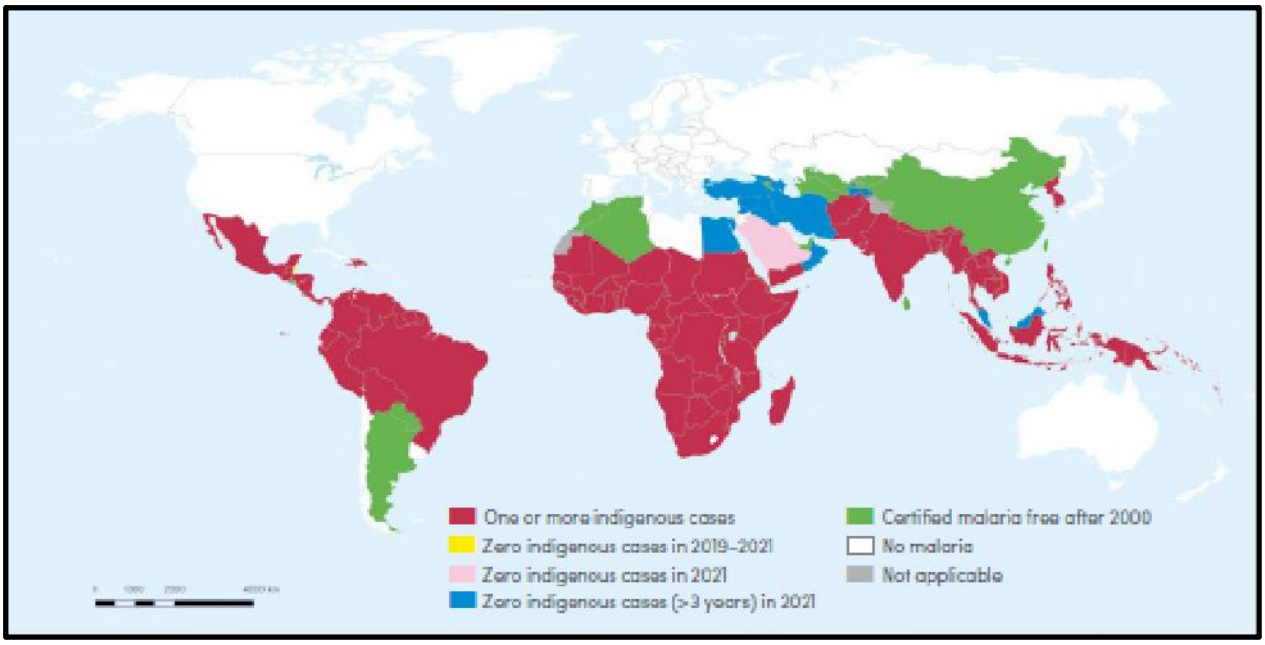


Figure 1.1. A world map showing the burden of malaria infections across the globe. Figure adaptation of World Malaria Report, 2023.

India accounts for 66% of malaria incidences in the SEA region, with almost 46% of all cases being *P. vivax* infections. Approximately 88% of the Indian population is at risk of malaria infection. But presently, 82% of infections happen in a 'high-risk' individual group comprising 20% of the population. These 'high-risk' zones are 200 regions in Andhra Pradesh, Gujrat, Jharkhand, Madhya Pradesh, Karnataka, Maharashtra, Odisha, West Bengal, and northeastern states. Although malaria incidences in India have been reduced drastically from the 2000s to 2020, we still need robust implementation of malaria control to eradicate the disease. A National Framework for Malaria Eradication program aims to end malaria by 2030 with zero indigenous cases and maintenance of malaria-free states (*12, 13*).

Many efforts are devoted to the prevention and treatment of malaria. The endemic regions use long-lasting insecticide-treated nets (LLINs), residual spraying of insecticides, anti-malaria drugs, and combination therapies. The recent approval of two vaccines by WHO has increased the hopes for malaria prevention (*14-16*).

1.3 Malaria symptoms

The malaria infection shows symptoms only during the life cycle's intra-erythrocytic (blood stage) phase. When in the blood, the parasites are exposed to the immune system, which leads to high cyclic fever (coinciding with the parasite release), headaches, chills, nausea, vomiting, and weakness. Other uncommon symptoms of malaria are diarrhea and abdominal pains (*17*). A classic three-stage symptom or paroxysm can be seen with alternating bouts of normal and symptomatic periods in malaria infections. The first stage shows extreme cold and shivering, lasting about 15 to 60 minutes. This is followed by a high fever reaching up to 41 ℃ and lasting 2 to 6 hours, and a third phase of cooling down and sweating—this paroxysm in *P. vivax* and *P. ovale* shows a tertian pattern (fever every 48 hours), while *P. malariae* shows a quartan pattern (every 72 hours). The most lethal malaria, *P. falciparum,* has a tertian pattern but need not necessarily occur every 48 hours. Splenomegaly and hepatomegaly are common in malaria infection but do not determine diagnosis (*18*).

P. falciparum malaria, if left untreated, can lead to severe and complicated forms which can be fatal. The most severe outcomes are cerebral malaria and anemic conditions. In cerebral malaria, obstruction in the brain capillaries due to parasite-expressed proteins can be malignant,
and this form often has a mortality rate between 15 to 50%. Other complications include hyperparasitemia (>3 to 5% of RBCs infected), hypoglycemia, lactic acidosis, shock, seizures, and hepatic or renal failure. Children below the age of five, pregnant women, immunocompromised individuals, and older people are at most risk of developing severe malaria (*19, 20*).

Although malaria can be fatal, the observations in endemic regions show that the severity of the infection drops with multiple exposures. The first-time or naive infections can progress to lethal stages, but the immunity against the parasite also broadens as the number of infections increases. Over time, the infection bouts become milder or asymptomatic. Interestingly, sterile immunity is not achieved in the case of malaria infection (*21*).

1.4 Malaria prevention and control

There are 30-40 species of *Anopheles* mosquitoes that transmit malaria to humans. An upward-pointing abdomen characterizes anopheline mosquitoes (*22*). Only females consume blood meals to support the nutritional requirements of proteins for egg production. Of all species, *A. gambiae* and *A. funestus* have a high capacity to transmit malaria (*23*). Once inside the mosquito, the parasite takes 10-21 days to complete its sexual life cycle (*24*). Within this period, the mosquito's immune system recognizes the foreign parasite and secretes multiple small molecules from the midgut, hemocyte, and fat bodies (*25-27*). The parasite also faces harsh conditions in the mosquito digestive tract and is known to deregulate the expression of certain digestive enzymes. Many ookinetes are killed in the mosquito gut as the host produces nitric oxide synthase (NOS) and antimicrobial peptides. Mosquitoes respond via complement activation and phagocytosis of sporozoites by hemocytes (*26, 28-30*). The most efficient way of tackling malaria and other mosquito-borne infections is by using insecticides and bed nets. The dichlorodiphenyltrichloroethane (DDT) is the most effective insecticide extensively used for mosquito elimination. However, the emergence of insecticide-resistant mosquitoes has marked concerns in vector control (*31*).

In India, six Anopheles species are found, of which *A. culicifacies* transmits around 65% of malaria (*32, 33*). Currently, the National Malaria Elimination Program is responsible for reducing the transmission burden in endemic regions and maintaining the malaria-free zones in India. The program aims to eliminate malaria in India by 2030 with zero indigenous cases and no emergence of new incidences (*11, 12*).

1.5 Emergence of drug resistance against malaria

Malaria infection therapy presents complications as the parasite in liver cells and blood cells cannot be treated with the same drug. The tissue schizonticides (liver-stage drugs) are necessary for *P. vivax* and *P. ovale* infections that show liver hypnozoites, while blood schizonticides are enough to control and treat *P. falciparum* infection (*34*). Many drugs have been tried and tested

against malaria, with artemisinin combination therapy (ACT) being the current gold standard front-line drug against the blood stage of infection (*35*).

A major concern in controlling and eliminating malaria is the independent emergence of parasite resistance towards anti-malarial drugs currently in clinical use. The first report of resistance was in the 1950s to 1960s against chloroquine drugs in several regions of Southeast Asia and South America (*36, 37*). Detailed studies showed multiple mutations in the Pfcrt gene conferring resistance against chloroquine (*38*). Resistance to mefloquine, sulfadoxine/ pyrimethamine, and halofantrine was observed shortly after (*39-42*). In the late 1990s, a gold treatment standard was introduced with a combination of artemisinin derivatives and partner drugs (*35*). By the early 2000s, a decreased parasite response to artemisinin had been reported in Cambodia, and it later spread to Southeast Asian countries (*43-45*). In 2021, artemisinin resistance was confirmed for the African continent (*46, 47*). Several of these resistance phenotypes are attributed to mutations in specific parasite genes. For example, a mutation in the PfKelch13 gene is associated with artemisinin resistance (*47-49*). It has particular dominance in South Asian countries, while genes such as Pfcrt, Pfdhfr, Pfmdr1, copy number variations in Pfplasmepsin1, etc., have known associations with other antimalarials (*36, 38, 41, 50*). Many reports have found an emergence of artemisinin tolerance in parasites independent of PfKelch13 mutation, suggesting more than one pathway for acquiring resistance (*45, 51-54*). Recent reports also indicate the possibility of co-existing mutations in the background genome that assist resistant parasites in survival (*55, 56*).

The first observation of artemisinin resistance in India was made in the Kolkata region of West Bengal, which also shares a border with Bangladesh (*53*). Studies have reported several PfKelch13 mutations in Indian patient isolates from 7 states and the emergence of PfKelch-independent artemisinin tolerance from central India. The genomic surveillance of 53 isolates from the West Bengal region showed definitive Pfcrt and Pfmdr mutations with PfKelch13 mutations absent. Nevertheless, a 10-15% ACT-resistant population is seen in this region, possibly assisted by background mutations in the ubiquitination and vesicular transport pathways (*54*).

Anti-malarial drugs are promising areas for malaria control and treatment. Still, they will work effectively only when other prevention domains, such as chemoprophylaxis and vaccines, synergize with the treatment.

1.6 *Plasmodium* genus

Malarial parasites are unicellular eukaryotes belonging to the phyla Apicomplexan. This phylum has obligate intracellular parasites such as *Plasmodium*, *Toxoplasma, Cryptosporidium*, *Eimeria, Theileria, and Babesia*. These are uniquely termed Apicomplexa due to the presence of an apicoplast organelle and an apical complex (*57, 58*). This apical complex localized at the apical pole harbors microneme, rhoptry bodies, and granules storage for invasion-specific proteins. While the apicoplast has essential pathways such as DOXP for synthesizing isoprenoids and fatty acids. This parasite carries other organelles such as mitochondria, food vacuoles, nucleus, Golgi apparatus, and endoplasmic reticulum (*59*).

The *Plasmodium* genus comprises over 250 species, with various hosts from primates, rodents, reptiles, and avians (*14, 60, 61*). Five known species of *Plasmodium* infect humans– *P. falciparum, P. vivax, P. malariae, P. ovale, and P. knowlesi*. *P. falciparum* is known to be highly lethal and responsible for significant mortality associated with malaria, while *P. vivax* is the most prevalent infection. *Falciparum*-induced malaria is majorly found in Africa, Asia, and Latin America, with the highest mortality in Africa (*62*). Indian subcontinent predominantly has *P. vivax* infections, followed by *P. falciparum (63)*. *P. ovale* is mostly found in Africa and, along with *P. vivax*, can show a dormant liver stage called hypnozoites that shows a relapse of infections (*34, 64*). *P. knowlesi,* a parasite known for infecting macaque monkeys, was recently found in human infection in the Sarawak state of Malaysia (*65*). Now, the *P. knowlesi* infection is found in multiple Southeast Asian countries (*66, 67*).

1.7 The life cycle of *Plasmodium falciparum*

Plasmodium parasite has a complex life cycle involving a human host and a female *Anopheles* mosquito wherein asexual and sexual development occurs, respectively (Figure 1.2) (*68*). Infected mosquitoes inject motile and infective sporozoites into a human host during a blood meal. These sporozoites reach the liver using lymphatic and vascular networks. Once inside a hepatocyte, the parasite remains there for 5-16 days and undergoes schizogony to produce multiple merozoites, which are then released into the blood vascular system and are capable of invading RBCs (*69*). In *P. vivax* and *P. ovale,* a dormant form called hypnozoites can persist in the liver and cause a relapse of parasites months later (*34*). During this asexual phase, the *P. falciparum* parasite remains in RBCs for about 48 hours, going through a dormant and transcriptionally silent ring stage, which lasts about 18 hours, the trophozoite stage, lasting roughly 40 hours post-invasion and finally asexually divides into schizont form. Once matured, parasites egress from the RBCs, releasing multiple invasive daughter merozoites capable of reinvading into uninfected RBCs (*68, 70*). Within each intra-erythrocytic cycle, a small proportion of parasites develop into sexual forms, namely, male and female gametocytes, which are taken up by mosquito vectors from an infected human. Inside the midgut of *Anopheles*, gametocytes mature into gametes and fuse to form a zygote, which later develops into an ookinete. Within the midgut wall, ookinete matures into an oocyst that releases thousands of sporozoites that travel to the salivary gland and are ready to infect the next host. Although gametocytes ensure the further transmission of parasites, they do not contribute to disease pathology (*71-73*).

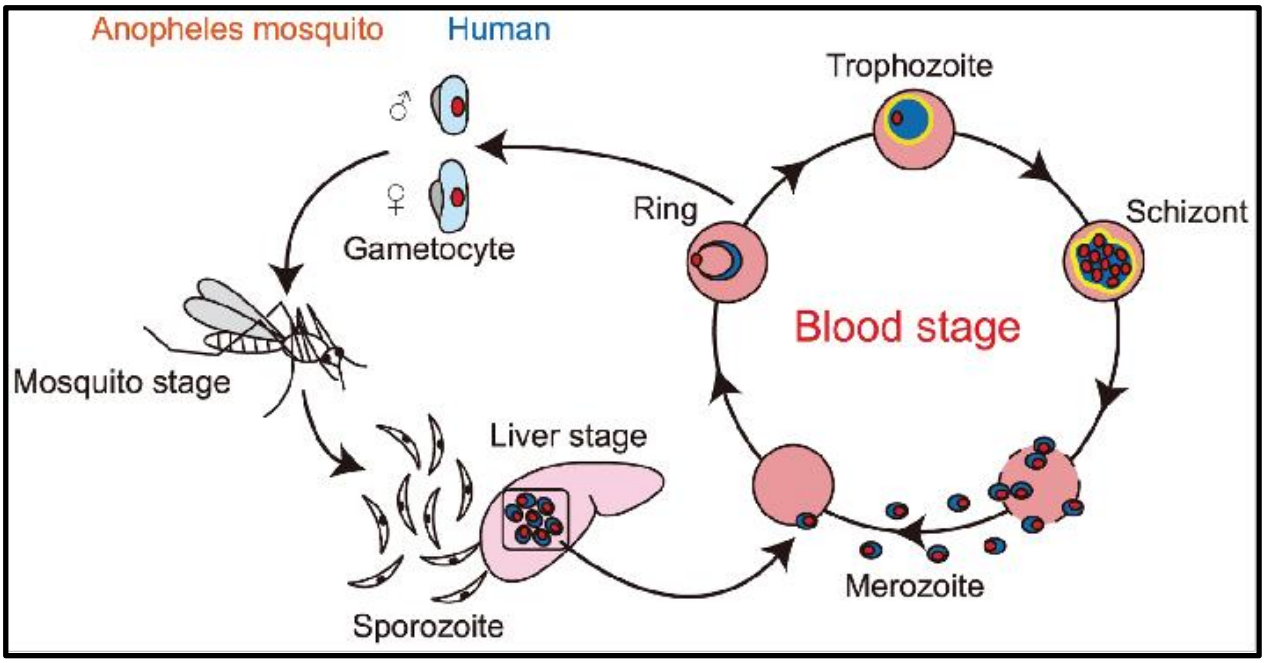


Figure 1.2. A life-cycle of Plasmodium falciparum parasite. (Adapted from Enomoto et al., Plos one, 2012 (68))

1.8 Host immunity against malaria

1.8.1 Host immune response against sporozoite stage

The malaria infection is known to elicit both innate and adaptive responses. The parasites are introduced to the host dermal lining via a mosquito bite in the form of a sporozoite. These are recognizable to dendritic cells through PAMP molecules (*74*). The DCs, upon phagocytosis of the sporozoites, present it to the CD4+ and CD8+ T cells through MHC class II and MHC class I molecules, respectively. The CD4+ T cells produce IL-12 and IFN-ɣ, while the CD8+ T cells produce IFN-ɣ, TNF-α, and iNOS as a line of defense (*74-77*). Given that naive infections show a higher frequency of malaria infections, the time taken for the T cell activation is far slower than required. Also, the gliding rate of sporozoites is estimated to be 1-2 µm/sec, while that of immune cells is 0.1 µm/sec. This ten-fold higher rate of movement makes it difficult for the immune cells to capture the sporozoites (*78, 79*). In semi-immune or vaccinated adults, most sporozoites are cleared by the B cell-produced cytophilic IgGs (IgG1 and IgG3) by target neutralizing and marking the sporozoites for antibody-mediated phagocytosis process done by neutrophils (*80, 81*).

1.8.2 Host immune response during hepatocytic invasion

Once the parasites are in hepatocytes, the infection remains asymptomatic but is recognized by the host immunity. Majorly, the intracellular parasite elicits the type I and II IFNs, which act further to eliminate the parasite. The parasite RNA molecules act as a PAMP and get recognized by a pattern recognition receptor (PRR) called MDA-5 (*82*). This receptor further activates MAVS (other sets of PRR called mitochondrial antiviral signaling molecules). It leads to the production of IFN- and IFN- (IFN type I) that subsequently activate the IFN-stimulated genes (ISGs) (*69, 83, 84*). The AT-rich parasite DNA stem-loop structures are also identified as PAMPs in bone marrow cells and are eliminated by a similar mechanism (Figure 1.3) (*85*). The IFN-ɣ, a type II IFN, is also essential in clearing the parasite multiplication through noncanonical autophagy (*86*).

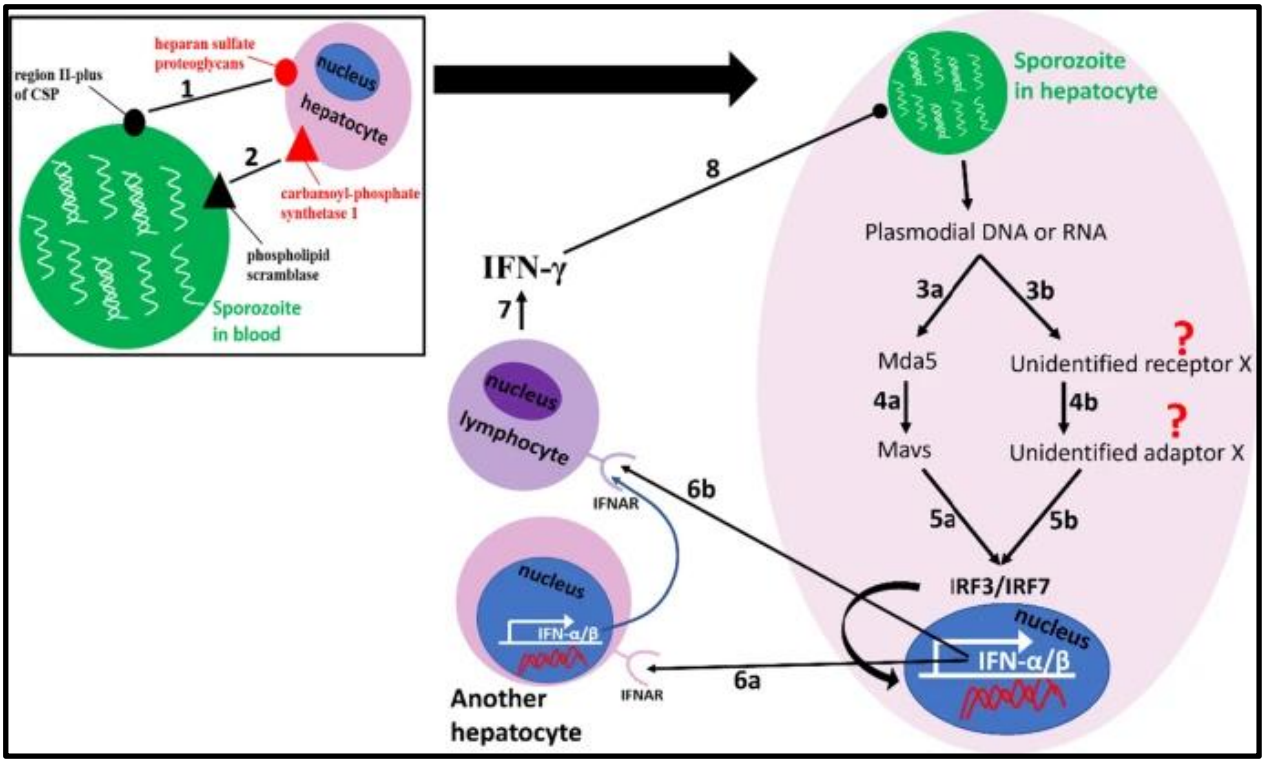


Figure 1.3. A schematic of host immune response toward malaria infection during hepatocytic stage. (Adapted from Ezema et al., Parasitology Research, 2023 (84))

1.8.3 Host immune response against blood stage of infection

During the blood stage of the infection, the parasites exist in two forms: inside RBCs, wherein they complete their asexual growth, and outside RBCs, in the form of merozoites. The merozoite form is more readily recognizable to the immune system and easy to target. The primary route of merozoite targeting is antibody neutralization and phagocytosis. However, this requires a prior infection or vaccination with merozoite or merozoite-specific proteins. While there have been multiple attempts at making a merozoite invasion blocking vaccines, complete protection is not yet observed, as the merozoites use redundant protein pathways for invasion and polymorphism (*87-91*). The merozoites are also known to induce a subset of T cells, which release granulysin– a merozoite-sensitive cytotoxin (*92-94*). The iRBCs, on the other hand, are protected from the immune response as the RBCs do not have MHC molecules and, hence, cannot activate T cells. Still, DCs are known to identify and engulf the iRBCs by recognizing parasite proteins and modifications on the RBC surface. This phagocytosis is dose-dependent, but a higher iRBCs to DCs ratio induces apoptosis in DCs, making this mode of parasite clearance unreliable (*92, 95*). iRBCs also release multiple molecules that are recognizable– phosphoantigens released in the DOXP (1-deoxy-D-xylulose 5-phosphate) pathway (activates T cells and release of IFN-ɣ), hemozoin/heme-containing parasite DNA/RNA (differentiates monocytes into macrophages and recruitment of DCs), GPI (activates natural killer T cells) (*96, 97*). The neutrophils show NET traps, complement-dependent phagocytosis, and ROS (reactive oxygen species) production (*92, 98-100*).

The iRBCs show altered cellular skeleton and rigidity due to the hemoglobin trafficking and incorporation of parasite-derived proteins into the host cytoskeleton. The restructuring of RBCs makes them susceptible to splenic clearance (*100, 101*). As a defense against the host, this clearance is avoided by the PfEMP1 proteins (*Plasmodium falciparum* Erythrocyte Membrane Protein 1). These variant surface antigens, along with scaffolding proteins, are known to be trafficked onto the host surface and show affinity for endothelial cell receptors. This interaction leads to parasite sequestration in the blood vasculature and hides the parasite from clearance (*102, 103*). The PfEMP1 proteins are immunodominant and are recognized by the B cell receptors, marking it for neutralization and antibody-mediated elimination (*104, 105*). However, the parasite has a repertoire of 60 PfEMP1 genes that show mutually exclusive expression in the

population with a certain synchronicity. Once the PfEMP1 is recognized, the PfEMP1 switches to another variant, and parasitemia persists (Figure 1.4) (*102, 103, 106*). Having an anti-PfEMP1 antibody pool against diverse PfEMP1 proteins is correlated with protection against disease severity (*107*). Similarly, PfEMP1 and RIFIN families of proteins induce binding of iRBC with other uninfected RBCs, called rosette formation. These rosettes again help the iRBCs to evade the immune response. Together, the protein redundancy, polymorphism, sequestration, and strategies such as switching enable the malaria parasite to evade the host immune response (*103*).

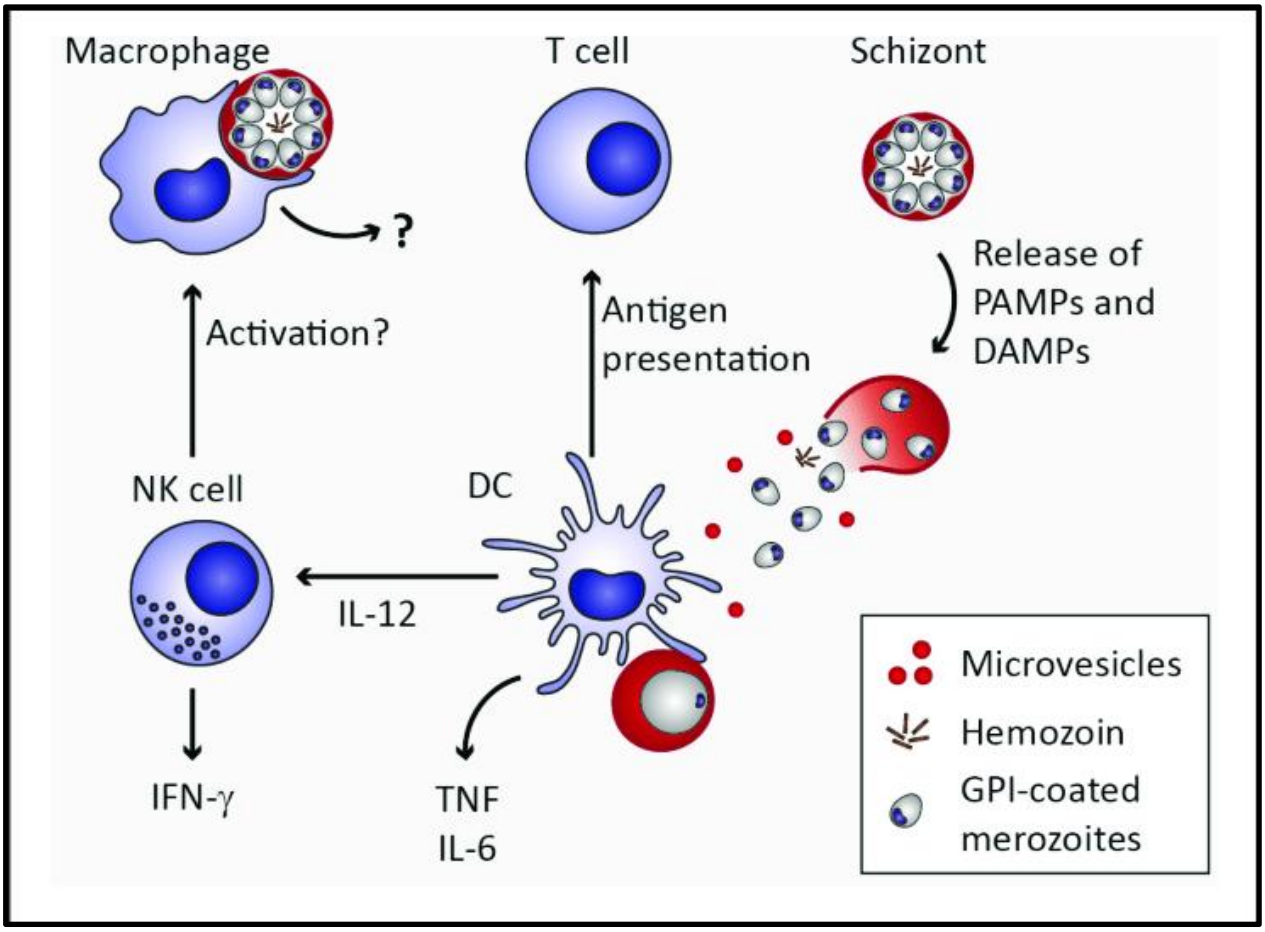


Figure 1.4. An innate host immune response towards the blood stage infection of malaria. (adapted from Dunst et al., Frontiers in Cellular and Infection Microbiology, 2017 (108))

1.9 Vaccines

The quest for a malaria vaccine started when alleviated symptoms were observed in people with repeated exposures. The initial search for a vaccine was started in 1965 by immunologist Dr. Ruth Nussenzweig. This initial search was quite disappointing for the scientists as targeting the

parasite proved difficult owing to the complex life cycle, redundant pathways, immune evasion, and absence of sterile immunity (*109-111*). A whole sporozoite vaccine showed promising results in a mouse malaria model in 1965, which later went in for human trials in 1973 (*112-114*). The parasites' scalability was the major obstacle in generating a whole sporozoite vaccine, and hence, efforts were redirected to developing an antigen-specific vaccine instead of an entire organism. This led to a hunt for the best possible parasite protein as a vaccine target (*115*).

A collaborative effort in 1987 between GlaxoSmithKline Pharmaceutical and Walter Reed Army Hospital resulted in a pre-erythrocytic vaccine against a single recombinant protein of the sporozoite stage. The circumsporozoite protein on the surface of sporozoites presented as a promising candidate during pre-clinical studies as the antibody responses were seen to reduce the infection rate in P. *falciparum-induced* malaria (*116*). Multiple attempts led to a monovalent recombinant vaccine containing truncated central repeat regions having T-cell epitopes fused with hepatitis surface antigen formulated in lipoprotein particles (RTS,S). This RTS,S formulation showed robust CD4+ T cell activation and IgG titers reaching 100 mg/ml. RTS,S with AS01 adjuvant (GlaxoSmithKline formulation - 'Mosquirix') was in multiple pilot trials from 2009 to 2019 and was approved by WHO for use in October 2021 (*16, 117-119*). However, the protection against malaria infection was 30-50%, with a decline in the absence of booster doses. Later, a modified version of RTS,S called R21 formulated in Matrix-M adjuvant was made by Jenner Institute, Oxford, UK, that showed ~75% protection in CHMI studies (*15, 120*). In October 2023, R21/Matrix-M was approved by WHO, marking it as a second vaccine against malaria (*121*). Notably, both the approved vaccines are against the pre-erythrocytic stage of malaria and specific against *P. falciparum* only. Any escape of parasites from this vaccine efficacy can still establish a malaria infection.

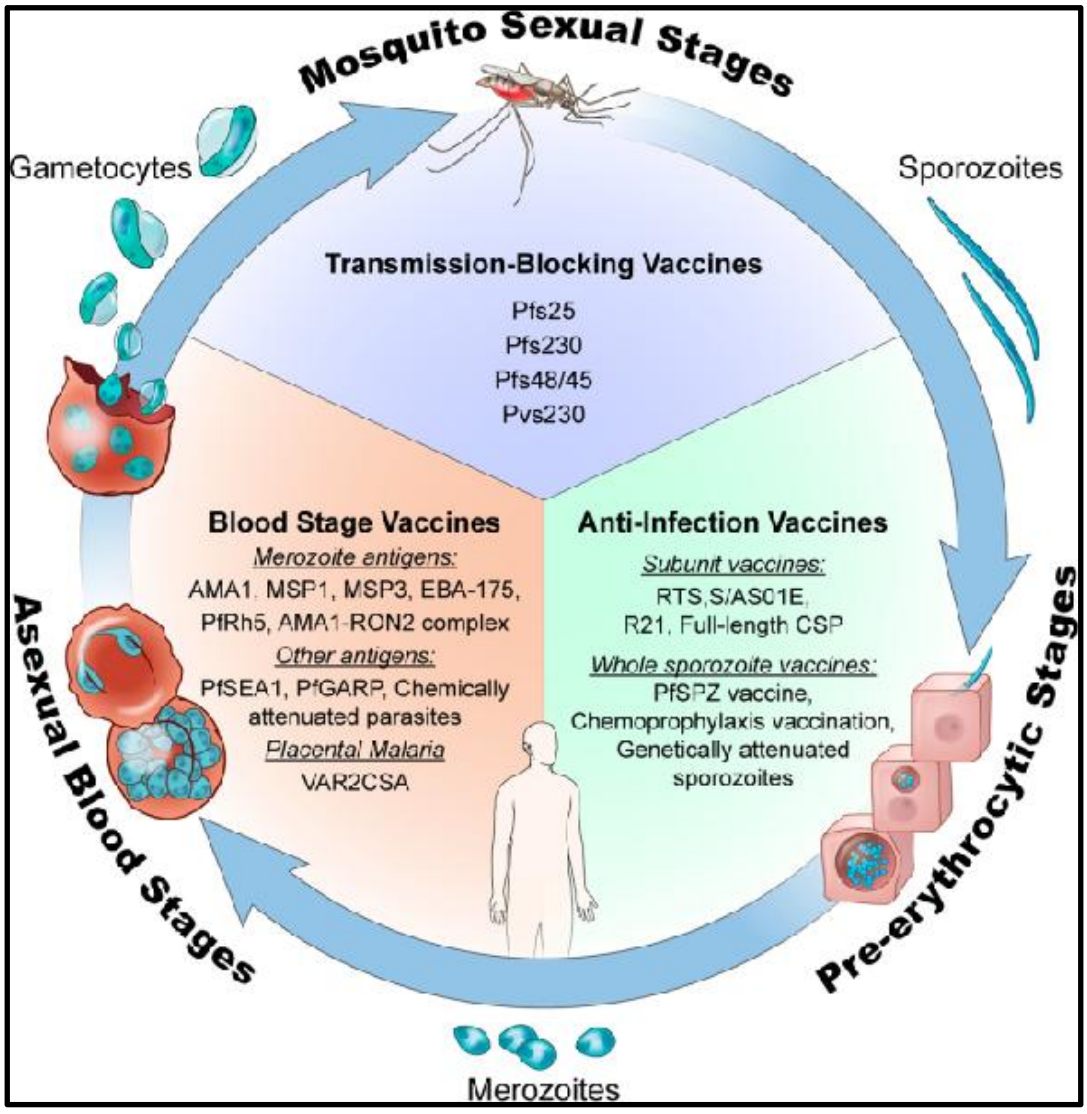


Figure 1.5. A schematic representing the different stages of the Plasmodium life cycle and the vaccines formulated in each stage. (Adapted from Duffy PE and Gorres GP, npj vaccine, 2020 (122))

1.9.1 The anti-infection vaccine (Pre-erythrocytic stage)

The RTS,S, and R21 are two successful examples of anti-infection vaccines that were recently approved (*117, 121*). Apart from these two, active efforts are being made to formulate whole attenuated sporozoite vaccines under phase trials.

Given that the large-scale production of live sporozoite is a challenging step, Sanaria, a biotechnology company in 2010, developed a platform that allowed isolation of PfSPZ from aseptic mosquitoes fed on culture strains. These PfSPZ could be purified and cryopreserved using the liquid nitrogen vapor phase and could then be considered for trial upon multiple ways of attenuation (*110*). Radiation-based attenuation (PfSPZ vaccine), chemo attenuation achieved in vivo using anti-malarial drugs (PfSPZ-CVac, Chemoprophylaxis vaccine), and genetic attenuation of sporozoites (PfSPZ-GA1) (*123-126*). Phase I for these vaccines is done, while PfSPZ and PfSPZ-CVac are currently in phase II (*127*). The immunity to these vaccines is strain and dose-dependent but has shown better efficacy than RTS,S vaccine (*122*). A cell traversal protein found on sporozoite and ookinete (CelTOS) has also been tested as a recombinant protein as a potential pre-erythrocytic vaccine in mice and showed complete sterile immunity to sporozoite challenge (*128*).

1.9.2 Transmission Blocking Vaccine (Mosquito Stage)

The mosquito takes up the male and female gametocytes in the human host during a blood meal, and their fusion happens in the mosquito's midgut region (*72, 129*). The idea of a transmission-blocking vaccine is to inhibit this fusion so that a zygote formation does not occur, block the oocyst formation of zygote to sporozoite transition, or inhibit the sporozoite entry into salivary glands (*130*). The antigens considered in transmission-blocking vaccines are Pfs230, Pfs-25, and Pfs-48/45, present on the surface of male and female gametocytes. The naturally acquired antibody responses against these proteins show fusion-blocking activity (*131-134*). The major drawback with these vaccines is that they can help reduce the transmission of the disease to the following individuals but are of no direct use to the infected person. Hence, they are also termed altruistic vaccines and require community mass vaccinations to reduce the spread of the disease. Due to this mode of action, these vaccines are not attractive for research or given enough incentives to improve further. Instead, transmission-blocking coupled with other vaccines may increase efficiency.

1.9.3 Blood stage vaccine (Erythrocytic stage)

Significant damage by malaria infection is caused during the blood stage. The exponential growth of parasites, rupture of RBCs, multiple symptoms, and organ-specific complications make this stage an attractive target for a vaccine design (*103, 135*). But exposure to the blood stage does provide immunity against clinical malaria mediated through parasite specific antibodies. This is further strongly supported by the fact that IgG transfer from semi-immune adults cleared the parasite infection in African children and later in Thai adults (*136, 137*). A merozoite-rich vaccine preparation shows complete protection in the primate model of *P. falciparum (138)*. The goal of the blood-stage vaccine is to elicit a threshold of immune response that can inhibit the entry of the merozoites into the next RBC, thereby leaving the merozoites free in the blood and flagging them for clearance by the immune system. The major challenge in using merozoites as a potential target is A. A brief time of action, as most merozoite reinvasion occurs within ~ 3 minutes. B. Redundancy in the reinvasion pathways. C. antigenic polymorphism was seen in invasion essential genes, and D. Exponentially growing parasite number needs targeting (*122*). As of July 2022, 44 vaccine formulations were tested for efficacy against the blood-stage *P. falciparum* malaria. All vaccines (except one) are recombinant protein formulations with different sets of adjuvants (Clinicantrials.gov). The significant candidates of blood stage are Rh5, AMA-1, MSP family, SERA-5, EBA-175, and GLURP (*87, 88, 139-144*). All these candidates elicited desirable IgG responses and, in the case of MSP-3, showed an antibody-dependent cellular inhibition, but unfortunately, the CHMI studies did not show promising evidence of protection (*145*). The AMA-1 antibodies in vitro had growth inhibition potential that did not translate in vivo upon homologous challenge (*139, 146*).

The leading blood-stage vaccine in the trial is currently formulated against RH-5. This protein is essential for RBC invasion and shows interaction with the basigin receptor. The protein is relatively conserved and elicits neutralizing antibody responses. The protective efficacy was also higher in primate infections with heterologous strains (*140, 141*).

Although the merozoites are attractive and promising targets, the parasites inside the RBCs for 48 hours are not entirely hidden by the immune system. The iRBCs can be detected by the

splenic macrophages and are cleared off from the circulation. To avoid this detection and splenic clearance, *P. falciparum* parasites have 60 PfEMP1 genes that show mutually exclusive expression and switching phenotype. These proteins, when expressed, are transported to the surface of the RBCs and show affinity for the receptors of the endothelial cells. The iRBC remains bound to the endothelial cells of the blood lining and does not actively pass through the blood circulation. This strategy allows the parasite to evade the immune response. These PfEMP1 proteins are highly immunodominant, and antibodies elicited against them are functional in inhibiting the parasite adhesion. Despite them being exposed, available, and immunodominant, a vaccine attempt against these proteins has not been tried (except for var2csa) for the following reasons, A. A parasite population shows an expression of only one PfEMP1 protein (although debatable) at a time, while the rest of 59 are epigenetically silenced. B. The parasite population can show the switching of PfEMP1 genes (with a rate of ~2.5% switch per generation). C. The PfEMP1 genes are also hotspots for recombination events, increasing the diversity of the repertoire (*102-104, 147*).

1.10 The var gene family

Plasmodium falciparum has an extensive repertoire of genes responsible for cytoadherence and sequestration. Mechanistically, they can impart adhesive qualities through three major interactions: adherence with endothelial receptors (*148*), rosetting with uninfected RBCs (*149*), and clumping with platelets (*150*) (Figure 1.6). Furthermore, a particular type of placental adhesion is observed during pregnancy wherein infected RBCs (iRBCs) adhere to syncytiotrophoblast cells, causing pregnancy-related severe malaria (*150, 151*). Since all kinds of sequestrations require exposing parasite-specific proteins to the outside environment, they are easily recognized by the host immune system. They are constantly under pressure of immune clearance. To avoid this, parasites have evolved to harbor multiple antigenic gene families such as var, rifins, and stevors, of which genes of the var family have been highly associated with severe forms of the disease. *P. falciparum* has ~ 60 var genes present in its 14 chromosomes containing haploid genome, which encodes for *Plasmodium falciparum* erythrocyte membrane protein- 1 (PfEMP1) responsible for mediating adhesion (*103*). Based on their 5’ upstream promoter sequence and location on chromosome, these var genes are classified into major upsA,

upsB, and upsC subtypes. upsA subtype var genes are located sub-telomerically, while upsB are more immediately adjacent to the telomere. The upsC subtype is located internally in clusters (*152*). It has been observed that upsA is more related to the severe form of malaria, while the upsB and upsC subtypes are associated with an asymptomatic form (*153, 154*). All PfEMP1 proteins are constructed of various combinations of Duffy-binding like (DBL) and cysteine-rich interdomain region (CIDR) domains present on exon one, which bind to different endothelial receptors such as CD36, ICAM-1, endothelial protein C receptor (EPCR), and chondroitin-sulfate A (CSA) (*155*).

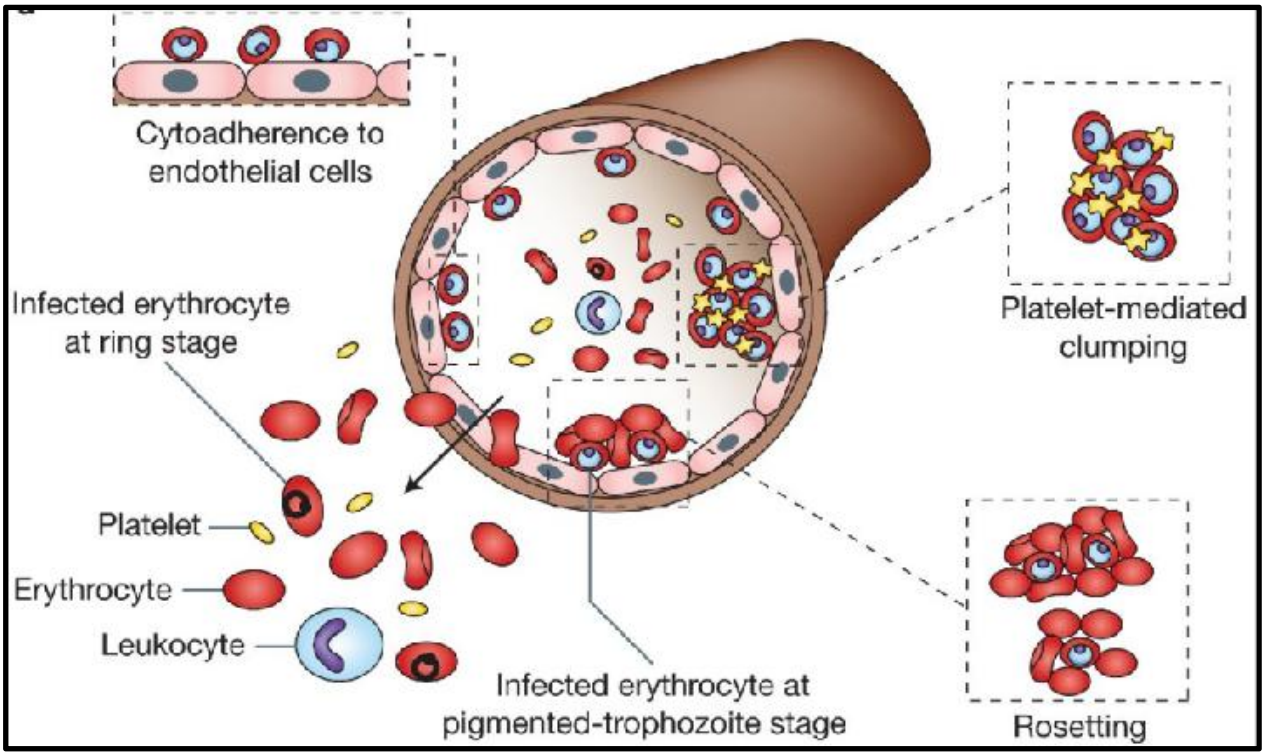


Figure 1.6. A representation of parasite cytoadherence, rosetting, and clumping mediated by surface-exported PfEMP1 proteins. (Adapted from Rowe JA et al., Expert Reviews in Molecular Medicine, 2009 (155))

1.11 The var genes and tissue tropism

The var gene organization is fairly similar across all gene repertoire (except for var2csa). Exon I codes for extracellular multi-domain structures, the DBL, and CIDR domain variants (Figure 1.7

A), while exon II codes for more conserved intracellular domains. The combination of DBL and CIDR determines the affinity of var proteins to the endothelial receptors (*103, 152, 155*). DBLα/CIDRα and CIDRα 2-6 domains facilitate the binding to CD36 (*156-158*) and EPCR binding is facilitated by CIDRα1 associated with DC8 and DC13 (*159, 160*). The ICAM-1 receptor is also critical in cerebral malaria, and upsA and upsB subtypes show binding to ICAM-1 through the DBLβ, and DBLβ domain of DC4 (*160-163*). A recent study in children developing cerebral malaria showed that these parasites had a binding affinity for both EPCR and ICAM-1 receptors (*160, 163*). In contrast, those with uncomplicated malaria showed more affinity for CD36 receptors (*164*). The precise affinities of each var gene domain to every endothelial receptor are unknown.

The sequestration of iRBCs is seen in multiple organ sites such as the brain, kidneys, lungs, intestine, and bone marrow (*154, 165*). The endothelial cells and their receptors vary in all these organs, indicating that the PfEMP1 binding repertoire is higher than just EPCR, ICAM-1, and CD36 (Fig 1.7 B). A comprehensive map of PfEMP1 and their binding affinities is yet to be determined.

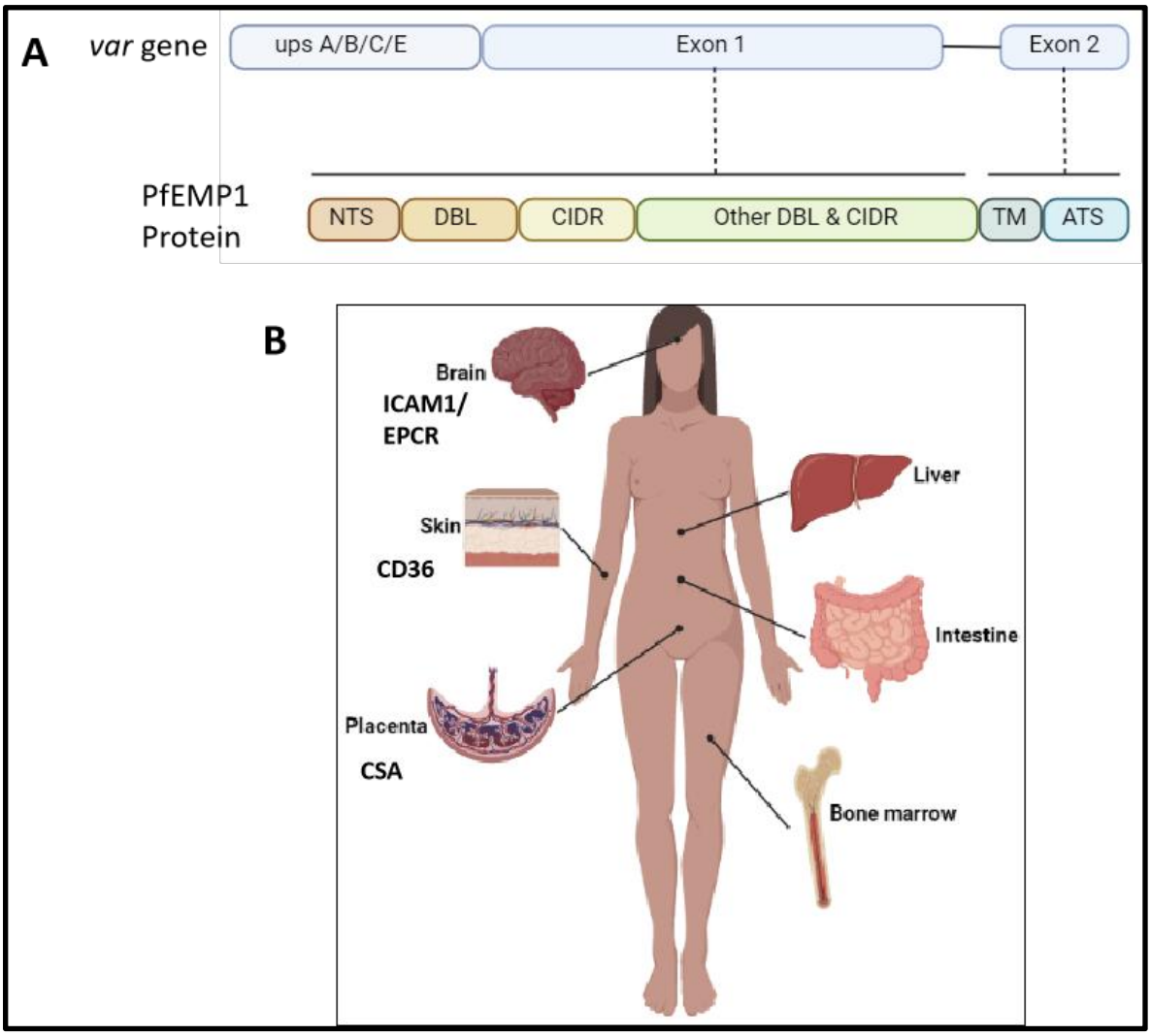


Figure 1.7. A. A structure of var gene highlighting the promoter type, exons, and intron. PfEMP1 protein structure with functional domains. B. Tissue tropism shown by PfEMP1 affinities in different organ sites. (Illustration created using biorender. com)

The immunity toward the PfEMP1 proteins is of keen interest as the presence of antibodies determines the disease outcome. The severe form of malaria is often seen in children < 5 years of age and pregnant women. In endemic regions, when malaria is a seasonal infection, children who have previous exposure tend to have uncomplicated malaria, while adults may get an asymptomatic form (*166*). This is owed to anti-PfEMP1 antibodies, which functionally inhibit the binding of iRBCs to the endothelial lining. This acquired immunity is believed to be achieved in an orderly manner (*167*). The expression of var genes in naive infections is more likely to be severe with the type of PfEMP1s causing sequestration in vital organs with stronger affinities.

When the breadth of anti-PfEMP1 antibodies increases, the parasites are forced to express other sets of PfEMP1 proteins that have sequestration in nonvital organs with weaker interactions. Many endemic region studies and CHMI experiments support this observation (*105, 107, 153, 168-170*). However, the direct effect of host immunity pressure on switching in experimental conditions is not well elucidated.

Based on these observations, a PfEMP1-based vaccine is possible. Targeting PfEMP1s will reduce the disease's severity by inhibiting the cytoadhesion and increase the possibility of detecting the iRBCs by the immune system or splenic macrophages. The PfEMP1-based vaccine is already tried for the var2csa type known for binding to chondroitin sulfate (CSA) present on the endothelial cells of the umbilical cord, leading to pregnancy-associated malaria (*171*). Technically, sampling from all PfEMP1 subtypes and the presence of a breadth of anti-PfEMP1 antibodies should work. The extensive repertoire, huge protein sizes (~150-250 kDa), antigenic variation, and recombination hotspots make these proteins difficult to target as a vaccine target (*104*).

1.12 Cerebral Malaria

The complications of severe malaria can lead to cerebral impairments. Yearly, around 50,000 deaths occur due to this severity, while the survivors usually live on with cognitive dysfunctions. Cerebral malaria (CM) shows symptoms within two weeks of infection with clinical features such as increased intracranial pressure, retinopathy, swelling, seizures, and breakdown of the blood-brain barrier (BBB) (*172-175*). The pathophysiology of cerebral malaria is multifactorial, with iRBC sequestration, immune inflammation, and loss of blood-brain barrier integrity playing a significant role in the development of CM (*176, 177*).

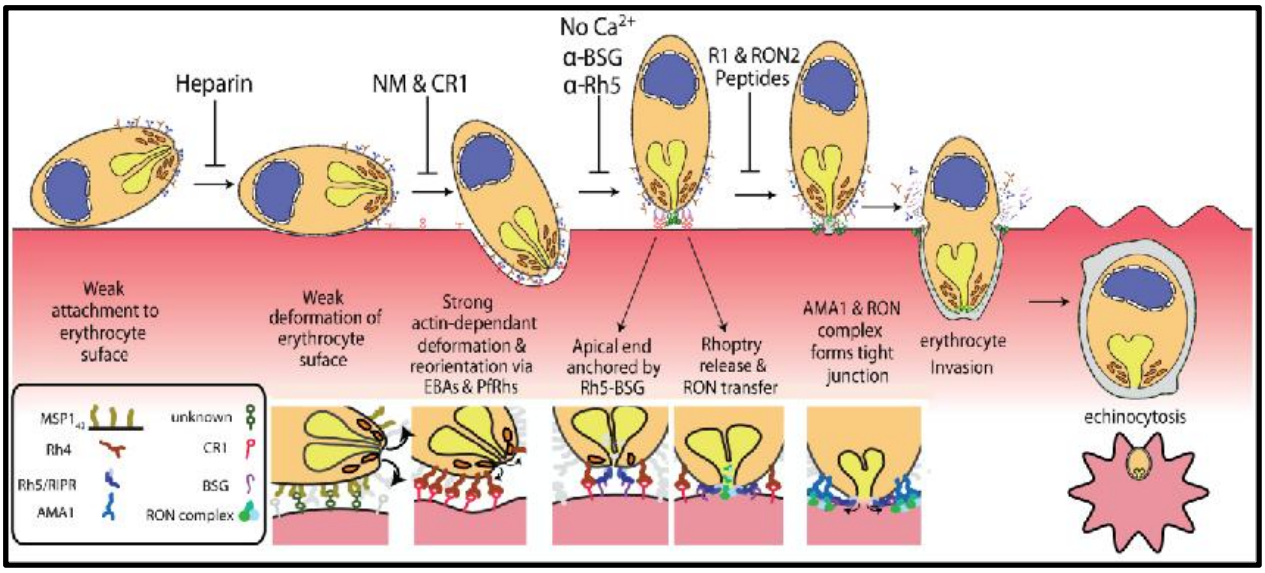
Histopathology reports of individuals deceased of malaria show pigmented late-stage parasites clogged in the vessels (*178*). This sequestration is mediated by PfEMP1 proteins that show affinity towards ICAM-1 and EPCR receptors of the endothelial cells that comprise the blood vessels (*104, 105, 169, 179, 180*). This sequestration is thought to be amplified by inflammatory cytokines such as TNF-α , IFN-ɣ, and IL-1β secreted by activated lymphocytes and microglial

cells (*181, 182*). This is followed by the activation of endothelial cells and an increase in the expression of endothelial receptors. The EPCR receptor disrupts the BBB via thrombin (*183*). The binding of PfEMP1 to ICAM-1 leads to rearrangements of tight junctions via phosphorylation (Rho-dependent) of cytoskeleton proteins, while the VCAM-1 binding induces stress fibers (*160, 180*). The CD8+ T cells also induce neuronal apoptosis via cytokine release, and taken together, the BBB breakdown causes nerve injury (*108*).

Multiple biomarkers are used to provide an early prognosis of CM—the presence of soluble EPCR and ICAM-1 correlated positively with the CM progression (*179*). Similarly, Angiopoietin -1 and Ang-2 are endothelial activation mediators, and reduction in ang-1 and ang-2 with an increase of ang-2 to ang-1 ratio are commonly seen in CM patients (*184, 185*). The recent emergence of multi-omics studies can better predict CM and non-cerebral severe malaria based on altered metabolomics and lipidomics (*186*).

1.13 Merozoite reinvasion

RBCs make a compatible host compartment for the parasite's growth as they lack a nucleus, do not have MHC molecules, and are slow metabolically. The hemoglobin-rich RBCs provide the amino acids for the parasite's growth. The RBC surface has an elastic surface skeleton that helps move through the capillaries and is rich in glycophorin, GPI anchors, Band 3, actin, spectrin, Kell, Duffy, Rh antigens, etc. The merozoites use all these surface receptors during the reinvasion process (*187-189*).



1.8. A model depicting the events of merozoite attachment, reorientation, and entry into host erythrocyte. (Adapted from Weiss GE et al., Plos Pathogens, 2015 (189))

1.13.1 Initial attachment of the merozoites

The merozoites contact RBCs through merozoite surface proteins (MSP family, MSP1 to MSP10) that are abundantly present on their surface. The attachment to RBC is through GPI anchors and is low affinity, reversible, non-specific, and leads to RBC surface deformity (*190, 191*). The immune system recognizes the MSP family and is also a target of neutralizing antibodies. Hence, these proteins have evolved to be polymorphic with some conserved regions. Given their crucial role in initial attachments, the MSP family is a well-considered vaccine target (*88, 89, 91, 144, 145*).

1.13.2 Reorientation to face the apical surface

The merozoites reorient to place the apical end toward the RBC surface and form a high-affinity interaction through EBL families or RH family proteins. The micronemes secrete the EBL families, consisting of EBL-175, EBL-140 and EBL-181 (*192, 193*). These proteins show sialic acid-dependent binding as the neuraminidase treatment of the RBCs (removes sialylated moieties) reduces the merozoite entry (*189, 194*). The RH family of rhoptry origin are PfRH1, PfRH2a, PfRH2b, PfRH3, PfRH4, and PfRH5, with PfRH3 being a pseudogene (*195, 196*). The binding

of PfRh1 to its receptor triggers the release of EBA-175 from the micronemes to the surface. The EBA-175 interacts with the glycophorin A receptor of RBCs, and this binding triggers the release of proteins from the rhoptry organelle through cytoplasmic Ca2+ changes (*197*). The PfRh5 shows binding with the basigin receptor, and the EBL and RH family is considered redundant as the RH family shows invasion in the sialic acid-independent pathway (*198*).

1.13.3 Formation of invasion bridge between parasite and host RBC

The parasite-derived AMA-1 and RON complex proteins form a tight junction with the RBC surface. This is essential in invasion events, and anti-AMA-1 antibodies have been shown to block this step with 100% efficacy in in vitro GIA assays (*139*). Meanwhile, the FMP2.1/AS02a, an AMA-1 recombinant vaccine, showed only partial efficacy in human trials (*139, 146*). AMA-1 promises to be an optimum target when used in multi-component combinations with other essential invasion proteins. The MTRAP proteins mediate the invasion movement and activate the actin-myosin motor to propel the parasite further inside the RBC. The initial binding to the invasion takes only ~60 seconds; hence, the window for antibody-mediated neutralization is relatively short. The abundance and specificity of the antibodies generated play a crucial role in invasion inhibition (*147*).

1.14 Immunodominancy and redundancy in malaria infection

In the entire blood stage of *Plasmodium falciparum*, the cycle can be divided into two phases based on the location of the parasite. I. When the parasite is inside the RBC, and II. when outside the RBC in the form of merozoites. Both these forms are susceptible to immune recognition via various proteins displayed and are known to be immunodominant. The PfEMP1 proteins are a great example of immunodominant yet redundant proteins of phase I, and the merozoite surface proteins also show the immune response, polymorphism, and redundancy (*104, 199*).

When considered a vaccine target, these proteins fail to elicit complete protection. However, increasing the breadth of antigens exposed through a vaccine route can mimic the multiple exposures of the infections and provide stronger immunity (*89, 90*). Hence, we aim to understand

if combining a multi-protein approach comprising essential and immunodominant antigens can work more efficiently than a canonical single-protein vaccine approach. This would require mixing the antigens from essential pathways in the proper ratios. The parasite proteins are high molecular weight proteins, and simply mixing the proteins in an adjuvant may not elicit a uniform immune response against all the proteins as their immunodominance may vary. Generating multi-protein chimeric vaccine targets would require precise peptide sequences from the antigens.

1.15 The strategy of chimera generation in infectious diseases

The requirement of multiple exposure, increased breadth of immune response, and the problem of redundancy are present in many infectious diseases. A new approach of considering multiple immunodominant epitopes in combined manner has been tried out for certain viral infections. A few studies have shown success in case of Dengue chimeric construct (Takeda Vaccines Inc.), Hepatitis, and Zika (VacDZ) vaccine generation (*200-202*). While, in-silico designing of multi-protein constructs have shown promising results in other parasitic diseases such as Ascariasis, Leishmaniasis, and Toxoplasmosis (*203-206*). Use of multiple antigens (up to four combined) has been used for the targeting of transmission and blood stages (Pfs48/45, MSP-3,and GLURP) of *Plasmodium* through the GMZ2.6 vaccine candidate. This candidate showed adequate naturally circulating antibodies in the malaria-exposed cohort and seemed to depend on the number of exposures tolerated (*142, 207*). These studies open up a new avenue for the design of chimeric vaccine antigens containing multiple epitopes arising from multiple parasite proteins. A careful selection of epitopes ensure the presence of highly immunogenic peptides hence reducing the antigen competition, eliminates the non-functional epitopes, provides the opportunity for trageting of multiple stages of the infection, and increases the breadth of the antigens presented. A canonical single protein or subunit vaccines lack the clear advantages provided by this strategy. In this thesis work, we show that combination of highly antigenic and redundant proteins from the blood stage of *Plasmodium falciparum* in the form of chimeric antigens work efficiently in reducing the parasite severity and multiplicity load.

Chapter 2: Design and construction of chimeric antigens targeting the blood stage of *P. falciparum*

2.1 Introduction

The recognition of a foreign invader takes place by both innate and adaptive immune systems. The innate system has limited recognition and acts based on identifying PAMPs and other non-host molecules. In contrast, the adaptive arm of the immune response can precisely identify the foreign antigens. The vaccine preparation in any model system tries to invoke the adaptive B (humoral) and T cell (cell-mediated) responses, as these two are essential players in destroying the pathogen. The B cell receptors (BCRs) recognize the epitopes present on the antigen surfaces and generate antibodies specific to them. In contrast, T cells identify the epitopes presented on MHC complexes by other antigen-presenting cells (APCs) and kill the pathogens by release of cytotoxins (*208*). These cells identify antigens through specific stretches of peptides, i.e., epitopes. Advances in immunoinformatics now allow the detection of epitope sites within a protein sequence using various parameters. In the 1990s, Kolaskar & Tongaonkar showed that the occurrence of hydrophobic residues (Cys, Leu, and Val) on the protein surface acts as a potential antigen. Their antigenic stretch determination method can accurately predict the epitopes with up to 75% confidence based on these amino acid residues and their frequencies (*209*). This has been extensively used for epitope selection in antibody preparation, and many emerging studies are using these resources for potential vaccine designs. Platforms such as Immune Epitope Database provide multiple parameters such as antigenicity predictor, beta-turn propensity, surface accessibility, flexibility, and hydrophilicity to assess the sequence of a protein (*210*). Multiple studies have focused on the design of vaccine candidates; however, the efficacy of such antigens has not yet been tested for malaria.

A *Plasmodium* parasite also harbors many potential antigens across all three stages of development. Given the efficacy rates and stage-specific expression of these antigens, a chimeric approach covering different stages and proteins holds the potential to provide complete protection against malaria infection. We selected the blood stage of the parasite since it is symptomatic and highly damaging to the host. Our studies focused on B cell epitopes as the

immune response to malaria is majorly driven by B cells, and the presence of specific antibodies correlates positively with a disease outcome specifically during the blood stage. Since malaria infection does not induce sterile immunity, the ideal vaccine would be a multi-protein antigen representing multiple phases of blood stage infection. Hence, we screened the important antigens of the blood stage of *Plasmodium falciparum* for a B cell epitope targeting the parasite while being inside as well as outside of the RBC. For this search, we considered the PfEMP1 family known for causing sequestration, related complications, and merozoite invasion-specific genes. These gene families are known to be antigenic and proteins of the redundant pathways. The PfEMP1 proteins mark the iRBCs for immune recognition and hence can be cleared by the immune system. Similarly, the merozoite forms of the parasite are ideal targets for vaccine development as they are available for immune recognition before entering into a new host RBC. This chapter discusses the generation of three chimeric antigens that comprehensively cover the blood stage of *Plasmodium falciparum*.

2.2 Materials and Methods

2.2.1 *In sillico* prediction of antigenic peptides

The eight proteins taken from varB subgroup (PF3D7_1200100, PF3D7_0500100, PF3D7_1300100, PF3D7_0324900, PF3D7_1100100, PF3D7_0937800, PF3D7_0300100, and PF3D7_0400100) and AMA-1, MSP-1, MSP-2 and MSP-3 along with EBA-175, Rh-5, SERA-5, and GLURP were subjected to the analysis in Immune Epitope Database- analysis resource (IEDB-AR) (*210*). A total of 6 parameters, including Bepipred Linear Epitope Prediction 2.0 (*211*), Chou & Fasman Beta-Turn Prediction (*212*), Emini Surface Accessibility Prediction (*213*), Karplus & Schulz Flexibility Prediction (*214*), Kolaskar & Tongaonkar Antigenicity (*209*) and Parker Hydrophilicity Prediction (*215*) were applied to each protein sequence. The scores for each amino acid were aligned, and the peptide stretch of 25 amino acids with an average of 0.6 and above were considered. For chimeric varB, chimeric MSP (AMA-1, MSP-1, MSP-2, and MSP-3) and chimeric InvP (EBA-175, Rh-5, SERA-5, and GLURP) construct a total of 29 peptides, 20 peptides and 24 peptides respectively were stitched together. The stitched sequence was converted to corresponding DNA sequences using backTransSeq and codon optimized for

expression in E. coli and cloned into a pET28a+ vector containing 6X histidine tag using NdeI and XhoI restriction sites.

2.2.2 Chimeric protein expression

The three clones (chimeric varB, MSP, and InvP) were separately transformed into a competent E. coli BL21DE3 expression system. The culture was grown till the optical density reached 0.6 in 600 nm spectra and induced using 0.5mM of isopropyl-1-thio-β-d-galactopyranoside (IPTG) at 18℃ for chimeric varB and at 25℃ for chimeric MSP and InvP for 8-10 hours. Only the bacterial mass was collected by centrifugation at 4000 RPM and sonicated using sonication buffer (10 mM Tris-Cl pH 7.5, 300 mM NaCl, 10% glycerol, 0.1% TritonX-100, 1X PIC, and 2 mM PMSF) at parameters of 3 sec ON/ 5 sec OFF/ 60% amplitude (Probe sonicator Thomas Scientific). The supernatant was separated by spinning at 12,000 RPM, and subjected to SDS-PAGE followed by coomassie staining and western blotting

2.2.3 Western blotting of chimeric antigens

The uninduced and induced supernatants of chimeric varB, MSP, and InvP proteins were used for western blotting. Briefly, 30 l of supernatant from different conditions (uninduced, induced with 0.5mM IPTG at 18 ℃ and 25 ℃) were denatured using 6X SDS dye (30% glycerol v/v, 10% SDS w/v, 10% -mercaptoethanol v/v, 0.02% Bromophenol blue w/v, 20mM Tris pH 6.8) and loaded onto 10% separation SDS-PAGE gel. The gel was transferred to the PVDF membrane using semi-dry transfer (Biorad) at 25V for 1 hour. The membrane was blocked using 5% skimmed milk made in TBST and probed using anti-his primary antibodies (1:2000 Bio Bharti Life Sciences BB-AB0010) overnight at 4 ℃. The membrane was washed three times using TBST and probed using anti-rabbit secondary conjugated with HRP (Biorad 1706515) for one hour at RT. The blot was developed using the Clarity Western ECL substrate (Biorad) in the LAS4000 system (GE life science).

2.2.4 Purification of chimeric antigens

The sonicated supernatant fractions of chimeric varB, MSP, and InvP proteins were subjected to purification using Nickel affinity chromatography. Briefly, supernatants arising from sonication of 2 liter culture were separated and Ni-NTA agarose beads (Qiagen 30230) were added to the lysate and incubated for 4 hours at 4℃. The elutions were taken by adding 50 mM, 100 mM, 150 mM, and 300 mM elution buffer (10 mM Tris-Cl pH 7.5, 150 mM NaCl, 10% glycerol, and varying imidazole). The elutions were run on 10% SDS-PAGE gel and stained using Coomassie brilliant blue solution. The elutes containing purified fractions were pooled, dialyzed (10 mM Tris-Cl pH 7.5 and 150 mM NaCl), and concentrated. The purified protein was re-run on SDS-PAGE to confirm purity and concentration and stored at -80 ℃.

2.2.5 Confirmation of chimeric antigens using Mass-spectrometry

For validation, the purified proteins were reduced using 10 mM Dithiothreitol, alkylated using 10 mM Iodoacetamide, and trypsinized using sequencing grade modified trypsin (Promega V5113). The samples were desalted and run on Sciex TripleTOF6600. The peptide identification and analysis were performed using MaxQuant. The reference proteome file used for analysis was customized to accommodate *E. coli* BL21DE3 proteome along with sequence of respective chimeric antigens.

2.3 Result

2.3.1 Selection of proteins for generating chimeric antigens

To cover the entire blood stage, we divided the stage into two phases: 1. During the iRBC phase by targeting PfEMP1 and 2. During the merozoite phase, targeting merozoite surface and invasion proteins. As a selection criteria we considered proteins that are A. surface exposed and available for immune recognition, B. highly immunodominant and known to have antibody response in natural infections, C. essential for cytoadhesion or invasion pathway (*104, 199*). We re-analyzed the RNA-seq data of 1027 patients (Mok et al., 2015) (*48*) to identify the clinically relevant PfEMP1 genes expressed. The expression of var subtype B was dominant in most patient samples compared to the other subtypes (Figure 2.1). This was partially expected as the

endemic regions have uncomplicated malaria events that are likely to be mediated by the varB subtype (*167*).

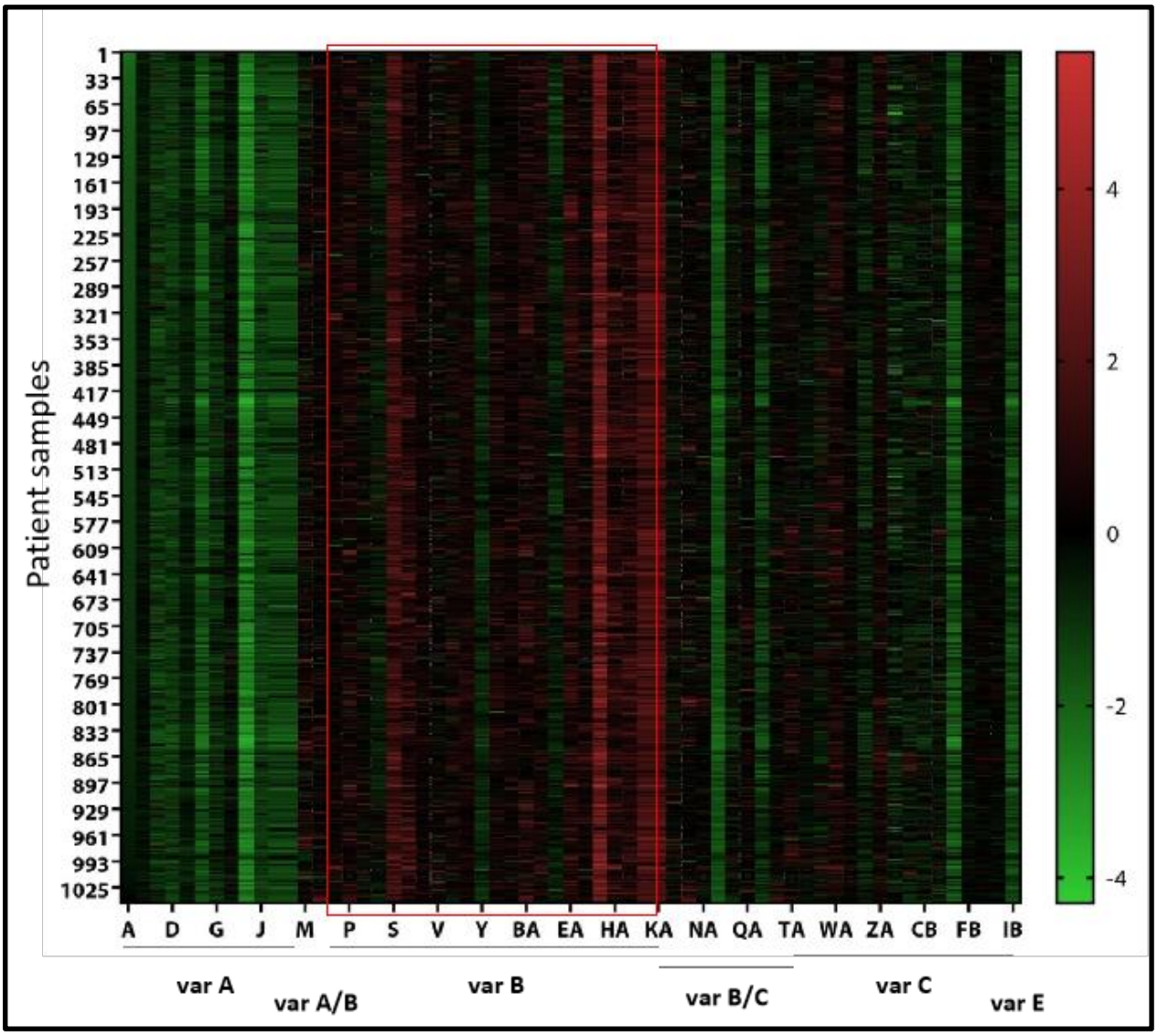


Figure 2.1. A heatmap showing expression of PfEMP1 subtypes in P. falciparum-infected individuals. The subtype B (highlighted in red box) shows higher expression across most patients. (Reanalyzed from Mok et al., Science, 2015 (48))

As proof of principle, we picked eight proteins (PF3D7_1200100, PF3D7_0500100, PF3D7_1300100, PF3D7_0324900, PF3D7_1100100, PF3D7_0937800, PF3D7_0300100, and PF3D7_0400100) belonging to group B, which also had dominant expression in the lab strain

3D7 (Figure 2.2). This overlap of gene expression made it feasible to use the lab strain for further downstream experiments.

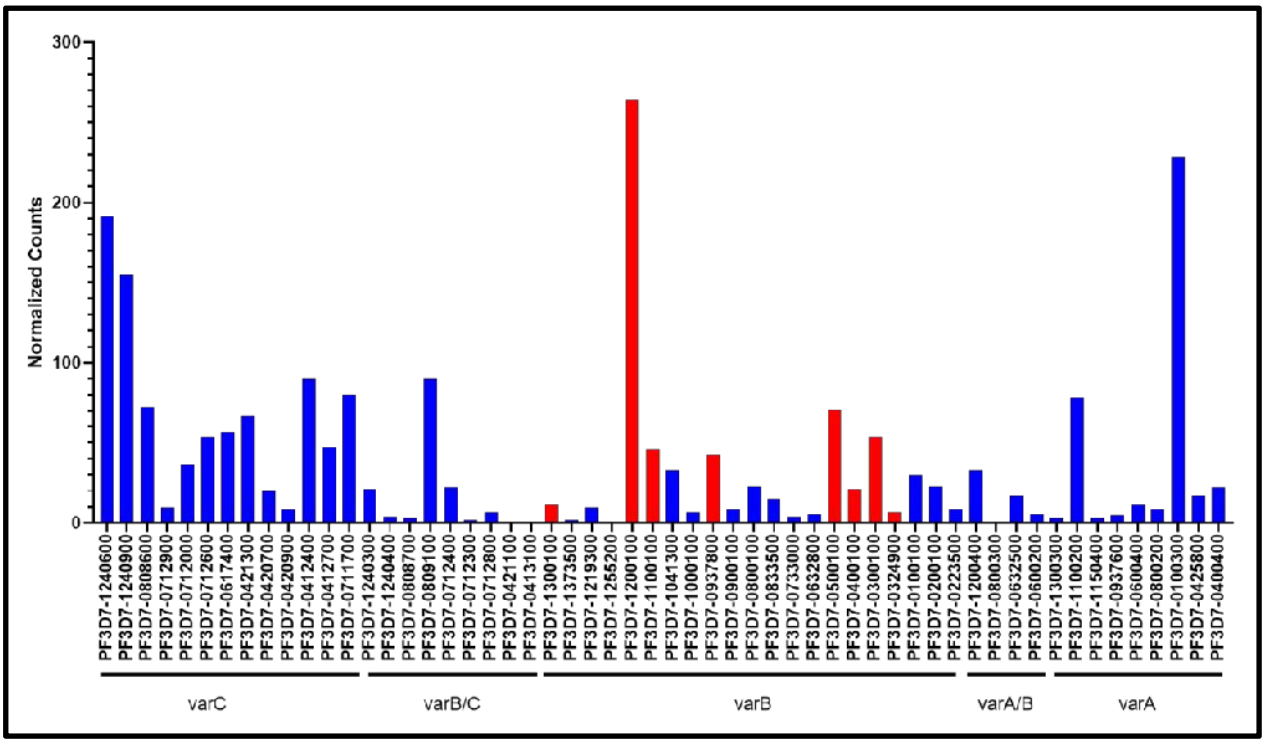


Figure 2.2. The expression profile of PfEMP1 genes in lab strain 3D7 was identified using RNA sequencing. The subtype B is highlighted in red and considered for generating the chimeric varB construct. (Data reanalyzed from Rawat et al., Microbiology Spectrum, 2021 (216))

Similarly, we selected the invasion and merozoite-specific proteins (MSPs) known as immunodominant and have already validated them as potential vaccine candidates individually. We focused on the merozoite entry mechanism and divided it into two stages 1) The initial attachment and reorientation process and 2) formation of invasion complex. The initial attachment process is mediated by MSP family proteins that show reversible, low affinity for GPI anchors present on the RBC surface (*91, 199*). There are multiple MSP proteins known and they cover the merozoite surface as a thick fibrillar coat of proteins. Being surface-exposed, they are highly immunodominant and can be blocked through antibodies (*191*). The MSP-1, 2, and 3 are of particular interest as multiple studies have shown the presence of antibodies against them correlating positively with disease survival (*87, 88, 90, 91, 143-145*). Another essential protein

AMA-1 is known to form tight junction bridges between merozoite and RBC once the initial attachment is established and the blocking of this interaction through anti-AMA-1 antibodies is known to inhibit merozoite entry (*139, 146*). AMA-1 is also highly immunodominant and its vaccine formulation in animal models shows complete protection (*217, 218*). Based on their early mode of action and essentiality during merozoite attachment, we combined MSP-1, MSP-2, MSP-3, and AMA-1 in one single chimeric construct.

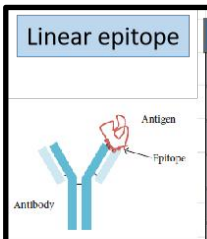
The invasion process of merozoite can take place through either sialic acid dependent or independent pathway. Recent reports suggest that parasites may use both these pathways alternatively to enter the host RBC. Microneme-secreted EBL family proteins mediate the sialic acid dependent invasion while the rhoptry-secreted RH family mediate the sialic acid independent pathway of invasion. It is important to target both these pathways simultaneously to completely inhibit the invasion process. Hence we considered EBA-175 (from EBL family) and RH-5 (RH family) antigens as they are already proven to be essential in invasion and individually characterized as possible vaccine candidates (*140, 147, 195, 196, 198, 199*). Apart from these two proteins, we have considered SERA-5 protein from the SERA family that helps in parasite egress and GLURP protein that has recently emerged as a possible vaccine target for blocking the parasites (*142, 143, 219-222*). Together, EBA-175, SERA-5, RH-5, and GLURP were combined in a single chimeric antigen designed to block the merozoite invasion.

2.3.2 Generation of antigenic peptidome library

To construct chimeric varB antigen representing eight of selected PfEMP1 subtype B proteins (PF3D7_1200100, PF3D7_0500100, PF3D7_1300100, PF3D7_0324900, PF3D7_1100100, PF3D7_0937800, PF3D7_0300100, and PF3D7_0400100) were subjected to IEDB-AR platform (*210*). Herein, we aligned each amino acid of the protein for six different scores– BepiPred, beta turn propensity, surface accessibility, flexibility, antigenicity, and hydrophilicity (*209, 211-215*). The criterion of 0.6 score for BepiPred was set for defining a stretch of amino acids as epitope. This is slightly stringent that 0.5 score that is regularly used. Followed by BepiPred we gave priority to beta turn propensity (known to be more antigenic than alpha helices) and surface accessibility of the epitope. Apart from the antigenicity scores, we considered the functionally

essential domains of these proteins. An example of score alignment is shown in Figure 2.3. A stretch of 25 amino acids satisfying all above criteria were marked as epitopes for generation of chimeric antigens.

Similarly for constructing chimeric MSP, we predicted highly antigenic peptide stretches of 25 amino acids from AMA-1 (PF3D7_1133400), MSP-1 (PF3D7_0930300), MSP-2 (PF3D7_0206800), and MSP-3 (PF3D7_1035400), and stitched them together. A chimeric InvP (invasion proteins) construct was generated by stitching the highly antigenic peptides from EBA-175 (PF3D7_0731500), SERA-5 (PF3D7_0207600), RH-5 (PF3D7_0424100), and GLURP (PF3D7_1035300).



Position	Residue	Assignment	BepiPred	Peptide	Beta Turn	Surface Acc	Flexibility	Antigenicity	Hydrophobicity
408	R	E	0.615	GGGRRQK	1.224	1.737	1.096	0.902	5.314
409	R	E	0.63	GGRRQKR	1.137	3.438	1.088	0.902	5.1
410	Q	E	0.641	GRRQKRS	1.119	4.656	1.095	0.921	5.214
411	K	E	0.657	RRQKRST	1.033	3.431	1.093	0.926	5.143
412	R	E	0.663	RQKRSTH	1.033	2.383	1.087	0.96	4.843
413	S	E	0.654	QKRSTHS	1.101	1.844	1.082	0.979	5.171
414	T	E	0.654	KRSTHST	1.099	1.331	1.062	0.964	5.057
415	H	E	0.643	RSTHSTK	1.099	1.359	1.052	0.964	5.057

Figure 2.3. An example of amino acid score alignment. For identifying the epitope stretch of peptides, the scores of BepiPred, beta-turn (Chou & Fasman), surface accessibility (Emini's), flexibility (Karplus & Schulz), antigenicity (Kolaskar & Tongaonkar), and hydrophilicity (Parker) was considered (*209, 211-215*)***. The major filter set was for a BepiPred score of 0.6 or above for calling peptide stretches as epitopes. (Analysis done using IEDB-AR tool (210))***

2.3.3 Selection of antigenic peptides

A total of 29 peptides originating from the functional domains of a length of 25 amino acids were stitched together to create the chimera varB (Table 1). The chimeric MSP antigen was designed by stitching the 20 peptides belonging to AMA-1, MSP-1, MSP-2, and MSP-3 (Table 2). The chimeric InvP was made by stitching 24 peptides belonging to EBA-175, SERA-5, RH-5, and GLURP (Table 3). All three chimeric constructs had an average antigenicity score of 0.6 and above, which marks a stringent criterion for an amino acid epitope stretch. The protein sequence

was back converted into a codon-optimized DNA sequence, cloned into pET28a+ plasmid with N-terminal 6X histidine tag, and expressed in the *E. coli* system under the control of the T7 promoter and used for further assays. The DNA sequence used is presented in Appendix 1. The alignment of the selected peptides on the 3D structure of protein is present in Appendix 2.

No	Protein ID	Peptides (Stitched in this same order)	start site	End site	Average antigenicity score
1	PF3D7_1200100	TSDKGSEPTARGHSHVARSADGAPS	862	886	0.653
		PNGNPLPQPGTNGTSNEPISQYQYD	1099	1123	0.628
		NTTASGNNTTASGKNTPSDTQNDIP	1794	1818	0.671
		STSGNKHSDIPSGKLSDTPSDNNIH	2012	2036	0.675
2	PF3D7_0500100	TTQVETQASGGNTETSQVSG	931	950	0.656
		ETTPQGQTPSESEAQTASQD	951	970	0.636
		TKRQSVLPLLEPINGDTISDDNNPE	999	1023	0.625
		NTTASGNNTTASDTQNDIQNDGIPS	1895	1919	0.629
3	PF3D7_1300100	TEAQAGGDEATEASVPLGDGVSKNP	933	957	0.647
		KEKEERERENAGLDPFGGSVDDEAS	989	1013	0.664
		TTASGKNTPSDTQNDIQSDDIPSSK	1827	1851	0.646
		VDSNPNQVDDTYVDSNPDNSSMDTI	2069	2093	0.608
4	PF3D7_0324900	EQEEEEKGAGEDEAASEAEASGPKV	795	819	0.618
		TKQNDSEGSEGGHRSKRHTESSDST	872	896	0.668
		TTASGNNTTASGNNTTASGKNTPSD	1844	1868	0.676
5	PF3D7_0300100	KKAYGKNGTTTKETSNGPINNLYVG	394	418	0.64
		GGGNTAASQGSGEAAQPVTV	910	929	0.65
		TQPQASGGNTQVAVSPGGAASTSTT	930	954	0.66
6	PF3D7_1100100	DFKNVNSSSGSGGGEGSNKTFSHTE	459	483	0.62
		GNSVVSSSSARGNGASRDKNGGSDS	557	581	0.66
		DNTNGGPPTQDGEVKNALLDDNNKP	1170	1194	0.65
7	PF3D7_0937800	RSTSVEMKALSGAGGGPELTGSGSD	1032	1056	0.68
		NTTASGNNTTASGNNTTASGNNTTA	1897	1921	0.66
		DIPNDYTSGTIPTNTNITTTSRHNV	1962	1986	0.643
		NDLYNGKNNLYSGQNNVYSGIDPTS	2080	2054	0.665
8	PF3D7_0400100	KGSKSQESGKAEGTSESSGSEASSP	1347	1371	0.67
		LDEKKKQQRESGLVGALDGNSGNVD	1429	1453	0.656
		TASGNNTTASGNNTTASGNNTTASG	2294	2318	0.662
		YNGKNNLYSGQNNVYSGIDP	2421	2440	0.666

Table 1. A list of proteins and the peptides stretches taken to construct chimeric varB. The table also denotes the start sites, end sites, and the average antigenicity score for each peptide. The peptides were stitched in the same order as shown without introducing linker sequences.

No	Protein ID	Protein Name	Peptides (Stitched in this same order)	start site	End site	Average antigenicity score
1	PF3D7_1133400	AMA-1	LPTGAFKADRYKSHGKGYNWGNYNT	379	403	0.6
			DEIMKEIERESKRIKLNDNDDEGNK	447	471	0.61
			GNAEKYDKMDEPQDYGKSNSRNDEM	570	594	0.63
2	PF3D7_0930300	MSP-1	TKGASAQSGASAQSGASAQSGASAQ	59	83	0.62
			AQSGTSGPSGPSGTSPSSRSNTLPR	94	118	0.62
			EDGGHSTHTLSQSGETEVTEETEET	726	750	0.64
			EEQKQITGTSSTSSPGNTTVNTAQS	901	925	0.64
			ATHSNSQNQQSNASSTNTQNGVAVS	926	950	0.63
			HDPLTVLSISNDLKGIVSLLNLGNK	960	984	0.64
			DVTPSPLSVRVSGSSGSTKEETQIP	1253	1277	0.61
3	PF3D7_0206800	MSP-2	IRRSMAESKPSTGAGGSAGGSAGGS	38	62	0.64
			GSAGGSAGGSAGSGDGNGADAEGSS	65	89	0.64
			TTNDAEASTSTSSENPNHKNAETNP	106	130	0.65
			KGKGEVQEPNQANKETQNNSNVQQD	131	155	0.68
			QTKSNVPPTQDADTKSPTAQPEQAE	157	181	0.64
			SAPTAEQTESPELQSAPENKGTGQH	183	207	0.64
			HGSRNNHPQNTSDSQKECTDGNKEN	211	235	0.69
4	PF3D7_1035400	MSP-3	LNNNSQIENEENVNTTITGNDFSGG	40	64	0.6
			NAYEKAKNAYQKANQAVLKAKEASS	164	188	0.61
			EEENDKKKEQEKEQSNENNDQKKDM	273	297	0.64

Table 2. A list of proteins and their respective peptide stretches used in constructing chimeric MSP. The table also denotes the start sites, end sites, and the average antigenicity score for each peptide. The peptides were stitched in the same order as shown without introducing linker sequences.

No	Protein ID	Protein Name	Peptides (Stitched in this same order)	start site	End site	Average antigenicity score
1	PF3D7_073150	EBA-175	DSRINNGRNTSSNNEVLSNCREKRK	138	162	0.61
			LVKSVLNGNDNTIKEKREHIDLDDF	432	456	0.6
			NNEQTSQEAVPEESTEIAHRTETRT	754	778	0.619
			DERKNQEPANKDLKNPQQSVGENGT	779	803	0.61
			GVNHGIPKGEDQTLGKSDAIPNIGE	825	849	0.63
			RSQINHSHHGNRQDRGGNSGNVLNM	1278	1302	0.61
			RSNNNNFNNIPSRYNLYDKKLDLDL	1303	1327	0.62
2	PF3D7_020760	SERA-5	NTGGGQAGNTGGDQAGSTGGSPQGS	29	53	0.65
			VSVSQTSTSSEKQDTIQVKSALLKD	93	117	0.62
			SSSSSSSSSSSSSSSSSSSSSSS	207	231	0.699
			HVDTTLEKEDTLSYDNSDNMFCNKE	545	569	0.62
			EQCPKVEDHWMNLWDNGKILHNKNE	669	693	0.61
			YFKNFNVGKKNLFSEKEDNENNKKL	852	876	0.62
			NYIIFGQDTAGSGQSGKESNTALES	879	903	0.64
3	PF3D7_042410	RH-5	IKKEIDNDKENIKTNNAKDHSTYIK	59	83	0.6
			EHPYDINNKNDDSYRYDISEEIDDK	238	262	0.61
			DETEEVEDSIQDTDSNHTPSNKKKN	268	292	0.63
4	PF3D7_103530	GLURP	NESSDIISVNNKSNKVQNHFESLSD	131	155	0.63
			TQIHKDYKEKNLINEEDSEPFPRQK	199	223	0.62
			EHIDQSQHNINVLQENNINNHQLEP	365	389	0.62
			TVSQESNPEKADNDGNVSQNSNNEL	460	484	0.63
			ESSLEEGHHEEIVPEQNNEESGESK	504	528	0.63
			EFEPDQNDSELSENELVESEKSVSE	629	653	0.63
			EVKEKENVSEVVEEKQNSQESVEEI	768	792	0.62

Table 3. A list of proteins and their respective peptides used in constructing chimeric InvP. The table also denotes the start sites, end sites, and the average antigenicity score for each peptide. The peptides were stitched in the same order as shown without introducing linker sequences.

2.3.4 Expression and purification of chimeric constructs

We cloned and expressed chimeric varB, MSP, and InvP in the bacterial expression system using a pET28+ vector containing an N-terminal 6X histidine tag. The expected proteins were validated using anti-his western blotting (Figure 2.4). The chimeric proteins were seen at precisely double the size owing to the unnatural folding patterns. The originally expected sizes are 72 kDa, 55 kDa, and 66 kDa for chimeric varB, MSP, and InvP, respectively. The chimeric proteins in soluble fractions of bacterial lysates were purified using Ni-NTA affinity chromatography (Figure 2.5). The purified proteins were further used for assays.

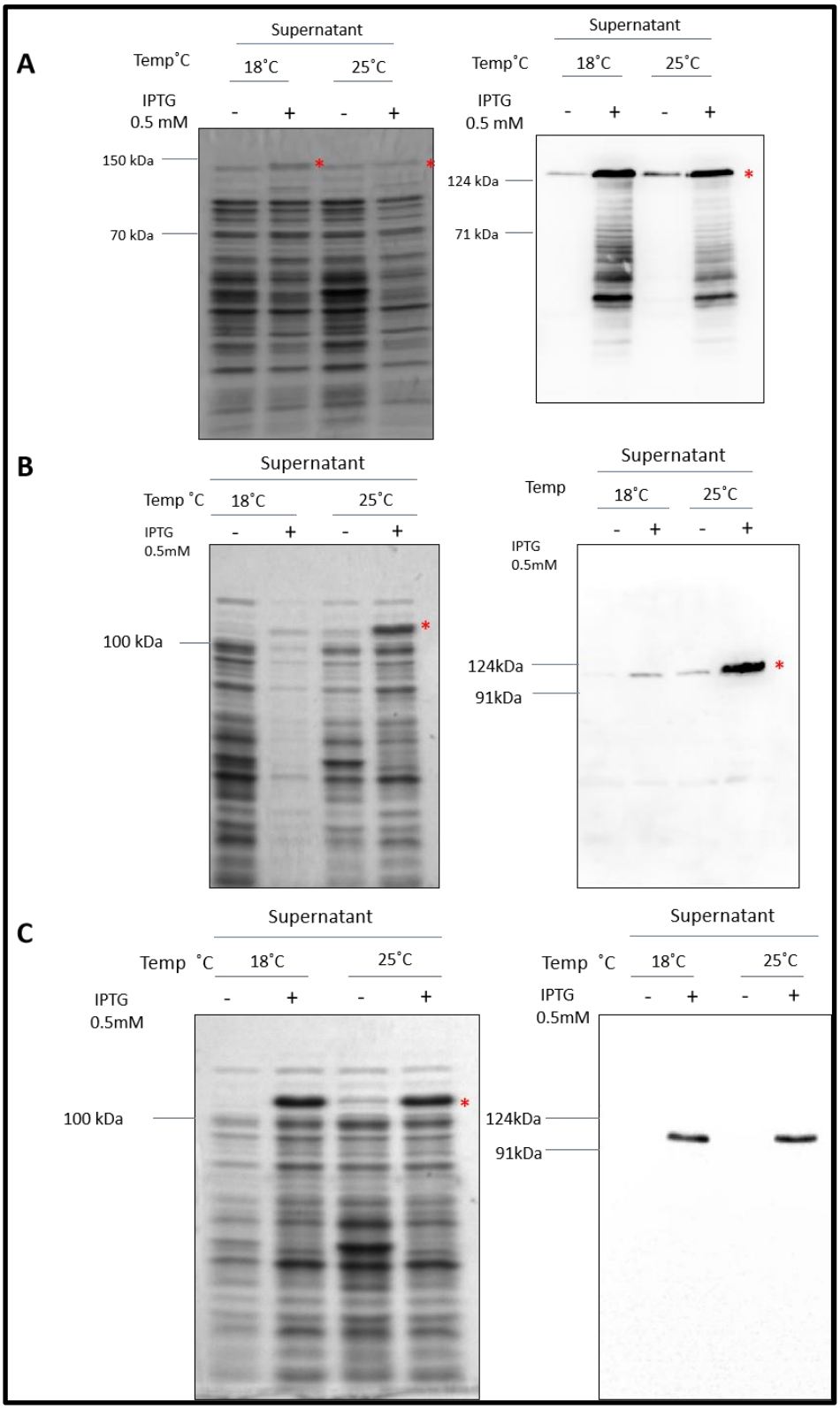


Figure 2.4. An expression profile of A. chimeric varB, B. chimeric MSP, and C. chimeric InvP antigens induced in the Bl21DE3 expression system using 0.5 mM of IPTG at 18 ℃ and 25 ℃.

The panel represents each antigen's Coomassie gel images (left) and anti-his western blot images (right) after sonication and separation of supernatant fraction only. The red asterisk represents the corresponding sizes of the chimeric antigens in Coomassie gel and western blot. The observed sizes are 140 kDa (chimeric varB), ~120 kDa (chimeric MSP), and ~120 kDa (chimeric InvP)

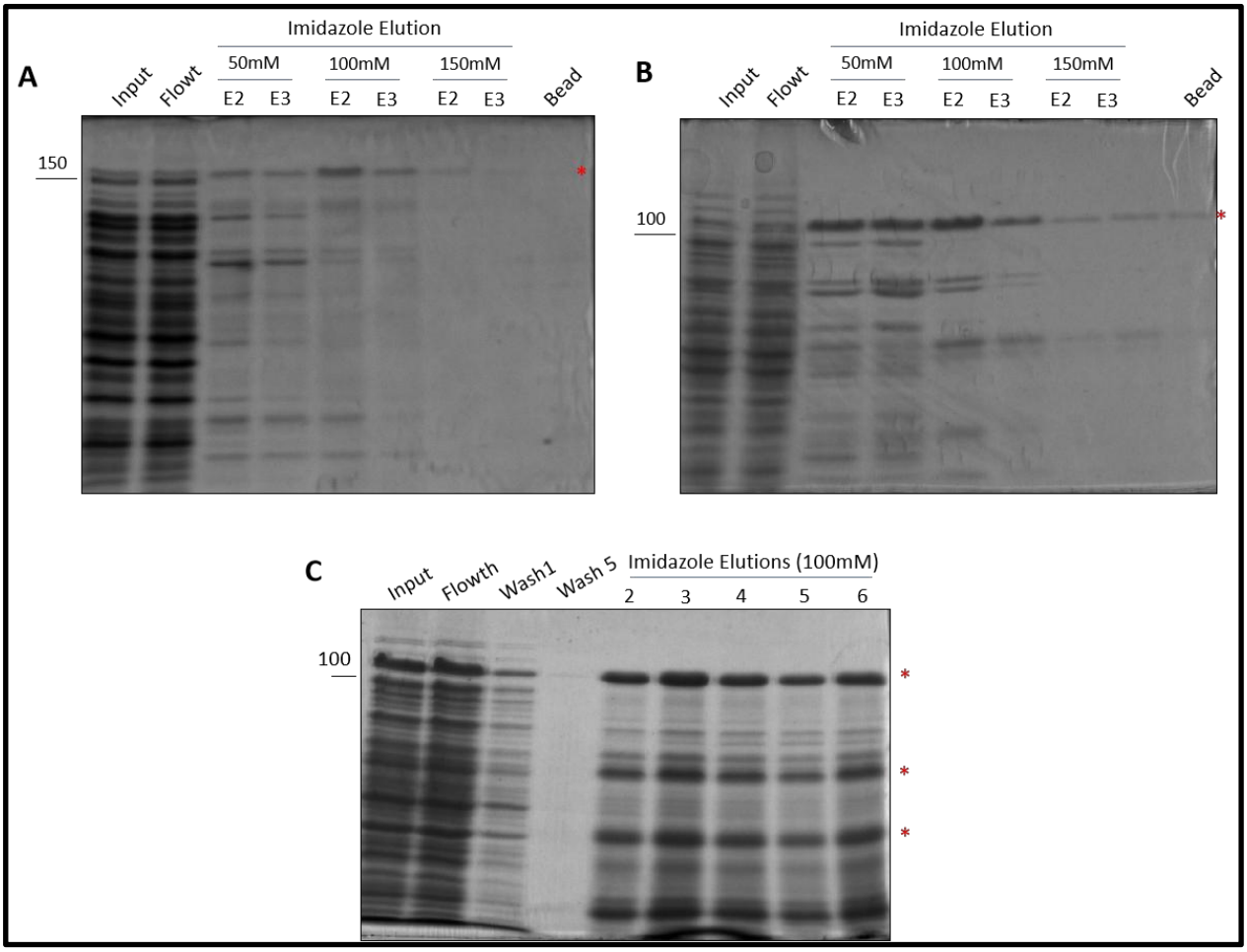
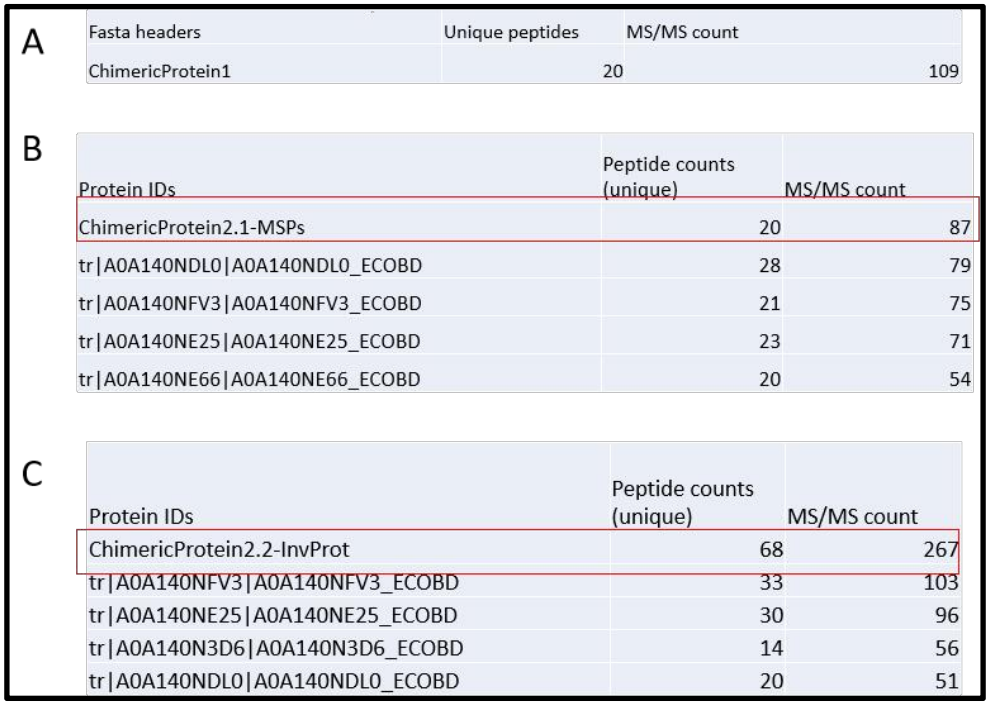


Figure 2.5. An SDS-PAGE followed by a Coomassie staining image of A. chimeric varB, B. chimeric MSP, and C. chimeric InvP antigens after affinity purification using Ni-NTA.The chimeric InvP construct upon purification show three distinct bands (also corresponding to western blot using anti-his) which are possible cleaved products.

2.3.5 Mass-spectrometry validation of chimeric antigens

The purified proteins were validated using mass-spectrometry. The analysis with a 99% confidence score showed the purified proteins had the highest number of unique peptides and MS/MS counts (Figure 2.6). A fasta file containing *E. coli* BL21 proteome combined with the sequence of the chimeric protein was created to use as a reference proteome file in analysis.



A

Fasta headers	Unique peptides	MS/MS count
ChimericProtein1	20	109

B

Protein IDs	Peptide counts (unique)	MS/MS count
ChimericProtein2.1-MSPs	20	87
tr|A0A140NDL0|A0A140NDL0_ECOBD	28	79
tr|A0A140NFV3|A0A140NFV3_ECOBD	21	75
tr|A0A140NE25|A0A140NE25_ECOBD	23	71
tr|A0A140NE66|A0A140NE66_ECOBD	20	54

C

Protein IDs	Peptide counts (unique)	MS/MS count
ChimericProtein2.2-InvProt	68	267
tr|A0A140NFV3|A0A140NFV3_ECOBD	33	103
tr|A0A140NE25|A0A140NE25_ECOBD	30	96
tr|A0A140N3D6|A0A140N3D6_ECOBD	14	56
tr|A0A140NDL0|A0A140NDL0_ECOBD	20	51

Figure 2.6. A mass-spectrometry analysis of A. chimeric varB, B. chimeric MSP, and C. chimeric InvP showing highest hit for unique peptides and MS/MS counts.

2.3.6 Additional confirmation of chimeric constructs using linker sequences

Since the chimeric construct showed higher size during SDS-PAGE analysis, we also introduced linker sequences (GGGSGGGS) in between each peptide in chimeric varB construct to induce flexibility (*223*). The sequence for the same is included in Appendix 3. After incorporation of linker sequences the gene was cloned into a pGEX4T1 vector containing GST tag. The expected protein size is ~90 kDa with 26 kDa GST tag (total 116 kDa), but in anti-GST western blot we observed the size to be around 180 kDa (Figure 2.7). The peculiarity of the proteins to run higher than expected sizes is not due to flexibility.

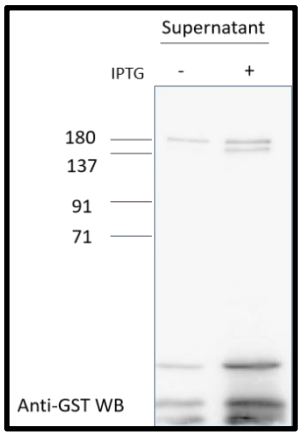


Figure 2.7. An anti-GST western blot image showing chimeric varB with linker protein appearing at 180 kDa. (Expected size is ~ 116 kDa)

2.4 Discussion

The blood stage of malaria infection poses a threat of multiple complications. The exponential increase in parasitemia per cycle drastically affects the RBC levels and leads to severe anemic conditions. The cyclic fever along with associated symptoms are a result of merozoite egress and reinvasion. Many vaccine strategies have tried to disrupt this cycle to alleviate the symptoms and reduce the parasite burden but till date no vaccine is approved against the blood stage of *P. falciparum* infection (*21, 92, 122, 135*). Similarly, the cytoadhesion and sequestration shown by late stage parasites contribute to the disease severity by causing organ damage. Both these stages have been proven to be difficult to target owing to the redundancy of proteins and antigenic polymorphism. Moreover, the PfEMP1 family causing cytoadhesion shows mutually exclusive expression with no defined sequence of switching (*103*). The three chimeras we designed (varB, MSP, and InvP) target these proteins in a combined fashion and hence increase the breadth of antigen target and cover the entire blood stage. The chimeric varB antigen can potentially disrupt the varB mediated cytoadhesion and sequestration. The peptides selected for the generation of chimeric varB belong to the functional domains known for endothelial receptor affinity (Table 4). The chimeric MSP antigen holds the potential of inhibiting the merozoite attachment and tight junction formation while the chimeric InvP can inhibit the parasite invasion into the host RBC. Other than neutralizing effect, having cytophilic IgG responses towards these antigens can mark the iRBC or merozoites for antibody-mediated complement activation and phagocytic clearance.

We successfully cloned, expressed, and purified these three chimeric antigens. A peculiarity about these proteins is that they seem to run higher on SDS-PAGE gel and are independent of flexibility or dimerization (tested through 8M urea denaturation). Hence, we also validated them through mass-spectrometry analysis. We aligned the peptide hits from mass-spectrometry and observed the full length proteins being covered proving that the proteins are being expressed. Given that we have taken only the beta sheets and highly antigenic stretches the folding of the proteins is unnatural and requires further analysis using structural studies.

Protein ID	Functional domain of the peptide
PF3D7_1200100	DBLδ
PF3D7_0500100	DBLδ
PF3D7_1300100	DBLδ
PF3D7_0324900	DBLα, DBLδ
PF3D7_1100100	DBLα, CIDRα, DBLδ
PF3D7_0937800	DBLδ
PF3D7_0300100	DBLα, DBLδ
PF3D7_0400100	DBLδ

Table 4. A list of functional domains considered per subtype B PfEMP1 protein for generation of chimeric varB.

The approach of reverse vaccinology has allowed scientists to identify the antigens of interest and further use it for designing vaccines. Many studies, especially in viral pathogens, have utilized this approach to narrow down multiple essential antigens (*202, 204*). To generate a single target representing the pool of selected antigens, only the B-cell and T-cell-specific peptides are taken and stitched to make a chimera. The advantage of this system is the simultaneous representation of multiple proteins in a single administration, which cannot be achieved in canonical vaccine preparations. This approach also gives the flexibility of choosing the epitope to be displayed to the immune system, reducing the possibility of non-neutralizing, non-specific, or otherwise unnecessary antibodies (*224*). Promising results are already shown in flaviviruses, HPV, monkeypox virus, etc (*225-227*). At the same time, research is ongoing on

parasitic diseases such as leishmaniasis, filariasis, ascariasis, and toxoplasmosis (*203, 204, 206, 228*).

Recent studies have used the IEDB-AR based epitope prediction for identifying the malarial antigens on whole proteome levels. These findings also show that CSP and LSA-1 protein during liver stage and MSP family, TRAP, and EMP proteins during blood stage are marked as proteins containing significantly higher B cell epitopes (*205*). Interestingly, the AMA-1, MSP-1, PfEMP1 family, and GLURP are also characterized to have potential IL-10 inducing ability which helps counterbalance the detrimental inflammatory response seen during blood stage infection. Another study showed MSP-3, EBA-175, and SERA-5 to be highly immunogenic within the pool of 14 merozoite antigens considered. Interestingly, the SERA-5 disordered region of sequential serine residues (Table 3, SERA-5 peptide aa 207-231) is also shown as a strong antigenic region with multiple epitopes by Azimi-Resketi et al in 2022. Their immune simulation also showed SERA-5 to elicit highest amounts of IgG and IgM responses, but this has not been validated in natural infections (*229*). Instead, MSP-3 and EBA-175 are known to have higher IgG titres in malaria infected individuals (*89*). The RH-5 protein scored lower than other invasion proteins in immunoinformatics approaches. Also the IgG titres of naturally infected individuals against RH-5 antigen was suboptimal as compared to MSP family or AMA-1 proteins. Surprisingly, the vaccine formulation of specific RH-5 stretch has shown promisingly high IgG responses and neutralizing activity in trials emphasizing on the use of epitopes instead of whole protein vaccines (*140*). With our chimeric antigens covering the blood stage successfully validated, we used them for further assays to confirm their antigenicity and subsequent functionality.

Chapter 3: Assessment of human immune responses against chimeric antigens

3.1 Introduction

The *Plasmodium* infection elicits both innate and adaptive immune responses. The innate response consists of activation and clearance through the complement system and phagocytosis through PAMP (*27*). The adaptive immune response mediated by T and B cells acts through antigen recognition and subsequent antibody generation. These antibodies, primarily generated against sporozoites and blood-stage antigens, neutralize the target or help in parasite clearance through complement activation and antibody-mediated phagocytosis. The number of exposures to the disease plays a crucial role in building protective immunity over time. Since the population in endemic regions faces multiple infections, adults usually have a protective repertoire of antibodies or so-called premunition that lowers the risk of clinical disease but does not provide sterile immunity. This premunition is acquired slowly over time, is strain-specific, and predominantly mediated through cytophilic IgG titer (*89, 90, 107*). Sero-epidemiology studies involving IgG quantification have consistently proven effective in understanding malaria transmission, surveillance, correlation of protectiveness, and identifying potential vaccine candidates (*230, 231*).

The blood stage of malaria infection presents the parasite to the human immune system in two distinct phases: i) the infected RBC phase, wherein the virulence proteins are exposed on the surface of parasitized RBC, and ii) the merozoite phase, where the parasite is yet to invade into a new RBC. Both these forms elicit an antibody response upon recognition by the human immune system (*104, 199*). Mainly, the cytophilic IgG1 and IgG3 responses are known to be protective and correlate with higher protection against the severity of the disease (*87, 232*). Recent studies also demonstrate that IgM responses are crucial in parasite clearance and memory response (*233*).

During the iRBC phase, antibodies against PfEMP1 proteins show a reduced possibility of severe malaria by inhibiting the blood capillaries' cytoadhesion, sequestration, and rosetting. A longitudinal study in Papua New Guinea demonstrated that DBLα group-specific antibodies strongly correlated with disease outcome (*107*). Although the PfEMP1 proteins are known for

their diversity and mutually exclusive expression, a unique small subset of antibodies against as little as 5% of PfEMP1 proteins is enough to keep the infection in a non-severe state. Similarly, patients with clinical malaria having multiple rosettes show less abundance of anti-PfEMP1 antibodies, while individuals with uncomplicated malaria have relatively higher antibody titer (*105, 107, 147, 167-170*). These studies indicate the essential role played by anti-PfEMP1 IgG-specific antibodies in deciding disease outcomes in two possible ways such as 1) The blocking of PfEMP1 and endothelial receptors/ RBC proteins adhesion reduces the sequestration and hence subsequent low blood perfusion to the organs, 2) It likely keeps the iRBCs in circulation increasing the probability of iRBC destruction via immune recognition and splenic clearance. However, no evidence exists of higher anti-PfEMP1 antibodies and higher splenic clearance. In iRBC phase II, the parasite, in the form of merozoite, is directly exposed to the immune system. Several merozoite surface proteins elicit an immune response, and the generated antibodies for many of the proteins are known to be neutralizing. IgG response against MSP antigens, AMA-1, GLURP, SERA family of proteins, RH-5, RAMA, cyRPA, etc, are positive correlates of disease outcomes, with many validated as potential vaccine candidates (*87, 88, 139-145, 195, 222*). As many as 44 blood-stage antigens are considered for vaccine trials, and most of them had shown promising IgG titers in patient samples upon natural infections (clinicaltrials.gov). However, now it is well established that the breadth of an immune response against multiple of these antigens is more important than the abundance of IgG against a single protein (*89*).

Hence, we wanted to test the IgG and IgM responses to the whole chimeric antigens and their peptide counterparts.The proteins selected for making the chimeric antigens individually are known to have neutralizing IgG and IgM responses, but are not considered collectively. IgG and IgM responses in naturally occurring infections show promise that these antigens will be functional as potential vaccine candidates.

3.2 Materials & Methods

3.2.1 Sample Collection

The patient samples were collected from the region of Kolkata (Gautom laboratory), West Bengal, and Bikaner (S.P. Medical College), Rajasthan—a total of 30 severe malaria samples, 29 of non-severe malaria and 30 samples of unknown severity. As a control, 19 samples of healthy people who had no infection at the time of collection were also collected.

3.2.2 ELISA Assay

The purified chimeric antigens varB, MSP, and InvP at the concentration of 2 µg in 100 µl of 0.05 M carbonate buffer pH 9.6 (0.293 g $NaHCO_3$ and 0.159 g Na_2CO_3 in 100 ml) per well were coated onto the 96-well plate at 37°C for 1 hour. The wells were blocked using 5% Bovine Serum Albumin (BSA) made in 0.01 M PBST pH 7.4 for 1 hour at 37°C. The plasma separated from patient samples was diluted to 1:2000, and 100 µl per well was added and incubated for 1 hour at 37°C. The wells were washed five times using 0.01 M PBST pH 7.4, then probed with Goat anti-human IgG secondary antibody with HRP conjugated (Invitrogen 62-8420) for 1 hour at 37°C. The wells were washed five times and developed using TMB substrate solution (ThermoScientific N301) for 15 minutes in dark conditions. The reaction was quenched using 0.2 M H_2SO_4, and the absorbance reading was taken at 450 nm in an Ensight plate reader (Perkin Elmer). A tetanus toxoid positive control and BSA negative control at the concentration of 2 µg per well were used for every assay. Each antigen was probed in duplicate, and the entire ELISA assay for patient samples was done at least N=2 times. The OD value was normalized and plotted using GraphPad Prism 7.

3.2.3 Epitope Mapping Assay

A 16-array slide containing peptides specific to chimeric varB, varA, varC, MSP, and InvP, along with control HA and polio peptides, was designed by PEPperPRINT Gmbh, Germany. The peptide sequences for each construct with precise locations are in the Appendix 4. The handling and protocol were followed as per the manufacturer's instructions. Briefly, the slides were hydrated using the wash buffer (0.05% Tween-20 in PBS pH 7.4) for 15 mins at room temperature, followed by blocking for 30 mins using blocking buffer (Rockland blocking buffer MB-070). Only secondary antibodies were added and incubated for 45 minutes to capture the background signal noise (if any). The malaria-infected patient samples were used at dilution levels of 1:1000 and 1:2000. A total of 19 patient samples that showed higher scores in ELISA

were taken for this assay. For detection of IgG and IgM-specific antibodies, goat anti-human IgG with DyLight 650 (Invitrogen SA5-10137) and goat anti-human IgM with DyLight 550 (antibodies-online ABIN612139) secondary at a concentration of 1:100 were used, respectively. The in-house rabbit-generated antibodies against chimeric varB, MSP, and InvP were probed at a dilution of 1:500. For IgG detection, goat anti-rabbit IgG tagged with cy3 (Invitrogen A10520) at the concentration of 1:100 was used. All the primary antibodies were incubated overnight at 4 ℃ at 140 rpm shaking. The secondary antibodies were incubated for 45 minutes at room temperature at 140 rpm. The images were taken using the Agilent SureScan G2600D system. At the end of the assay, an anti-HA mouse monoclonal antibody with cy3 at the concentration 1:2000 was added to visualize the control HA peptides. Mapix software was used to analyze fluorescence intensities. The rabbit-specific anti-varB, MSP, and InvP antibodies were probed N=2 times on two separate microarray slides.

3.2.4 Epitope Mapping Assay Analysis

During the assay, images were taken three times. 1. After only secondary incubation to detect any background signal. 2. After primary and secondary incubation. 3. After adding HA-specific antibodies as technical control. For further analysis, image number 2 was uploaded to Mapix software in tiff format and aligned to the proper orientation. The grid containing the peptide location was placed on top of the peptide array, and fluorescence intensity was measured. After background normalization, the values were plotted as arbitrary fluorescence units in GraphPad Prism 7.

3.2.5 Immunoprecipitation using malaria-infected human serum

Plasmodium falciparum 3D7 parasites were harvested using the saponin lysis method at 10% parasitemia and 3% hematocrit. The infected RBCs were washed with 1X PBS buffer, treated with 0.15% saponin solution made in PBS, incubated at 37℃ for 15 minutes, and vortexed vigorously. After lysis, the solution was centrifuged at 6000 rpm for 15 minutes at 4℃. The parasite pellet was collected and further washed with PBS until clear and stored at -80℃ until use. The pellet was lysed using lysis buffer (250mM Tris-Cl pH 7.5, 1mM EDTA, 1% IGEPAL, 5% glycerol, 1X PIC, 1mM PMSF, 150mM NaCl) by freeze-thawing in liquid nitrogen three times. The lysed supernatant was separated at 12,000 rpm for 15 minutes at 4℃. The lysate was

further used for pull-down using human serum. The lysate was pre-cleared by adding Sepharose protein G beads (Invitrogen 101242) for 1 hour at 4℃. The pre-cleared lysate of 500 µg was then added to a human serum sample, either infected with malaria at the time of collection or control (10 µl per tube) and incubated overnight at 4℃ and 8 rpm. For antibody pulldown, protein G beads at a fraction of 1/20th were added and further incubated for 4 hours at 4℃ and 8 rpm. The antibody-bound beads were washed using PBS and eluted using 100 mM glycine pH 2.5.

3.2.6 Mass-spectrometry

The elute collected from immunoprecipitation was reduced using 10 mM of dithiothreitol (Sigma D9779) for 45 minutes at 60℃ and 8 rpm, alkylated using 10 mM Iodoacetamide at room temp dark condition for 15 minutes (Sigma A3221), and trypsinized using sequencing grade modified trypsin (Promega V5111) overnight at 37 ℃ and 800 rpm. The trypsinized peptides were acidified using 1% formic acid and desalted on the C-18 column. The mass-spectrometry run was done on the Sciex tripleTOF6600 system, and analysis was done on MaxQuant software. The peptides having a unique peptide count above five and absent in control conditions were considered as hits.

3.3 Result

3.3.1 The chimeric antigens show the presence of naturally circulating antibodies

The chimeric antigens constructed have the antigenic stretches stitched together to form a protein. It is essential to validate the exposure of the human immune system to these peptides and measure the extent of naturally circulating antibodies present against the chimeric antigens. To understand the human immune response towards these antigens we performed ELISA assay and quantified the IgG titer against purified chimeric antigens. Malaria-infected individuals react significantly against chimeric varB, MSP, and InvP compared to healthy controls (Figure 3.1). The mean OD of malaria-infected individual serum for chimeric varB, MSP, and InvP was observed to be 0.483, 0.559, and 0.56, respectively. We divided the serum samples based on their disease severity status into severe malaria (as defined by WHO guidelines), non-severe malaria, random malaria (where the severity status was unknown), and control group. The severe malaria samples react significantly more toward the chimeric MSP and InvP construct (Figure 3.2).

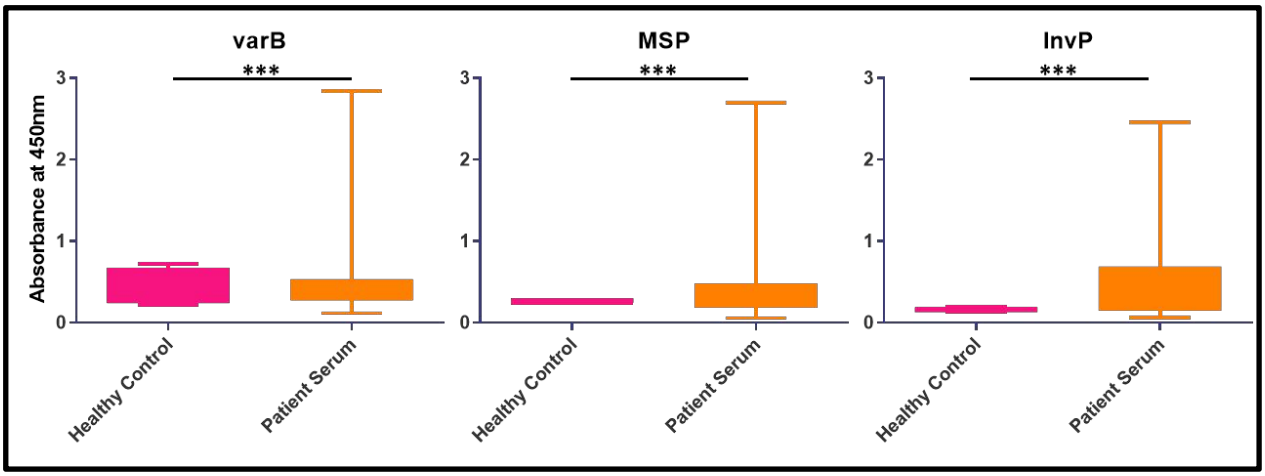


Figure 3.1. The chimeric antigens varB, MSP, and InvP show naturally circulating antibodies in malaria-exposed individuals. The plots depict OD values of IgG response against chimeric varB, MSP, and InvP in healthy individuals vs malaria patient samples.

One of the 30 severe malaria patient samples had a significantly higher response toward the chimeric varB construct. This could be owing to the diversity of PfEMP1 protein expression during infection. Since the construct has eight PfEMP1 proteins combined in antigenic stretches, the selected cohort in India may have exposure to the PfEMP1 subtype other than varB. We validated the constructed chimeric varB, MSP, and InvP antigens through ELISA and observed a significant titer of naturally circulating IgG antibodies.

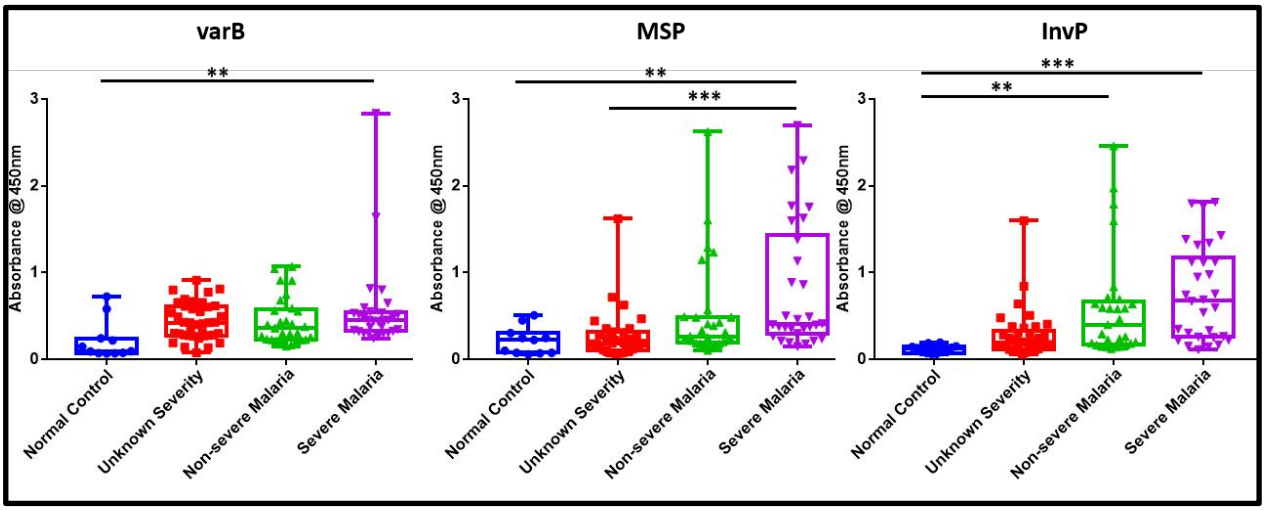


Figure 3.2. Chimeric antigens show the presence of significant IgG titers in severe forms of malaria. The plot depicts the OD of IgG responses against the chimeric varB, MSP, and InvP

antigens in healthy individuals compared with malaria-exposed individuals categorized in non-severe and severe malaria. (Unknown severity are patients diagnosed with P. falciparum infection, but the severity status was undefined)

3.3.2 Individual peptides show the heterogeneity of immune response

The ELISA assay accounts for the immune response to the entire chimeric construct but not at the peptide level. The precise contribution of each selected peptide in the immune response seen is crucial to understanding the immune response against these chimeric constructs. We performed epitope mapping peptide-microarray to achieve a peptide-level resolution of antibody responses, allowing the in-depth understanding of antibody responses against unique peptides and heterogeneity seen in the human immune response. The 16-array slide containing 20-mer peptides of chimeric varB, MSP, InvP, varA, and varC, along with HA and polio control, were probed with serum of malaria-infected individuals (Figure 3.3).

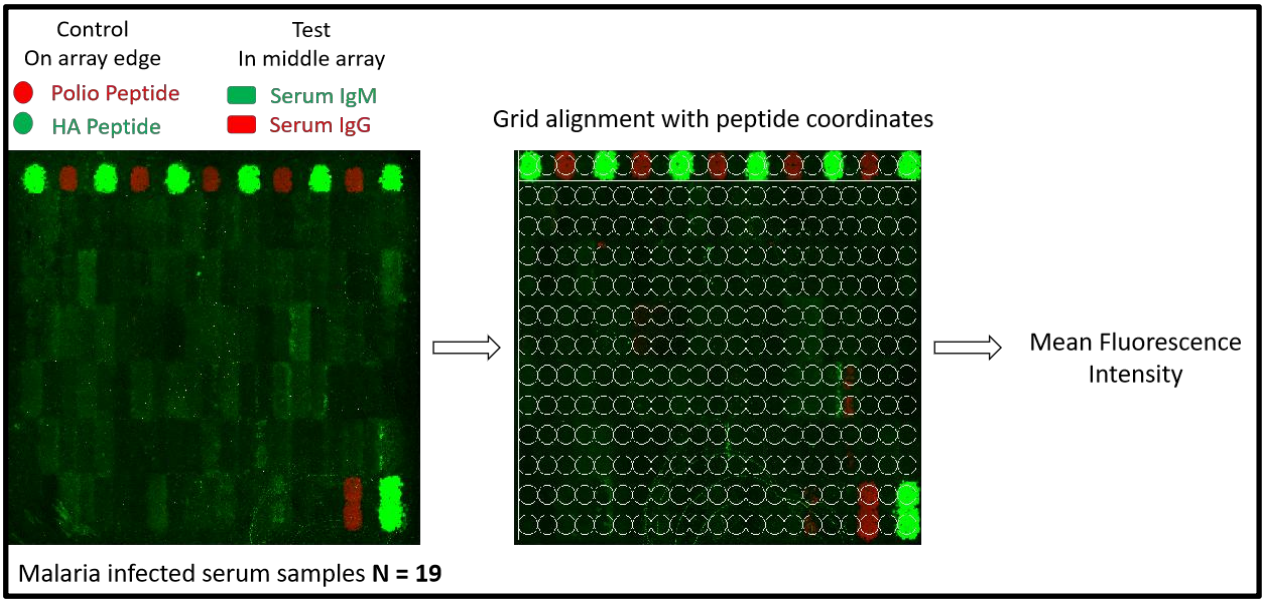


Figure 3.3. A single array image containing peptides against chimeric varB, MSP, InvP, and control varA and varC, along with HA and polio peptides. Once the image is captured, a grid containing peptide coordinates is aligned on top of the image, and fluorescence intensity is taken.

We observed the human IgG and IgM responses against the selected peptides through the assay. As expected, a wide range of reactivity was observed, positively correlated with the ELISA assay. All the peptides selected had IgG reactivity against them with maximum towards the peptide from proteins PF3D7_1300100 and PF3D7_1200100 belonging to chimeric varB (Figure 3.4). The average IgG and IgM response shows a wide range of heterogeneity, which was expected since the PfEMP1 genes are known to switch and have diverse expression in natural infection settings. Since not all PfEMP1 proteins are expressed in all individuals, a combined approach is more relevant and covers multiple virulent proteins.

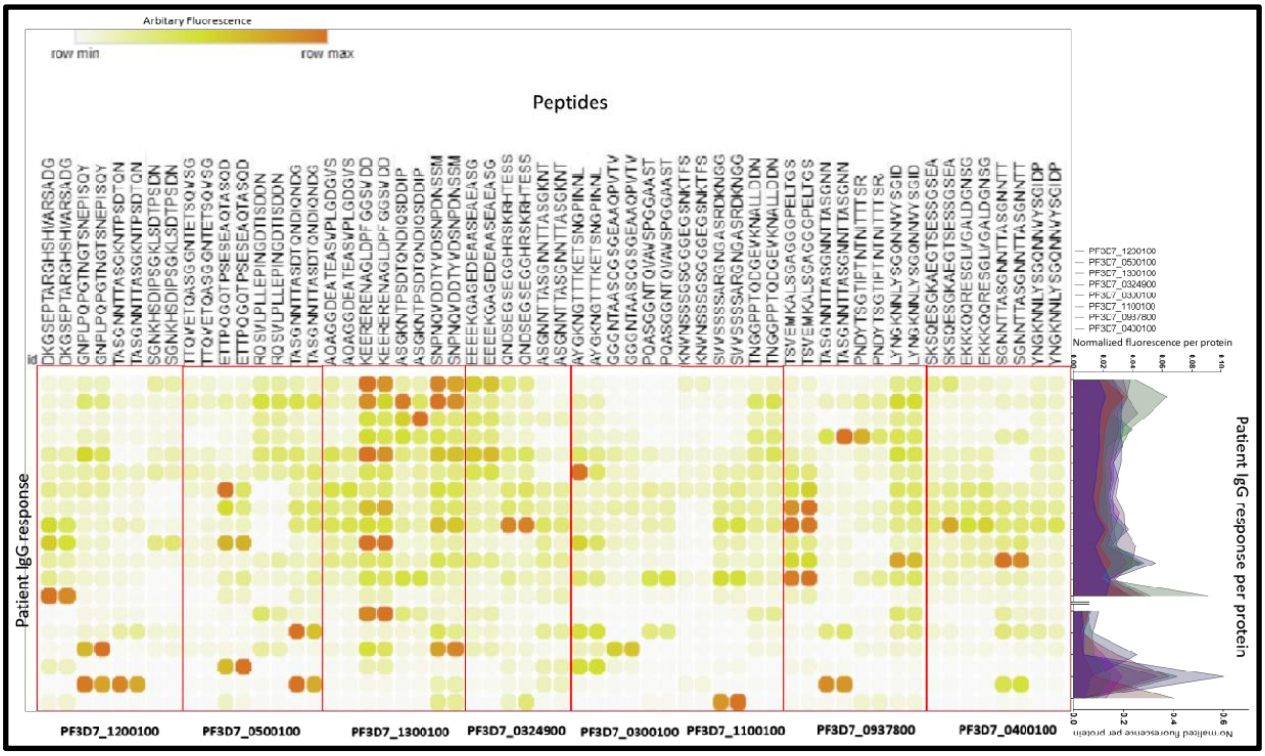


Figure 3.4. A peptide mapping microarray against chimeric varB peptides shows a heterogeneity of IgG responses in patient samples. A graph on the right shows cumulative IgG response per protein in each patient sample.

The chimeric MSP construct showed uniform reactivity across the peptides selected (Figure 3.5). Four patient samples showed reactivity against 75% of the peptides used, while a broad range of reactivity was seen against the peptides belonging to AMA-1 and MSP-3. The average IgG response per protein showed a trend where AMA-1, MSP-1, and MSP-2 showed the highest IgG

peaks in different patient samples with no overlap. While MSP-3 antibodies were present in lower titres, they were present across all 19 patient samples (Figure 3.5).

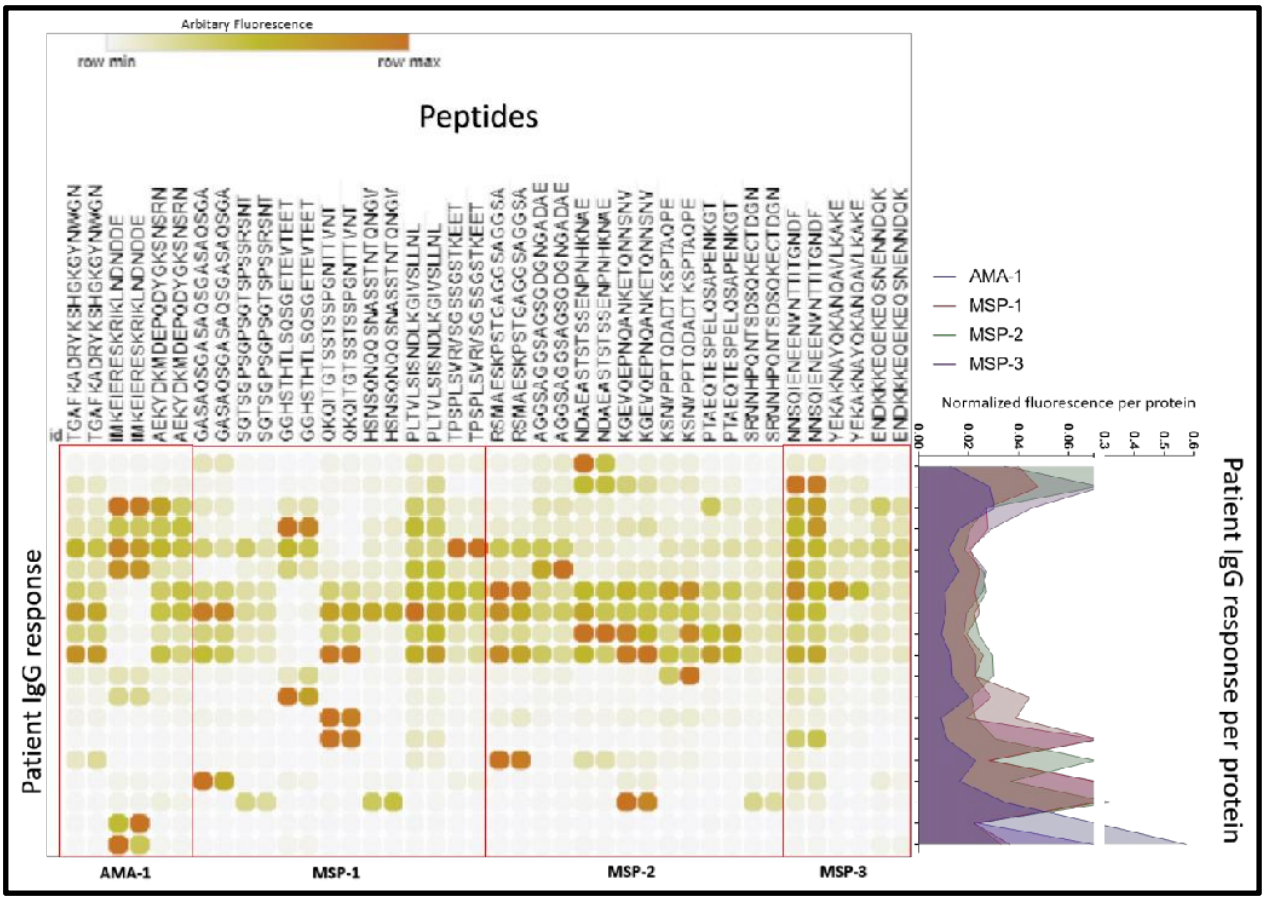


Figure 3.5. Peptide mapping microarray showing the heterogeneity of IgG response against chimeric MSP protein. A graph on the right indicates cumulative IgG responses per patient against individual proteins taken in the design of chimeric MSP.

The peptides of the chimeric InvP construct had a steady IgG reactivity across. The peptides belonging to RH-5 and SERA-5 proteins showed maximum reactivity in 8 out of 19 patients (Figure 3.6). After analyzing the average IgG per protein approach, we saw one dominating protein being recognized in the patient samples. The patient samples with the highest SERA-5 antibodies show a lower recognition by other proteins. Similarly, where the expression of EBA 175 or RH-5 was maximum, the IgG response to other proteins was lower (Figure 3.6).

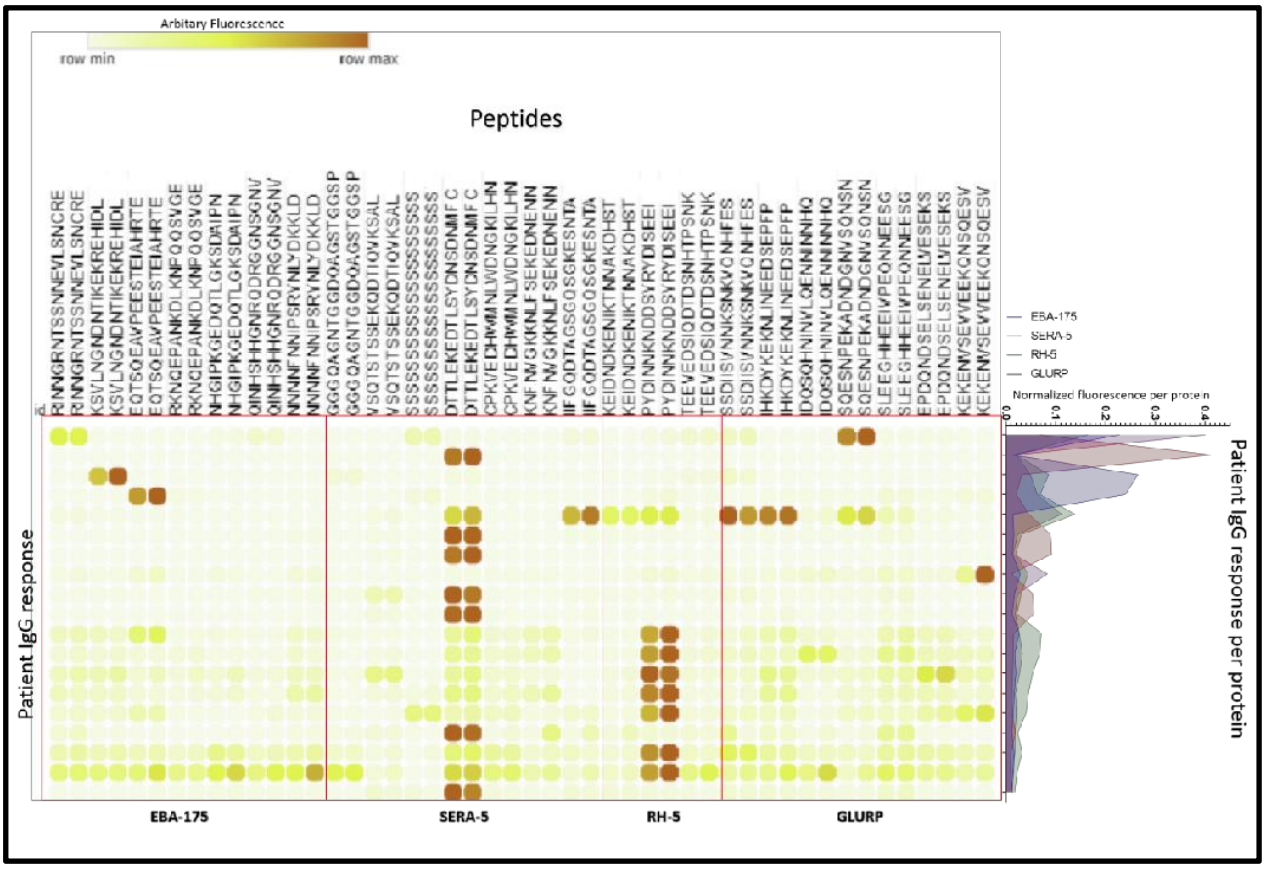


Figure 3.6. Peptide mapping microarray showing heterogeneity of IgG responses against peptides of chimeric InvP. A graph on the right indicates a cumulative IgG response per protein in individual patient samples.

We also looked for IgM responses against the antigens and observed a trend similar to that of IgG (Figure 3.7). The IgM response in chimeric varB was higher in peptides belonging to PF3D7_1300100, PF3D7_1200100, and PF3D7_0937800 (Figure 3.7 A). The heterogeneity expected in the exposure to the PfEMP1 proteins was seen across IgG and IgM response to the chimeric varB construct. Specific patient samples had antibodies against all of the peptides used in the construct, while others showed very protein-specific responses. IgM response against chimeric MSP showed higher breadth towards AMA-1 peptide followed by MSP-1. Around 10 samples out of 19 had strong IgM responses against all peptides used (Figure 3.7 B). For chimeric InvP, the IgM response was higher in peptides of RH-5, one peptide in SERA-5, and GLURP (Figure 3.7 C). All the proteins selected for the chimeric construction are known for

their polymorphic nature; hence, the immune response variation was as expected. Thus, a comprehensive analysis revealed extensive IgG and IgM responses in patient samples targeting the full spectrum of peptides incorporated into chimeric antigens and that every host produces varied levels of IgG responses against different proteins. This result clearly indicates why a single protein vaccine works only on a subset of the population and fails to elicit a protective antibody response in all individuals. To achieve a threshold of protective immune response considering multiple antigens is a necessity. This underscores the imperative to shift from singular protein candidates to multi-protein chimeric antigens when developing vaccines. This necessity arises from the intrinsic polymorphic diversity inherent in antigens, showcasing the essentiality of a broader immune response for effective vaccination strategies.

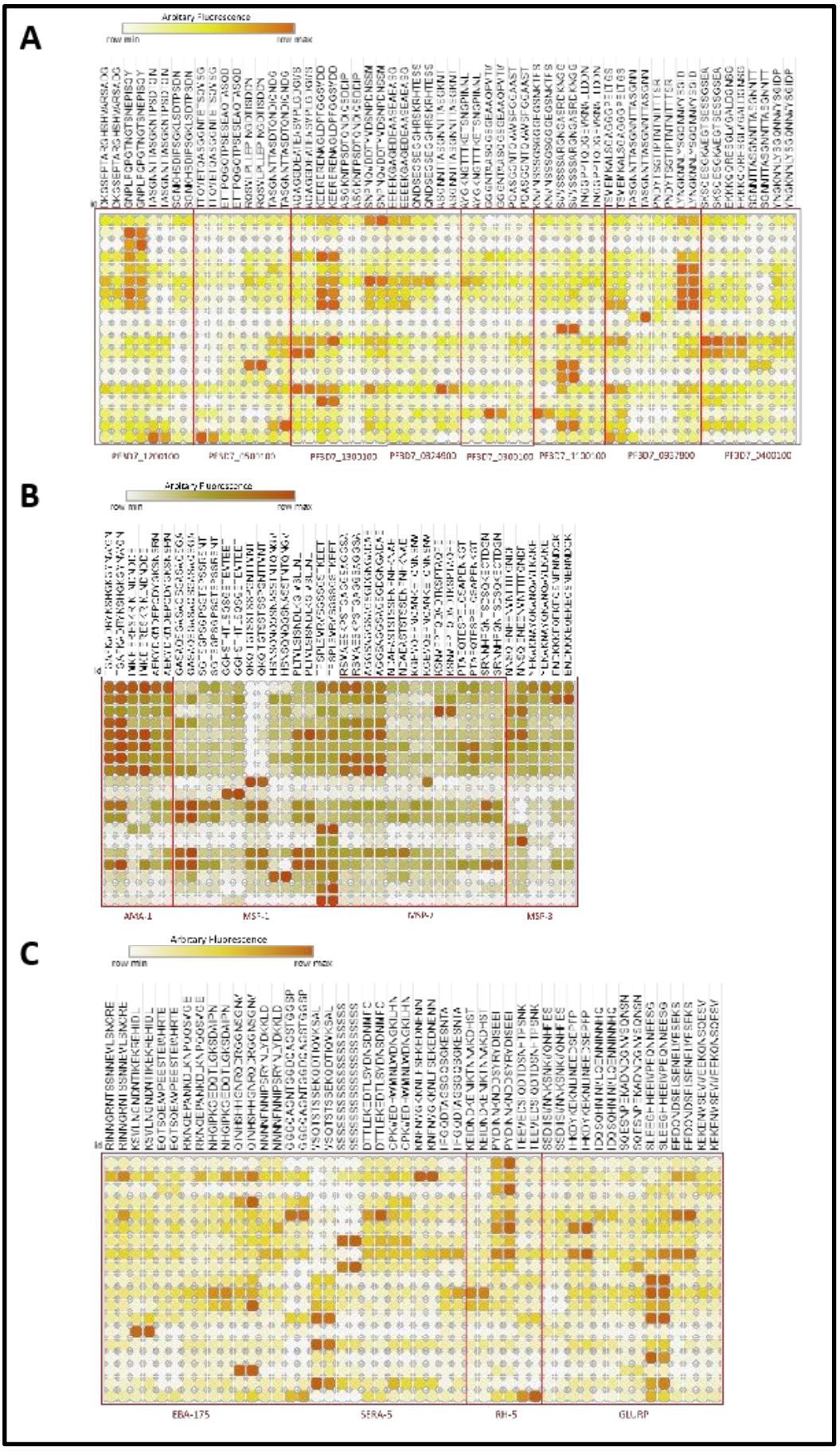

A
Arbitary Fluorescence
row min
row max
PF3D7_1200100
PF3D7_1300300
PF3D7_0824800
PF3D7_0900100
PF3D7_0937900
PF3D7_0400100
B
Arbitary Fluorescence
row min
row max
AMA-1
MSP-1
MSP-7
MSP-8
C
Arbitary Fluorescence
row min
row max
EBA-175
SERA-5
RH-5
GLURP

Figure 3.7. Peptide mapping microarray showing the heterogeneity of IgM responses against chimeric varB (A), MSP (B), and InvP (C).

3.3.3 Proteins selected for chimeric antigens are exposed to the Indian malaria-exposed cohort

We also performed Immunoprecipitation followed by mass-spectrometry of parasite lysate using serum samples of malaria-infected individuals of the Indian cohort. The selected eight proteins were also exposed in the patients during natural infection, confirming our selected chimeric antigens. The heterogeneity of var proteins expression and antibody titer was clearly seen within these candidates (Figure 3.8). A consistent immune response was observed against PF3D7_0300100, PF3D7_1133400, PF3D7_0206800, and PF3D7_1035400 across three patient samples selected. It is well known that cytophilic IgG antibodies against the proteins considered in the generation of chimeric antigens are known to be protective and correlate positively with disease survival. Hence, the IgG response against the designed antigens is also very likely to be highly protective against the infection.

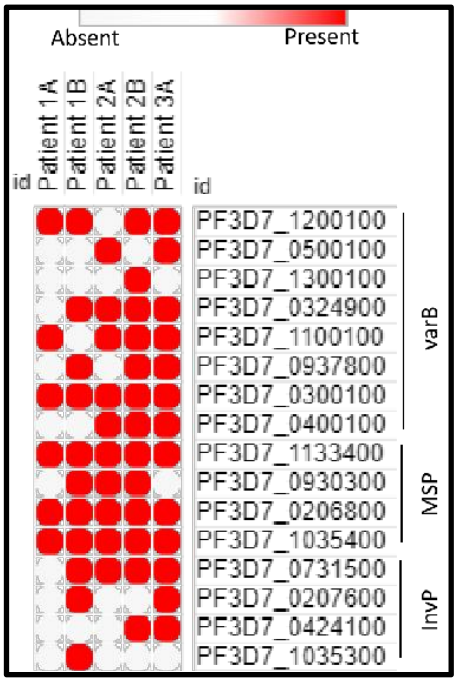


Figure 3.8. A mass-spectrometry analysis of patient serum IP shows the presence of IgG antibodies against the proteins taken for constructing chimeric varB, MSP, and InvP antigens.

The heatmap shows the presence or absence of IgG antibodies. The analysis considered a unique peptide count of 5 and above with a confidence score of 95%.

3.4 Discussion

The adaptive immune response towards the malaria antigen has been the basis of malaria detection, diagnosis, elimination, and vaccine preparations. The presence of cytophilic IgG and IgM often indicates that the antigens are immunodominant and are a point of target for immune clearance (*232, 233*). The proteins taken for designing chimeric antigens in their full-length expressed form are already known vaccine targets. The IgG responses against them are known to be functional either for neutralization or by antibody-dependent phagocytosis (*87, 88, 90, 140, 142-146, 195, 219, 222*). In our study, we see that the chimeric fusion of these proteins is well-recognized by the human immune system. The epitopes on the antigen surface show naturally circulating IgG (all subclasses) antibodies against them in patient sera. The titer of IgG antibodies was significantly higher in individuals diagnosed with severe malaria. This emphasizes that the epitopes selected are more exposed in severe malaria infection cases than non-severe, and hence, having antibodies against them can act as a severity-determining factor.

An entire chimeric antigen can have specific epitopes that are sterically unexposed. A better conclusion can be drawn when the human immune response is observed against individual peptides selected. The peptide mapping microarray showed that each selected peptide had IgG and IgM response in patient sera, confirming that the selected peptides were immunodominant. We also observed the heterogeneity in the titer of IgG and IgM against the peptides. This shows that not all proteins are exposed to the immune system with the same intensity, and parasite redundancy plays a role in determining the antibody responses. Especially in the chimeric varB construct, the DBL domain of PF3D7_1300100 had highest IgG reactivity and was present across 14 patient samples out of 19, followed by DBL domain of PF3D7_0324900 and PF3D7_0300100 having IgG response in 6 and 5 patient samples out of 19 respectively. The CIDR domain has a prominent IgG response in 3 patient samples. These domains are crucial in the process of cytoadhesion and having antibodies against them can potentially reduce the disease severity. The chimeric InvP construct showed a mutually exclusive group of patient samples that show IgG reactivity against SERA-5 and RH-5 indicating that either one antigen

was presented to the host system (Figure 3.9). While the seroreactivity to EBA-175 and GLURP was lower in most patient samples. We observed the IgM response to be more prominent than IgG in terms of abundance as well as the breadth of antibody responses. Since, the clinical data of sample collection time, stage of infection, age, and previous exposure status was unknown to us we could not conclude further regarding the difference in IgG and IgM responses. Most possibly these patient samples are early in the infection cycle (2-3 weeks) based on higher titer and breadth of IgM antibodies than IgG.

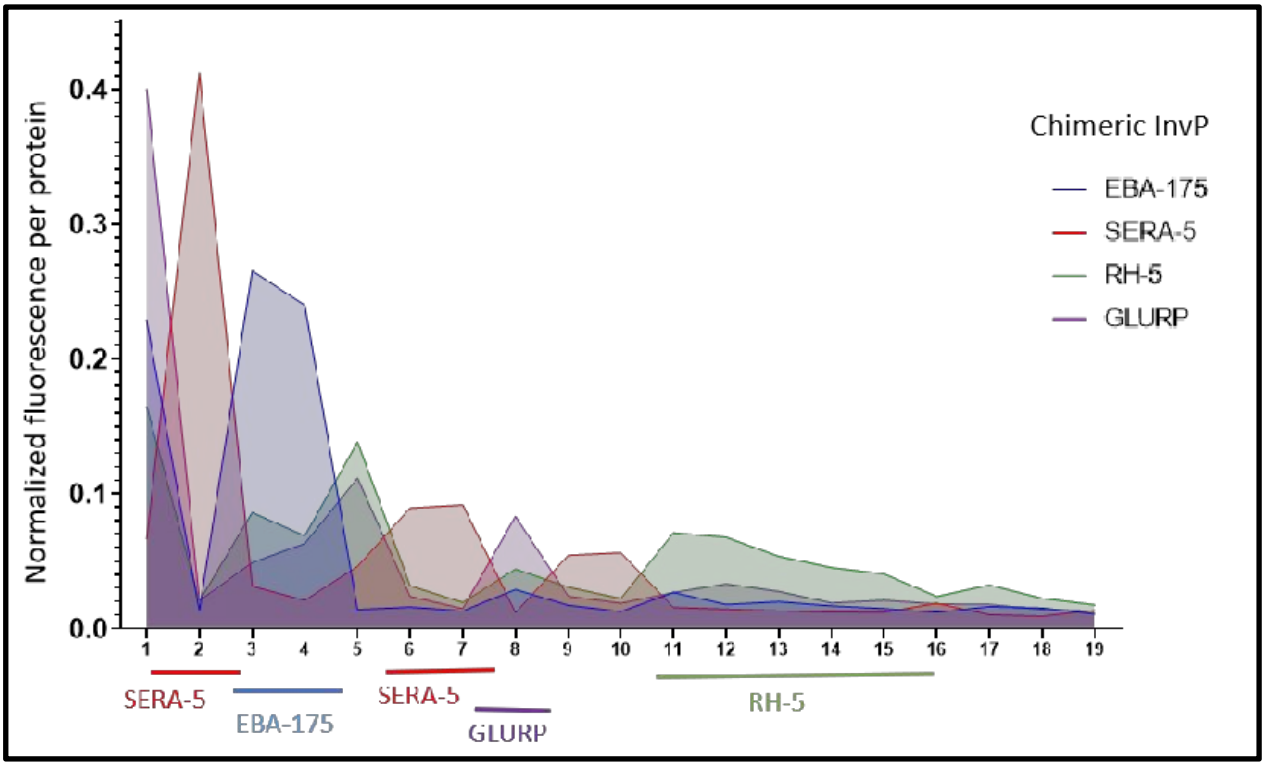


Figure 3.9. A graph showing normalized fluorescence intensity arising from each protein considered in generation of chimeric InvP across 19 patient samples. A clear mutually exclusive IgG reactivity is seen against SERA-5 and RH-5.

Our peptide mapping microarray considered only the *in silico* selected peptides of the selected antigens. The presence of antibodies against these antigens in their native form was also observed in IP-MS analysis of three patient samples. A comprehensive peptide mapping array of all immune-exposed blood stage antigens in their native conformation along with an IP-MS of higher patient cohort number can provide a better list of epitopes for future studies. Nevertheless,

the heterogeneity we observed with our selected peptides emphasizes the need for a vaccine that targets more proteins of essential pathways such as immune evasion and parasite reinvasion. Covering multiple epitopes may confer enough protectivity to keep the disease asymptomatic. Although we see the presence of IgG and IgM, it will be interesting to determine if these antibodies are functional through neutralization, antibody-dependent FCγR activation, and phagocytosis.

Chapter 4: Anti-chimeric varB antibodies can inhibit cytoadhesion

4.1 Introduction

During its erythrocytic stage, the parasite synthesizes and exports a large polymorphic antigenic protein PfEMP1. This protein expression is seen 18 hours post-invasion with abundant mRNA at the late ring stage (16-18 hpi) (*234*). Expressing these proteins renders two key phenomena to the parasite, i.e., cytoadhesion and rosetting. The cytoadhesion process allows the parasite to remain bound deep within capillaries and is absent from peripheral circulation. These late-stage deformed iRBCs hence can avoid the splenic clearance. Similarly, the rosette structure allows the iRBCs to remain sterically hindered by immune cells, delaying immune detection. This sequestration of iRBCs obstructs blood vessels and can lead to organ failure. Although the parasite is hidden well within the RBC, these PfEMP1 proteins are surface-exposed, recognized by the immune system, and cleared from circulation. A small proportion of parasites can switch the isoform of PfEMP1 protein and persist in the infection cycle—a typical lab strain of *P. falciparum* harbors around 60 var genes that act as switching repertoire (*235*). An additional complication of PfEMP1 is that they show mutually exclusive expression, which means a population of parasites majority expresses a single var gene at any given time. The synchronicity of the PfEMP1 expression and the mechanism behind switching are still being explored in the field.

The PfEMP1 isoforms have defined structural domains and are huge proteins (200-350 kDa). The var gene typically shows two exons, with one encoding the polymorphic extracellular domain and two encoding the more conserved intracellular domain. The extracellular domain contains semi-conserved N terminal sequences (NTS) followed by variable DBL, CIDR, and C2 domains. The NTS operates to transport the protein beyond the parasitophorous vacuole into the host RBC, while the DBL and CIDR domains show adhesive phenotype against the endothelial receptors. Further, the DBL domain is classified into α, β, γ, δ, ε and χ with each domain further classified into ten semi-conserved (A to J) and ten variable (1-10) blocks which impart the presumed affinity for binding. The CIDR domain is also classified into α, β, and γ. The arrangement of certain DBL and CIDR domains make up the domain cassettes (DC) that show

specificity in receptor affinity (Figure 4.1). The ATS is a relatively conserved region and is believed to function as an anchor for placing the PfEMP1 protein into the RBC cytoskeleton with the help of KAHRP proteins. The arrangement of PfEMP1 is such that NTS is always followed by DBL1α and can contain additional one to six DBL domains and one to two CIDR domains (*152, 236-238*). These domain structures in combination show affinity for CD36, ICAM-1, EPCR, VCAM-1, PECAM-1, thrombospondin, ELAM, E-selectin, and P-selectin, While CSA, hyaluronic acid and IgG are mediating molecules for placental malaria (*154*).

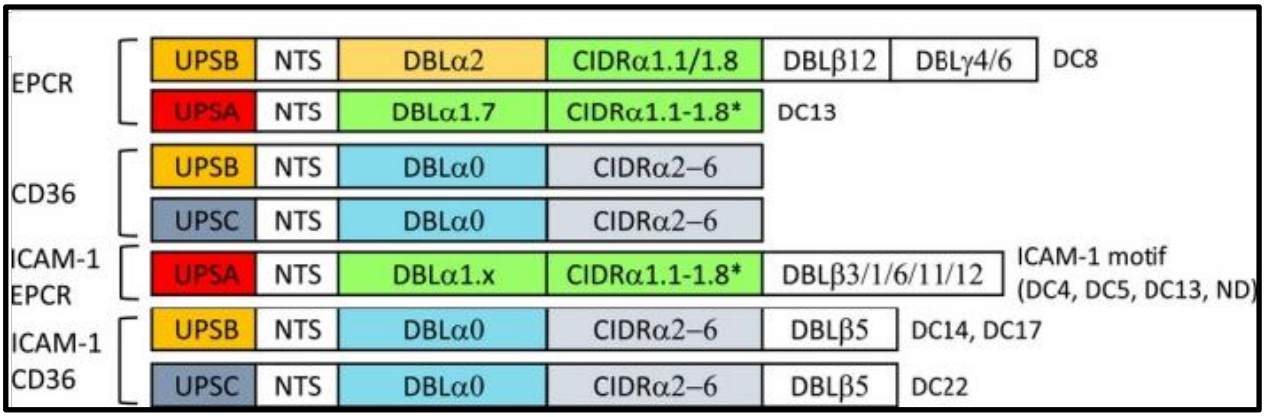


Figure 4.1. A schematic representing the PfEMP1 protein structure, domains present, and the possible receptor interaction. (Adapted from Jensen et al., Immunol Review, 2020 (104))

Out of all the endothelial recpetor ICAM-1 is a receptor of particular interest in the context of severe malaria. It is receptor belonging to the immunoglobulin superfamily and present on diverse cell types such as endothelial cells, leukocytes. It is a membrane glycoprotein of 85-110 kDa size and contains five IgG-like domains (*239*). It is known to be expressed on the endothelial cells of brain microvasculature and is known to get upregulated upon proinflammatory conditions such as the presence of TNF-α cytokine (*240*). The ICAM-1 expression was seen to be upregulated upon CM conditions and there was an evident colocalization of ICAM-1 expressing cells with sequestered iRBCs in patient autopsy samples (*241*).

It is observed that multiple exposures to malaria infection do not confer sterile immunity but instead reduce the severity of the infections, and the presence of anti-PfEMP1 antibodies is a significant contributing factor in the disease outcome. The acquisition of immunity against

PfEMP1 proteins causing severe malaria is believed to happen within a few exposures (early in life), probably because these genes are antigenically conserved. The PfEMP1 genes causing uncomplicated malaria are diverse, and acquiring immunity against these proteins takes many exposures and a higher breadth of antibodies against diverse PfEMP1s (*107, 167*).

It is shown that DBLα group 1-3 play a significant role in causing cerebral malaria through ICAM-1 and EPCR binding, and the presence of anti-DBL antibodies correlates positively with disease outcome (*170, 242*). Similarly, the CIDR domains show binding for CD36 receptors, and antibodies can inhibit this binding (*168*). Active efforts are being put into designing a vaccine for the var2csa gene that shows an affinity for chondroitin sulfate during pregnancy. Since this is a one-gene-one receptor interaction, it is easier to target as a vaccine. Variations in var2csa are still challenging, making a strain-transcending vaccine strategy difficult (*171*). Theoretically, an epitope mix vaccine covering the PfEMP1 repertoire should mimic the multi-exposure conditions. The idea is to build enough anti-PfEMP1 antibody breadth through vaccination to reduce the sequestration and, thereby, the severity of the infection. The chimeric varB antigen covers multiple DBL , CIDR , and DBL domains through the most antigenic B-cell epitopes. An immune response comprising antibodies against these peptides should be neutralizing in nature during the cytoadhesion process. To understand the blocking efficiency of chimeric varB antigen, we generated a polyclonal antibody response against the antigen in rabbits. The IgG fraction was purified and used in a cytoadherence assay. We find that the anti-chimeric varB antibodies can inhibit the ICAM-1 mediated cytoadhesion to human brain endothelial cells.

4.2 Materials & Methods

4.2.1 Generation of polyclonal antibodies

500 µg of purified chimeric varB antigen was loaded onto 10% SDS-PAGE gel and separated (this was done to separate only the antigen), and the band corresponding to varB was cut out. The gel pieces were crushed into a fine powder in a mortar and pestle by repeated freeze-thawing in liquid nitrogen. The fine powder was resuspended in 1x PBS mixed with an equivalent volume of Freund's complete adjuvant (Sigma F5881) and injected in a New Zealand white male rabbit sub-cutaneously (age ~ one year and four months, weight 3.4 kg). A pre-immune serum was collected just before the injection. A booster schedule of 3 weeks was maintained with 300 µg of protein injection with Freund's incomplete adjuvant (Sigma F5506) and bleed collection every two weeks. A total of five boosters were given, and five bleeds were collected. The antibody generation was done at National Facility for Gene Function in Health and Disease, IISER, Pune.

4.2.2 Purification of varB IgG fraction

The bleed 4 and 5 fractions were diluted in 1X PBS, passed through 0.2 µm filters, and incubated with sepharose protein G beads (Invitrogen 101242) overnight at 4℃ and 8 rpm. The supernatant was removed by centrifuging at 1200 rpm, and the beads were washed with 1x PBS thrice. The antibodies were eluted using 100 mM Glycine with pH 2.5, dialyzed against 1x PBS, and stored with 25% glycerol.

4.2.3 A) *Plasmodium falciparum* culturing

The 3D7 strain of *Plasmodium falciparum* was cultured as per the protocol given in (*243*). The culture was maintained in RPMI-1640 base media (Sigma R6504) having 0.5% AlbuMAX I (Gibco 11020021), HEPES 25mM, hypoxanthine 100 µM (Sigma H9636), Sodium bicarbonate 1.77 mM, glucose, 12,5 µg/ml of gentamicin and incubated in 37℃ humidified incubator having 5% CO_2. The parasitemia was maintained at 5% with 3% hematocrit using O+ human RBCs taken from random healthy donors (KEM hospital, Pune). The parasites were synchronized at the ring stage using 5% sorbitol and at matured schizont using percoll gradient at 63%.

B) Freezing and thawing of *P. falciparum* culture

For freezing the parasite lines, synchronized ring stage culture showing healthy growth for the last 3 cycles was pelleted down and media supernatant was removed. The pellet was mixed with equivalent volume of freezing solution (0.28% glycerol, 0.03% sorbitol, and 0.0065% NaCl) and immediately aliquoted in freezing vials. The vials were snap frozen in liquid nitrogen and stored. For thawing the parasite line the cryovial was incubated at 37℃ for one minute for a quick thaw. The pellet was transferred to a falcon and added with equivalent volume of sterile 3.5% NaCl solution drop-wise. The suspension was swirled well and incubated for exactly one minute at room temperature and immediately quenched by adding 5 ml of complete media. The suspension was centrifuged at 300 rcf for 5 minutes and the pellet was resuspended in complete media at the hematocrit of 3%. The growth was monitored everyday till ring forms were seen.

4.2.4 Endothelial cell culture

The human brain endothelial cells (HBEC-5i) were kindly gifted by Dr. Hem Chandra Jha (Indian Institute of Technology, Indore). The cells were always passaged between four and seven for cytoadhesion experiments. For cell growth and maintenance, DMEM-F12 with L-glutamine (HiMedia AL139A), 10% Fetal Bovine Serum (HiMedia RM 9955), and 0.04 mg/ml Endothelial cell growth factor (ECGS) (Sigma 02-102) were used. For sub-culturing, the cells were washed with DPBS solution trypsinized using 1X trypsin-EDTA; the confluency was kept between 70-90%, and the plates were coated with 0.1% gelatin before the seeding. The cells were incubated at 37℃ humidified incubators with 5% CO_2.

4.2.5 Western blotting

For inducing proinflammatory-like conditions, the cells were treated with 10 ng/ml of TNF-α (Invitrogen A42552) for 6-8 hours. The cells were harvested by trypsinization and lysed using a lysis buffer. For control, HEK-293T cells were used. Equal amounts of lysates were loaded and separated at 10% polyacrylamide gel and transferred to the PVDF membrane using a semi-dry transfer method using Towbin buffer. The blot was probed using anti-ICAM-1 antibody (Invitrogen PA596365),anti-CD 36 (Invitrogen PA527236), and anti-gamma tubulin (Sigma T6557).

4.2.6 Static cytoadhesion assay

The HBEC-5i cells at 70-90% confluency were washed with DPBS and later with RPMI-1640 complete media. The 3D7 parasite culture of 5% parasitemia and 3% hematocrit at trophozoite and schizont stage was added onto the HBEC-5i cells and incubated with or without anti-varB antibodies for 1 hour at 37℃ with intermittent shaking. The cells were washed with 1X PBS three times to remove unbound iRBCs. The bound cells were fixed using 1% glutaraldehyde and stained with 10% Giemsa solution for 20 minutes at room temperature. The bound iRBCs were visualized under 20X on a Leica DM750 microscope with a Flexacam C3 color camera. For analysis, 15-20 random fields were taken, and the number of HBEC-5i cells and iRBCs were counted. The data is plotted as a ratio of iRBCs to HBEC-5i cells.

4.2.7 RNA-sequencing

The iRBCs showing strong adhesion to HBEC-5i cells were removed with 1X PBS (stringent washes) and passed through cellulose-packed column filters. This separates the iRBCs from HBEC-5i cells. The enriched iRBCs were added to trizol (TAKARA RNAiso 9109), and total RNA isolation was done by adding 0.2X volume of chloroform to the trizol fraction and centrifuged at 13,000 rpm for 30 minutes at 4℃ followed by precipitation using 0.8X isopropanol for 30 minutes at room temperature. The RNA pellet was separated at 13,000 rpm and washed using 70% ethanol and eluted in 20 µl of nuclease free water. The RNA amount was tested using the Qubit fluorometer (Invitrogen). For mRNA enrichment, the NEBNext poly(A) mRNA magnetic isolation module (NEB E7490S) was used per the manufacturer's instructions. The RNA library prep was done using the NEBNext Ultra II RNA library prep kit (NEB E7775). The sequencing was done on the Illumina 550 platform with a high-output 75-cycle paired-end kit.

4.2.8 RNA sequencing data analysis

The raw files were demultiplexed using bcl2fastq. The paired-end files were subjected to quality control using FastQC. The adapter sequence was removed using TrimGalore. The sequences were aligned to the *Plasmodium* genome using HiSAT2 and converted to count files. All genes' transcript per million (TPM) were generated using StringTie. The TPM for var genes was plotted from highest to lowest using GraphPad Prism 7.

4.2.9 Rosetting assay

A) Wet Mounting

The 3D7 parasite culture was maintained at 5% parasitemia, and 3% hematocrit was supplemented with heat-inactivated A+ serum at 65℃ to facilitate the rosette formation. The Culture was incubated with or without anti-varB antibodies or heparin in a total of 500 µl of suspension at 37℃ for 1.5 hours at 8 rpm. For staining the rosettes, the suspension was added with acridine orange (HiMedia TC262) solution in equivalent volume and incubated for 20 minutes at room temperature at 8 rpm. A wet mounting was done under a coverslip, and rosettes were observed in an EVOS fluorescence microscope (at 488 excitation). Randomly, five fields per condition were taken, and a rosette was defined as a cluster of two or more RBCs surrounding a fluorescent positive RBC.

B) Flow cytometry

The protocol for counting rosettes by FACS was adopted from Chapter 37 (Malaria Immunology) (*244*). Briefly, the culture was maintained as mentioned above for rosette formation and stained with 1X DAPI and Dihydroethidium (DHE) for 1 hour at room temperature. The stained culture was split into aliquots of 500 µl and treated with or without anti-varB antibodies or heparin. The sorting was done based on area vs width, and the multiplet population was counted. The experiment was done N = 3 times and plotted as a comparison with the control condition, which had no antibody addition.

4.3 Results

4.3.1 HBEC-5i cells express the ICAM-1 receptor upon inflammatory conditions

The parasites show adhesion to host endothelial receptors using the virulence genes. Herein, we have used the model of HBEC-5i cells derived from the endothelial lining of human brain tissues. The sequestration of iRBCs in the brain microvasculature is known to cause obstruction and damage and is also the leading cause of cerebral malaria. The primary receptor for the PfEMP1 interaction during cerebral malaria is ICAM-1. Many reports suggest that fever-like conditions and inflammatory response during the malaria infection help in the process of cytoadhesion. Pro-inflammatory cytokines are known to increase specific endothelial receptors' expression and lead to vascular integrity loss. These changes further aid the parasite in adhering to the endothelial cells. One cytokine, TNF-α, is known to upregulate the expression of ICAM-1 by creating pro-inflammatory-like conditions (*105, 169, 240, 241*). To mimic these conditions, the HBEC-5i cells were primed with TNF-α, as previous reports suggest (*245*). Upon treatment, we observed the expression of the ICAM-1 receptor on the HBEC-5i cells, which was absent/not detectable without the TNF-α. We also checked for the expression of the CD36 receptor (known to be absent on HBEC-5i cells) and, as expected, could not detect the expression (Figure 4.2). We considered HEK-293T cells as a technical negative control for expression of ICAM-1 and CD36 as these receptor are known to be absent in HEK-293T cells.Therefore, the primed HBEC-5i cells can be further used for the cytoadherence assay.

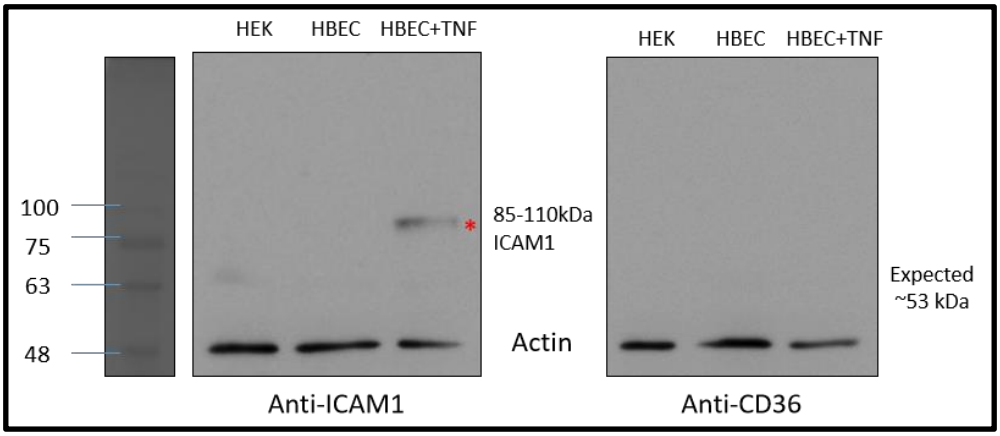


Figure 4.2. A western blotting image of HBEC-5i cells with and without TNF- treatment. Left blot (probed with anti-ICAM 1 antibodies) shows expression of ICAM-1 (85 kDa) upon

TNF- . Right blot probed with anti-CD36 shows absence of CD36 (expected size 53 kDa) in HBEC-5i cells. HEK293T cell lysate used as a negative control. Actin probing in all conditions show an equal loading.

4.3.2 Standardization of cytoadhesion assay

The primed HBEC-5i cells were co-incubated with healthy RBCs as control (at 3% hematocrit) or 3D7 parasite culture. The healthy, uninfected RBCs showed no affinity towards the HBEC-5i cells. The iRBCs were clearly seen to be adhering to the HBEC-5i cells (Figure 4.3 A). To further confirm that the bound RBC harbors a parasite within it, we stained the cells and observed them under 100X objective and could clearly observe parasites inside the RBCs displaying the cytoadhesion phenotype (Fig 4.3 B). It was evident that the 3D7 parasite line does show cytoadhesion to the primed HBEC-5i cells, and it can be further used to test the efficacy of anti-varB antibodies.

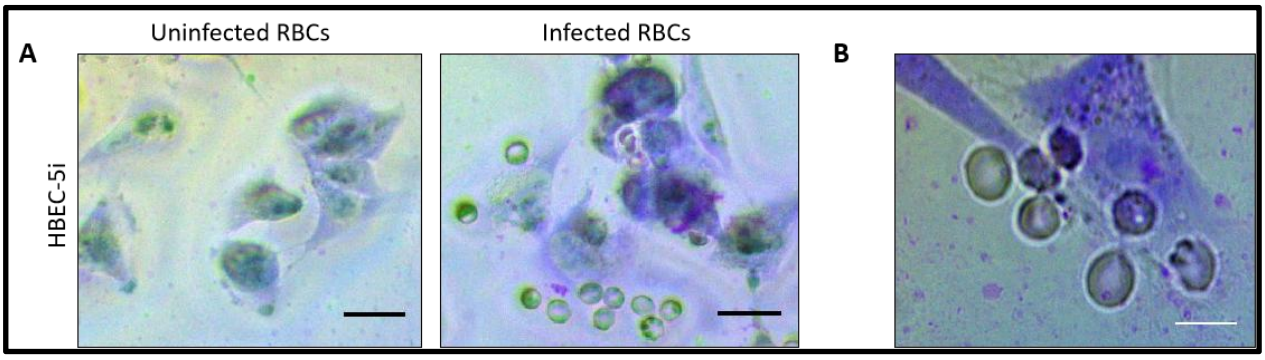


Figure 4.3. Static cytoadhesion assay done using co-incubation of primed HBEC-5i cells and iRBC culture A. Images showing the affinity of iRBCs for primed HBEC-5i cells while uRBCs do not show any affinity. B. A 1000X magnified image of cytoadhered iRBC showing harbored trophozoite. The cells were fixed and stained with 10% Giemsa and capture on Leica DM750 with Flexacam C3 color camera system. (Scale bar: 80 µm)

4.3.3 RNA sequencing shows enrichment of chimeric varB specific PfEMP1 genes

We could mimic the cytoadhesion using the primed endothelial cells, but the parasite is known to have a repertoire of 60 virulence genes that can mediate the cytoadhesion. To understand the var gene expression in the bound iRBC pool, we did RNA-sequencing of the adhered iRBCs. The bound iRBC sample showed 80.60 % mapping to the *Plasmodium* genome. Our primary interest was to observe if the genes selected in constructing chimeric varB are expressed in the bound iRBCs pool. As compared with the unbound 3D7 parasites, the adhered iRBC pool showed enrichment of varB genes. The most enriched gene was PF3D7_0420700, followed by PF3D7_0412400. Both genes belong to the subclass varC. The genes used in constructing chimeric varB appear to be enriched in the population, with PF3D7_1200100 being the third-most expressed. Pf3D7_0937800, Pf3D7_0400100, Pf3D7_0300100, and Pf3D7_0500100 were also expressed in the bound population (Figure 4.4 B). While in control, where parasites are not enriched, the most expressed genes were PF3D7_0711400, PF3D7_0412400, and PF3D7_1240600 (Figure 4.4 A). The genes selected for chimeric varB were among the least expressed in the non-enriched culture. Since the approach used is bulk RNA sequencing, the effect seen is an average of the population, and individually, a tiny subset of parasites may still express diverse var genes. With this RNA sequencing, we confirmed that our genes of interest are expressed in the adhered population, and the assay setup of cytoadhesion can be used to test the efficacy of anti-chimeric varB antibodies in inhibiting this interaction further.

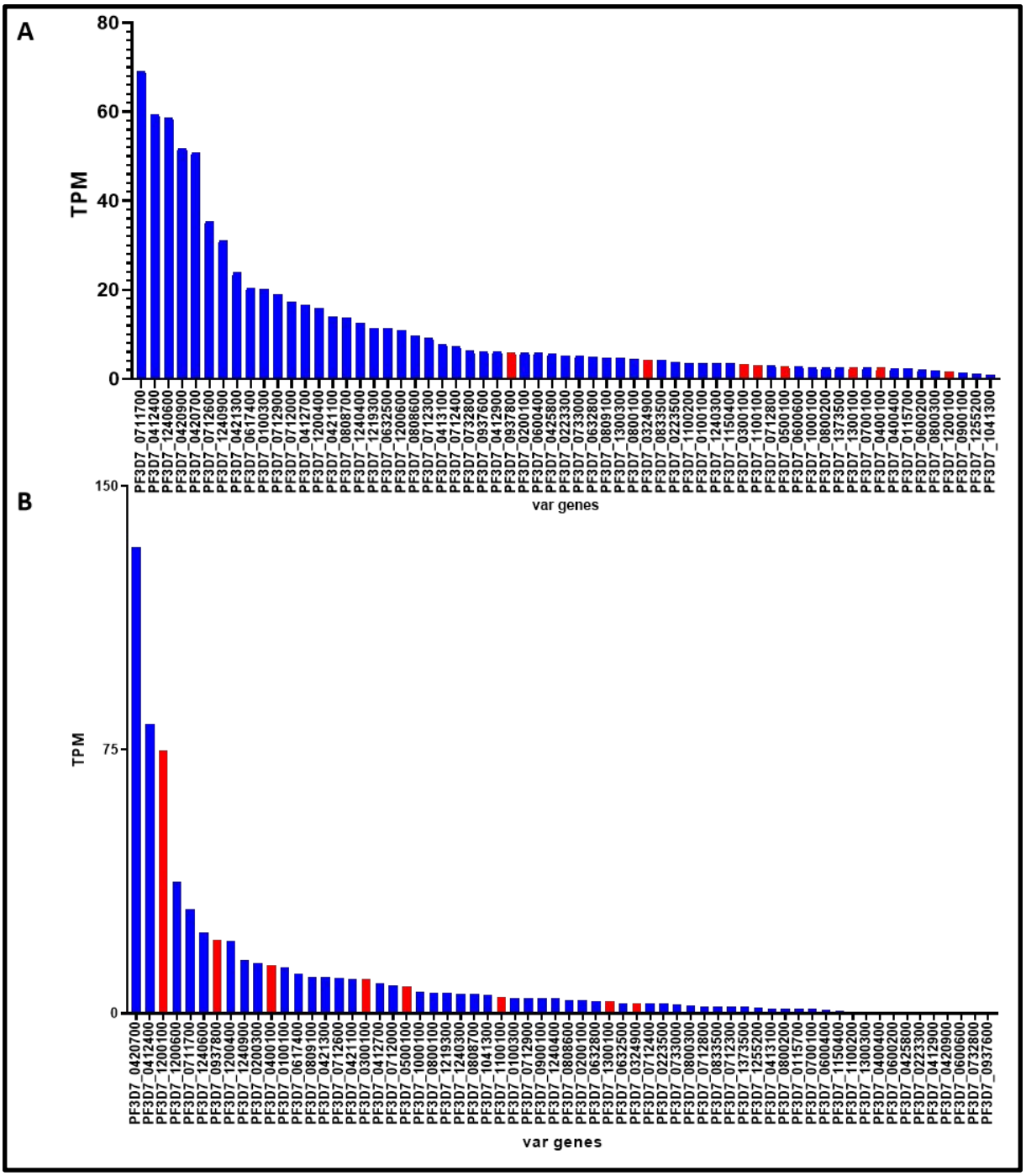


Figure 4.4. Transcript per million (TPM) of PfEMP1 genes in A. Control 3D7 line with no enrichment on HBEC-5i cells. B. 3D7 cells after enrichment for affinity against primed HBEC-5i cells. The genes considered in the generation of chimeric varB construct are highlighted in red bars.

4.3.4 Anti-varB antibodies show inhibition of cytoadhesion

To test the efficacy of the raised antibodies against the chimeric varB antigen, we co-incubated the cytoadherence assay setup with a range of anti-varB antibodies. An evident decline in the adhered parasites was seen in a range of 2.5 µg to 20 µg per 500 µl of culture (Figure 4.5). Surprisingly, the decline was not antibody-concentration-dependent as 2.5 µg and 20 µg showed more or less the same amount of inhibition. Moreover, we did not observe complete inhibition of cytoadhesion. Since the population expressed var genes other than those selected in chimeric varB, it is intuitive that baseline cytoadhesion may still exist.

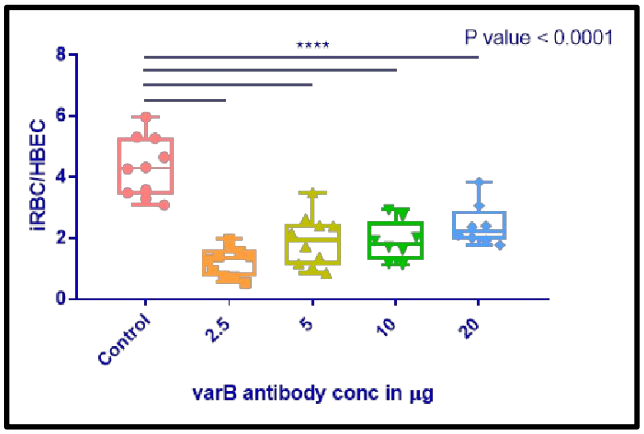


Figure 4.5. A boxplot showing the ratio of iRBCs per HBEC-5i cells across the anti-chimeric varB antibody concentrations seen in a cytoadherence inhibition assay. One-way ANOVA, Multiple comparison test P< 0.0001.

4.3.5 Anti-varB antibodies show inhibition of rosette formation

Apart from cytoadhesion, the virulence genes also show the ability to bind to uninfected RBCs. This rosetting phenomenon helps the iRBCs avoid immune detection. The PfEMP1 genes are known to form these rosette structures by interacting with the RBC receptors. The rosette structures were induced using 10% human serum addition, as mentioned in (*244*). The rosette structure of multiple uninfected RBCs surrounding the iRBC was clearly visible (Figure 4.6 A). The counting of rosettes was done using FACS sorting, where the area versus width of a rosette

cluster was considered (Figure 4.6 C). The uRBC control was set to demarcate the singlets; any deviation to the area versus width ratio was considered multiplets (Figure 4.6 B).

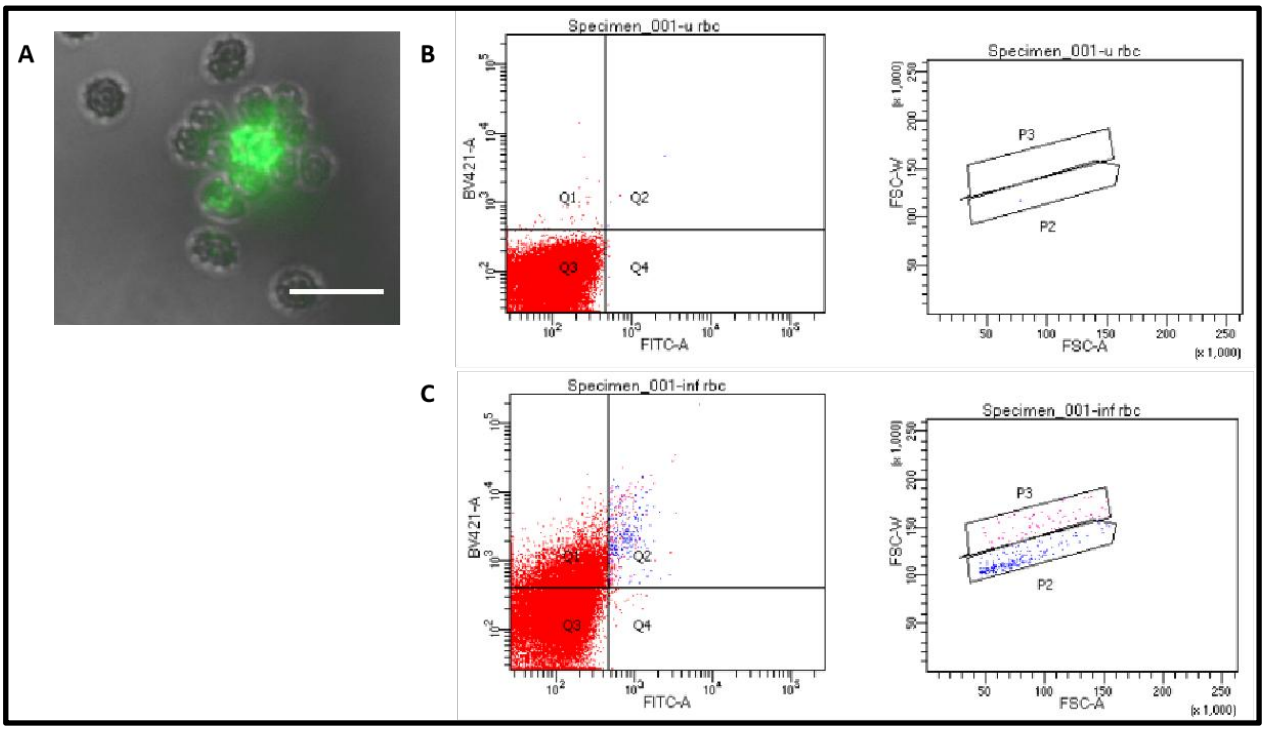


Figure 4.6. Experimental approach for identifying and quantifying the rosette structures. A. A 3D7 parasite line showing loose rosette formation in 10% human A+ serum. Central iRBC is stained using acridine orange dye. (Scale bar: 80 μ m) B. A gating was done using uRBC control. C. iRBCs positive for DAPI and DHE (Q2 quadrants) were subjected to width vs area analysis and gates based on low (singlet) and high (multiple) areas. (Method adapted from Quintana & Ch'ng, Malaria Immunology: Targeting the Surface of Infected Erythrocytes, Methods in Molecular Biology, vol. 2470, Chapter 37, 2022 (244))

An evident decline in rosette structures was seen after treating the culture suspension with anti-varB antibodies (Figure 4.7). For analysis, the rosettes formed in iRBCs without any treatment were considered 100%, and the test conditions were compared with this control. However, we did not see a complete decline dependent on antibody concentration. Since PfEMP1 proteins other than the chimeric varB family rifins and stevors are known to form rosettes, it is expected that rosette formation would not be affected entirely (*103*). Overall, we observe a decline in rosette formation when treated with anti-varB antibodies.

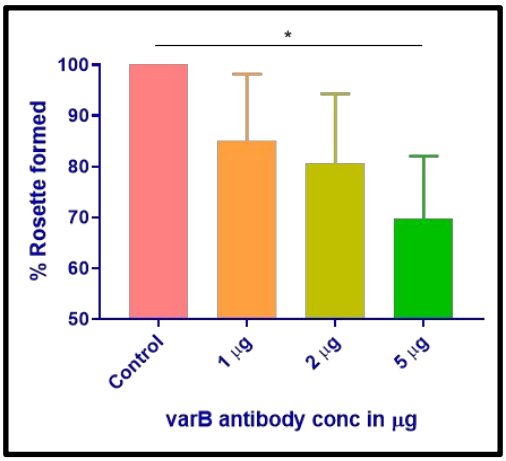


Figure 4.7. A plot showing % of rosettes formed in anti-chimeric varB antibody addition across different conditions. One-way ANOVA, Multiple comparison test P<0.05.

4.3.6 Rabbit IgG fraction is specific to chimeric varB peptides

As a further confirmation of rabbit IgG specificity for the chimeric varB antigen, we used the array designed in the peptide mapping microarray. We observed these IgG antibodies to be specific towards peptides of chimeric varB antigen (Figure 4.8). The intensities of chimeric varB specific antibodies were normalized to the intensities of only rabbit IgG control. All 29 peptides showed a presence of IgG fluorescence spot with 6 peptides showing higher intensity of immune response against them. These 6 peptides in comparison were more immunodominant and belonged to the PF3D7_1200100, PF3D7_1300100, and PF3D7_0400100 proteins.

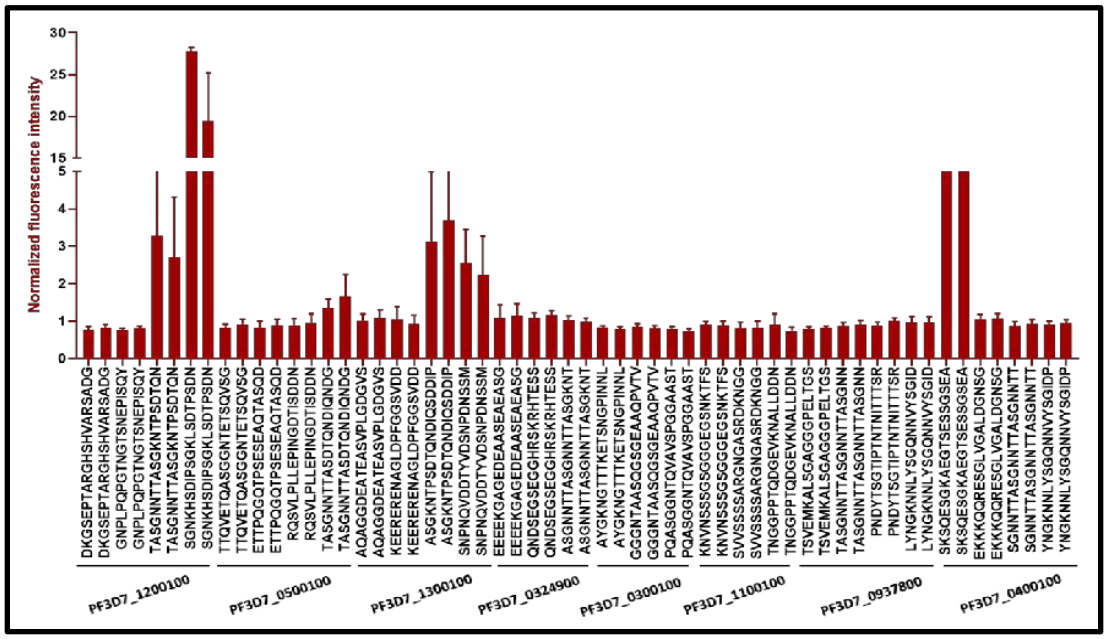


Figure 4.8. A plot showing the normalized fluorescence intensity of anti-chimeric varB antibodies (polyclonal IgG response of immunized rabbit) against the peptides used in the construction of chimeric varB antigen. All peptides are spotted in duplicate and plotted side-by-side.

4.4 Discussion

The cytoadhesion and sequestration led by the PfEMP1 proteins are majorly responsible for the severity associated with malaria. Specifically, the ICAM-1 and EPCR binding of parasite lead to sequestration in brain microvasculature and obstruction to blood flow (*103, 154*). It is well known that acquired humoral immunity to various PfEMP1 proteins correlates with reduced severity. Hence, the breadth of antibody response plays a major role in disease outcome (*107*). The varA subtype is more confidently associated with cerebral malaria and is thought to acquire immunity faster with the first few exposures (*105, 246*). Subtypes B and C appear later and manifest as uncomplicated malaria, and an antibody response is gradually built (*167*). In our construct, we have taken the functional domains belonging to varB as proof of principle. The antigenic peptides stitched originated from DBLα , CIDRα , and, majorly, DBLδ.

The 3D7 strain showed efficient binding to the primed HBEC-5i cells through the PfEMP1 genes selected to construct chimeric varB antigen. We observed that this binding was significantly reduced when the anti-chimeric varB IgG fraction was co-incubated with the cytoadhesion assay. The IgG antibodies generated in rabbits were specific to the chimeric varB antigen, confirmed using a peptide mapping array experiment (details of the method are in Chapter 3). Herein, we observed the inhibition of cytoadhesion with the ICAM-1 receptor, an interaction well known for causing sequestration in cerebral malaria cases. However, given that the peptides are taken from varB subtypes with higher affinity towards CD36, we predict these inhibitions will be enhanced CD36 receptor interactions. The antibodies could also partially inhibit the rosette formations, but the effect was not seen to be significant.

A combined approach in targeting the PfEMP1 proteins will help tackle the severity of malaria infection. The tissue-specific sequestration shown by different var proteins leads to severity in different organs. This tissue tropism is aided by differences in the endothelial receptors and var genes expressed. There are multiple significant sequestration sites, such as the brain, skin, kidneys, intestines, etc., that lead to complications during malaria (*154*). The PfEMP1 subtypes that are known to interact with these receptors also vary—a comprehensive map of the PfEMP1 subtype to endothelial receptor binding is still not elaboratively made in the field.

The major drawback with these cytoadherence assays is that the PfEMP1 to receptor affinities are tested in static conditions. A co-incubation in a culture plate fails to represent the complexities present in the human vasculature. The interactions are highly dependent on the lumen diameter, shear stress, and fluid rate, and it is essential to test the affinities and their subsequent inhibitions in the best physiological conditions possible.

Chapter 5: Anti-chimeric varB antibodies significantly inhibit cytoadhesion under physiological conditions

5.1 Introduction

The sequestration of parasites in blood vessels, blocking of microvasculature, and subsequent organ failure are the hallmarks of *falciparum* malaria (*154, 178*). The pathogenesis of sequestration caused by these PfEMP1 proteins interacting with various endothelial receptors is complex and highly dependent on host vascular biology. The PfEMP1-mediated pathogenesis is not replicable in any animal model with scalable results. Hence, designing and modeling a quantitative method of generating PfEMP1 interaction under human physiological conditions is essential. The dynamic nature of human blood circulation consists of vessel dimensions, endothelial cell receptors, microvascular niche, blood pressure, and flow rate, which are essential in determining sequestration outcomes (*181, 247-249*). Indeed, the binding affinities of PfEMP1 proteins are not uniform across different tissues. The preferential cytoadhesion or tissue tropism is exhibited based on endothelial receptors expressed, particularly the PfEMP1 protein present on the iRBC surface, and the fluid dynamics involved (*154*). A higher percentage of cytoadhesion is observed in smaller capillaries having a diameter lesser than 50μm and a fluid pressure between 4 to 40 mbar. Activating endothelial cells by pro-inflammatory cytokines also aids in the process of cytoadhesion by disrupting the vessel integrity and upregulating the endothelial receptors (*250*). Hence, static assays showing the one-dimensional affinity of endothelial cells and PfEMP1 proteins are not a suitable model for studying the effects of anti-PfEMP1 antibodies.

A better mimic of human vasculature has been demonstrated by Bernabeu et al., in which branched structures of capillaries having similar lumen diameters and perfusion rates was maintained. The cytoadhesion was indeed dependent on the flow rates of micro capillaries (*181*). Understanding the antibody-mediated blocking of this cytoadhesion would require not only the mimicking of microcapillaries but also a method to quantify the bound RBCs in real time. For this, we coupled an organ-on-chip system with a microfluidics device that can be mounted directly onto the microscope and visualize the cytoadhesion in real-time. The organ-on-chip system was lined with primed HBEC-5i endothelial cells, and the culture was perfused with

physiological parameters. The cytoadherence events were captured in a series of videos and further analyzed using machine-learning approaches. We observed slow rolling, firm adhesions, and weak interactions of iRBCs with HBEC-5i cells. We focused more on firm adhesion phenotypes for quantification as they are more likely to cause sequestration and blood clots. When tested under physiological conditions, the anti-chimeric varB antibodies inhibited the parasite sequestration by up to 90%. This quantitative microfluidic cytoadhesion assay is a newly developed tool that shows potential in detecting and quantifying cytoadhesion phenotypes in better mimicking conditions.

5.2 Materials and Methods

5.2.1 Seeding of HBEC-5i cells for generation of the capillary structure

The HBEC-5i cells in passages four to seven were grown to an 80-90% confluency. The cells were trypsinized and resuspended in 25 µl media (cell count ~ 180,000). The Be-on-Chip microfluidic chip was precoated with 0.1% gelatin for 1 hour at 37℃. The resuspended cells were seeded into the lane and allowed to adhere for 12 hours. The media was changed after adherence, and cells were supplied with fresh media added with TNF-α 10 ng/ml for 6 to 8 hours at 37℃. After 24 hours of seeding, the capillary meshwork was checked under a brightfield microscope. Once the capillary meshwork was adequately made (Figure 5.1), the capillary lane was used for the cytoadherence assay.

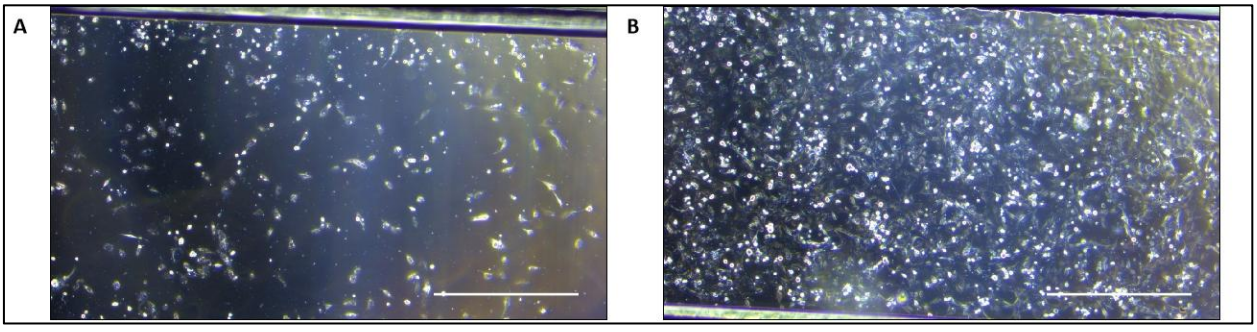


Figure 5.1. Seeding of primed HBEC-5i cells forming capillary meshwork. A. Inadequate meshwork formation due to lower seeding. B. Proper capillary meshwork formed with a

standardized number of primed HBEC-5i cell seeding. (Image capture at 4X magnification using Leica DM750 with Flexacam C3 system). (Scale Bar: 1000 µm)

5.2.2 Preparation of iRBCs for the dynamic cytoadherence assay

The infected RBC culture at the 5% matured trophozoite and schizont stage was diluted to a hematocrit of 0.75%. This hematocrit was adjusted to a lower-than-usual percentage to allow visualization of the cytoadhesion during live tracking. The anti-varB antibodies were added to the 0.75% hematocrit diluted culture at the concentration of 10 µg and 20 µg per 500 µl of culture (final 5 ng/µl and 10 ng/µl respectively) and incubated at 37℃ for 10 minutes before passing through the chip.

5.2.3 Microfluidic Setup

The entire dynamic microfluidic assay setup was set as shown in (Figure 5.2). The Fluigent pressure generator and controller were used to create and maintain the pressure of 25 mbar. The culture (control or treated) was loaded onto the reservoirs and connected with one end of a microfluidic chip. The cells were passed at 25 mbar pressure and a flow rate of approximately 236 µl/minute.

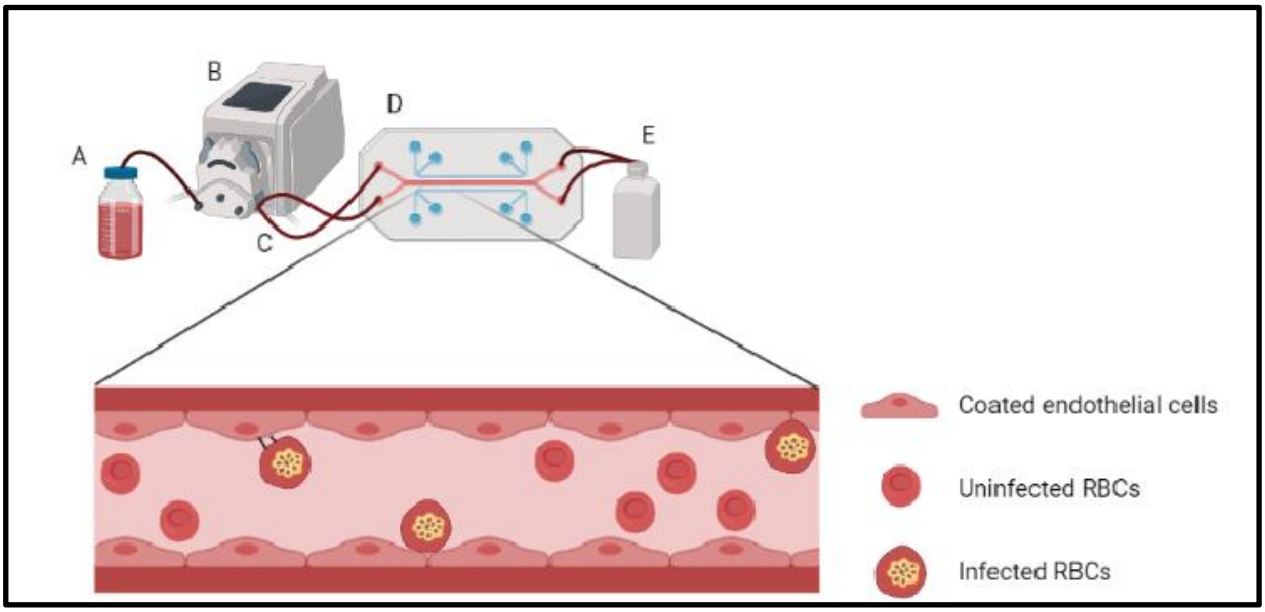


Figure 5.2. A model depicting the microfluidic setup. A. A culture suspension reservoir. B. Pressure generator and controller system. C. Tubings necessary for the flow of the culture to the chip. D. Organ-on-chip system containing the seeded meshwork of primed HBEC-5i cells. E. Culture discard container. (Illustration made using Biorender.com)

Dynamic viscosity of the culture media at 37°C = 0.8 mPa
Channel height = 372 μm
Channel width = 1.5 mm
Channel length = 45 mm
Channel volume capacity = 31 μl (max)
Resistance in the channel = 0.076 mbar.min/ μl

Tubing diameter = 500 μm
Tubing length = 1000 mm
Tubing resistance = 0.086 mbar.min/μl
Reynolds number = 4.399

The final flow rate in the capillary = 236.67 μl/min
The final shear stress = 1.095 dyn/cm2 or 0.1 pascal
While the cells were passing, a series of videos 2-3 minutes apart (Figure 5.3) were taken using a Flexacam C3 color camera mounted on a Leica DM750 microscope. Each video was 1 minute long and divided into 1800 frames (the camera speed was 30 fps, so 60 seconds X 30 frames = 1800 frames). These frames were used for further quantification of the cytoadhered RBCs.

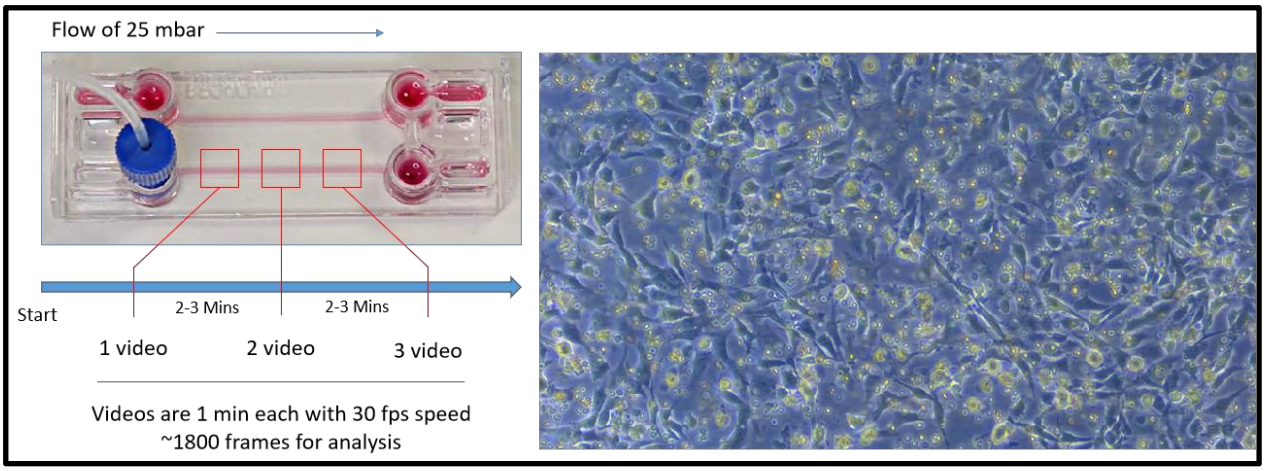


Figure 5.3. The figure shows a paradigm selected for video capture and analysis, along with the representative image of a frame showing capillary meshwork with iRBC suspension being passed. Please refer to addendum video 1 for visualizing the cytoadhesion. (Magnification using 10X lens on Leica DM750 with Flexacam C3 system)

5.2.4 Quantification of the adhered RBCs

We generated an in-house detection and quantification pipeline to identify the adhered RBCs (done by Dhruv Khatri, Prof. Chaitanya Athale Lab, IISER Pune). The videos were broken down into a series of 1800 frames. Since the RBCs in the microfluidic series of experiments show high contrast in the center, as previously described by (*251*), a Laplacian of Gaussian (LoG) filter was applied to enhance the local contrast. Furthermore, image binarization and centroid detection were done to identify the RBC coordinates. If the RBC coordinates remain the same across five consecutive frames, it is considered a stationary RBC. Further, to remove the background noise of RBC vs non-RBC objects, a CNN (Convolution Classification Network) was utilized to select the "in-focus RBCs" and discard the rest of the noise. This CNN network was manually trained by feeding 1000 images of in-focus RBCs and 1000 images of spurious background detections with a probability threshold of 0.93. With this classifier training, we achieved a confidence score of 95.57% in validation data. This pipeline was used on control and test conditions to detect and quantify the adhered RBCs in control vs test conditions.

5.3 Results

5.3.1 Standardization of dynamic microfluidic cytoadherence assay

To observe the efficiency of cytoadhesion, we first passed iRBC and uninfected RBC suspension at the hematocrit of 0.75%. The culture was loaded onto the reservoir and passed through the microfluidic chip. As expected, uninfected RBCs do not interact with the endothelial cell lining, and most RBCs simply pass along with the flow of the capillary. The iRBC suspension, when passed through the capillary, showed three types of interactions– 1) a tight adherence with the endothelial cells marked by complete stationary fixing of the iRBC, 2) a loose interaction wherein the iRBC was seen slowly rolling on the endothelial cell, 3) a momentary contact with the endothelial cell where iRBCs contact for a few seconds and detach (Addendum video 1). These are the different cytoadherence phenotypes previously mentioned and known to bind through solid and weak affinities of PfEMP1 proteins. Out of the three interactions, we were interested in quantifying the tight adhesion where iRBCs remained stationary for longer.

5.3.2 Detection of adhered iRBCs

The dynamic cytoadherence experiment was recorded as a 1-minute video series from subsequent time points after passing the iRBC suspension. These videos were further broken down into 1800 frames, and the movement of each RBC across the frames was tracked. Firstly, the images were fed to LoG filters to detect a local contrast in the image. Then, a CNN classifier was trained with images of in-focus RBCs vs non-RBC backgrounds. A confidence score of 95.57% was achieved in validation data in detecting the RBCs (Figure 5.4). The stationary RBCs present per five consecutive frames were plotted across the time series.

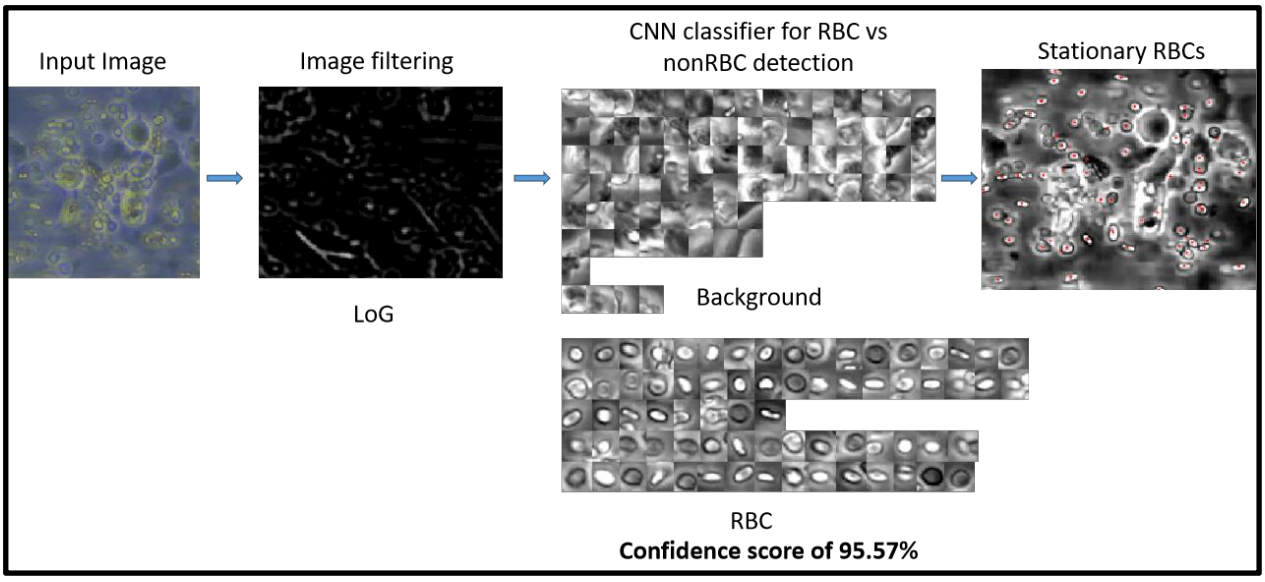


Figure 5.4. The workflow used for detection of adhered RBCs. (The analysis was done by Dhruv Khatri and Prof. Chaitanya Athale, IISER, Pune, India.)

5.3.3 Anti-varB antibodies inhibit the cytoadhesion significantly in dynamic conditions

In the iRBC suspension, a significant reduction in adhered RBCs was observed when pre-incubated with anti-varB antibodies at the final concentration of 0.02 mg/ml and 0.04 mg/ml. Visually, the control condition showed a cluster of adhered RBCs that did not move across the time and remained adhered for a long time. These firm-adhered RBCs were measured using the protocol mentioned above. We also observed loose binding/rolling RBCs on the endothelial cells that were not quantified. As for the anti-varB treated iRBC suspension, we observed that most RBCs passed by with the speed of the flow and did not show any interaction with the endothelial cells. An apparent decrease in the cytoadhesion was seen upon quantifying the RBC adherence.

During a series of three videos (each video 2-3 minutes apart), an increase in the number of cytoadhered RBCs was seen in the control condition. This was as expected since more cultures would be passed through the capillary, increasing the load of the iRBCs over the endothelial cells. As for the anti-varB pre-incubated culture, we did not see an increase in cytoadherence RBCs. This suggests that the inhibition is constant even when more culture is passed through the capillary (Figure 5.5). Our experiment consisted of tracking the iRBCs for 9 to 10 minutes, with

results showing consistency across time. With this assay, we further affirm that anti-varB antibodies, when pre-incubated at concentrations of 0.02 mg/ml and 0.04 mg/ml, can efficiently inhibit the binding of iRBCs to the primed endothelial cells under physiological conditions.

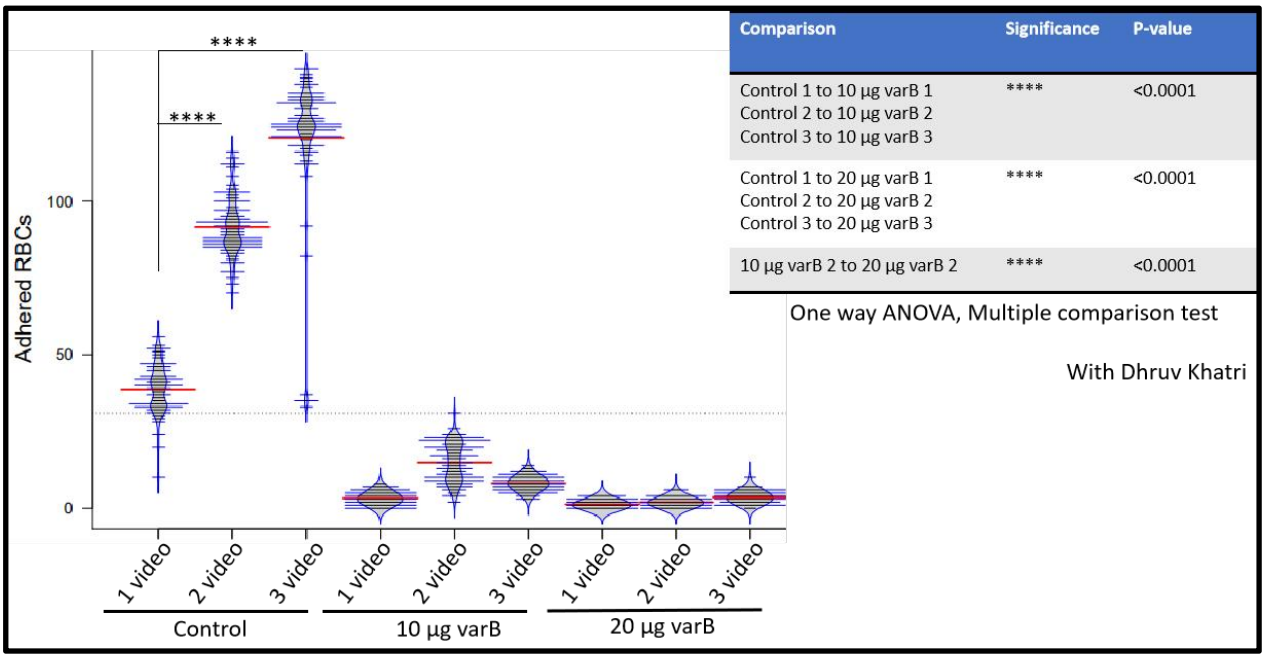


Figure 5.5. A graph showing the number of adhered RBCs present per frame across the time series of the dynamic microfluidic assay. A significant reduction in adhered RBCs can be seen when anti-chimeric varB antibodies are added. A table at the right corner shows the statistical significance of each condition. One-way ANOVA, Multiple comparison test applied with P value < 0.0001. (Analysis was done on the adhered RBC dataset with Dhruv Khatri and Prof. Chaitanya Athale, IISER, Pune, India.)

5.4 Discussion

The cytoadhesion and sequestration process is highly dependent on human vasculature parameters, and canonical static assays fail to consider the dynamic nature of these cell-cell interactions (*247, 249, 250*). A system mimicking the physiological conditions is necessary to understand the efficacy of anti-PfEMP1 response fully. A few studies have demonstrated using a 3D microenvironment of the blood-brain barrier that shows affinities to be flow-dependent (*181*). These tools are very crucial in understanding the cytoadhesion process. Many recent studies use

matrices made of collagen and other stiffness-inducing materials to understand the receptor interactions (*252*). Our developed tool mimics a capillary's pressure, shear stress, flow rate, and real-time quantification of adhered RBCs. This tool can be essential to visualize and quantify the cytoadhesion properties of PfEMP1 proteins against multiple receptors and cells.

The antibodies against the chimeric varB construct showed decreased cytoadhesion during static assays. However, this inhibition was not seen to be concentration-dependent. The dynamic cytoadhesion assay shows a more prominent inhibition due to the inclusion of physiological parameters. The construct contains the peptide stretches against DBL , CIDR , and the majority of DBL domains. All these domains are known to be essential for receptor binding. Our assay shows the effect on ICAM-1 expressing cells. However, given that the peptides were taken from the group B-specific PfEMP1 genes, a better affinity and inhibition can be seen with the CD36 receptor. Also, it will be interesting to see the inhibition potential of these antibodies against other endothelial receptors using the microfluidic assay.

Chapter 6: Anti-chimeric MSP and InvP antibodies show growth inhibition of *P. falciparum*

6.1 Introduction

The clinical manifestation of the disease begins in the blood stage of the parasite life cycle, wherein parasites multiply rapidly in the host erythrocyte. The exponential growth of parasitemia is maintained through continual cycles of parasite reinvasion. This invasion process is crucial in parasite survival and has evolved into an elaborate process. This sophisticated and multistep process is entirely driven by parasite-derived proteins that orchestrate efficient binding, reorientation, and invasion. Multiple parasite ligands are known to be expressed and bind different receptors on the host erythrocyte through sialic acid-dependent and independent pathways. The merozoite surface proteins and ligands associated with the invasion process show redundancy and polymorphism. The diversity of these proteins and multiple ligands performing a similar binding pattern allow for a successful invasion in a short time (*199*).

The phylum Apicomplexa means the presence of specialized compartments that help in the invasion process. The *Plasmodium* species have micronemes, rhoptry organelles, and dense granules that are present towards the apical tip and serve the function of attachment and entry into the host RBCs (*57*). The merozoites have a coat of merozoite surface proteins (MSP family) that help in the initial attachment to the RBCs by interacting with heparin, band 3, and glycophorin moieties. After this initial attachment, the merozoites get reoriented so that the apical tip faces the RBC surface (*199*). At the beginning of the invasion process, micronemes release the erythrocyte binding ligands (EBL family proteins) that comprise EBA-175 (binds to glycophorin A), EBA-140 (binds to glycophorin C), EBA-181 (binds to W, and Band 4.1), and EBL-1 (binds to glycophorin B) (*189*). The glycophorin receptors on the RBC surface are sialylated, and cleavage of sialic acid moieties using neuraminidase treatment drastically inhibits the function of EBL family proteins, leading to a nine-fold decrease in invasion efficiency. The EBL family mainly carries this sialic acid-dependent invasion, making it an attractive vaccine target (*253*).

The rhoptry organelles release Reticulocyte Homologue (RH family) proteins such as RH-1 (binds to a putative Y receptor), RH2a, RH2b (binds to Z receptor), RH-3 (pseudogene with a missense mutation), RH-4 (binds to CR1 receptor), and RH-5 (binds to a basigin receptor in a complex comprising of P113, RiPR, and CyRPA). These proteins show invasion through the sialic acid-independent pathway. The EBL and RH family proteins carry out the invasion process in synergy (*189*). Currently, RH-5 is the leading vaccine candidate for the blood stage of infection, showing promising results in the clinical trial phase (*140, 141*).

The invasion bridge made for entering the RBC is entirely parasite-driven. The AMA-1 proteins, along with the RON complex, form the irreversible bridge of invasion. Several studies show that targeting AMA-1, either full-length or in domain forms, inhibits parasite invasion. The FMP2.1/ ASO2a recombinant AMA-1 vaccine candidate shows partial, strain-specific efficacy (*139, 218*). All these candidates, AMA-1, MSP-1, MSP-2, EBA-175, RH-5, SERA family, and GLURP, have been individually considered as potential vaccine candidates (*88, 139, 142, 143, 145, 219, 222*). Previous vaccine formulations have not succeeded due to the complexity, redundancy, and polymorphism present in these proteins. The sialic acid-dependent and independent pathways also further increase the probability of the parasite invasion.

Considering these complications, a multi-protein antigen is also necessary for targeting the blood stage of *Plasmodium*. We generated chimeric MSP antigen comprising antigenic peptides from AMA-1, MSP-1, MSP-2, and MSP-3, targeting the initial attachment and bridge formation in the merozoite invasion process. The second chimera, InvP construct, has dominant antigenic peptides from EBA-175, SERA-5, GLURP, and RH-5, targeting both sialic acid-dependent and independent pathways—these two chimeras in combination cover most of the invasion process of *Plasmodium falciparum*. The design and construction of these chimeric antigens are discussed in Chapter No. 2 in detail.

Our primary interest is specific to two chimeric antigens, i.e., chimeric MSP and chimeric InvP, to observe the efficacy of the anti-MSP and anti-InvP antibodies in inhibiting parasite growth. Given that they have a broad range of action during invasion, we expected the efficiency to be

higher in combination with antigens. We observed that, indeed, when antigenic stretches of multiple proteins are combined, the growth inhibitory efficiency is significantly higher.

6.2 Materials & Methods

6.2.1 Generation of polyclonal antibodies against chimeric MSP and InvP antigens

The purified chimeric MSP antigen was loaded onto 10% SDS-PAGE and separated. The corresponding band was cut and crushed using liquid nitrogen. A 500 µg antigen mixed with an equivalent volume of Freund's complete adjuvant was injected into a New Zealand white male rabbit (age = 8 months, Weight = 6.485 kg). For the chimeric InvP antigen, a purified soluble protein of 500 µg was mixed with an equivalent volume of Freund's complete adjuvant and injected subcutaneously in male rabbit (age = 6 months, weight = 4.36 kg). The rest of the antibody generation protocol is mentioned in the generation of chimeric varB antibodies.

6.2.2 Purification of anti-MSP and anti-InvP antibodies

We purified antigen-specific antibodies for anti-MSP and anti-InvP serum bleeds 3,4 and 5. For generating antigen-specific columns, we used sulfolink coupling resins (Thermo Scientific 20401) for the irreversible binding of chimeric MSP and InvP antigens. Briefly, the antigens were reduced using TCEP and allowed to bind to sulfolink coupling resins to form a covalent thioether bond between the cysteine molecule and the resins. The coupled resin columns were washed and allowed to attach with diluted serum overnight at 4°C and 8 rpm. The column was washed using 10 mM Tris-Cl pH 7.4 and eluted using 100 mM Glycine pH 2.5. The elutes were pooled and dialyzed against 1X PBS and stored in 25% glycerol.

6.2.3 Peptide blocking assay

As a part of validating, the anti-MSP and anti-InvP antibodies were tested using peptide blocking assay. A late-stage schizont lysate was equally loaded and separated using 10% SDS-PAGE, transferred using semi-dry transfer on a PVDF membrane. The blot was cut into two parts. One part was probed with 1:500 dilution of purified antibodies (either chimeric MSP or chimeric InvP), and the other was probed with antibody dilution + 5 μg of purified antigen (either chimeric MSP or InvP) overnight at 4°C. Blots were washed using 1XTBST solution, and anti-rabbit HRP-conjugated secondary (Bio-Rad 1706515) was added at a dilution of 1:4000 for one hour at room temperature. The blots were developed using Clarity Max ECL western blotting substrate (Bio-Rad 1705062) on ImageQuant LAS 4000 system (GE Healthcare).

6.2.4 Immunofluorescence assay

Late-stage 3D7 parasites were washed and re-suspended in 1X PBS and fixed using 4% paraformaldehyde with 0.0075% glutaraldehyde at 37℃ for 20 minutes. Permeabalization was done using 0.1% TritonX-100 solution for 10 minutes at room temperature. Freshly prepared 3% Bovine serum albumin (in 1X PBS) was used for blocking for 1 hour at room temperature. Primary antibodies (purified chimeric antibodies) at concentration 1:500 were added to the suspension, incubated overnight at 4°C/ 8 rpm, and washed using 1X PBS five times. Anti-rabbit Alexa Fluor 488 (Invitrogen A32731) secondary antibodies were added at the dilution 1:500 for 1 hour at room temperature. Imaging was done on the Zeiss Multiphoton microscope.

6.2.5 Growth Inhibition Assay

Parasites at 1% parasitemia (synchronized ring stage) maintained at 3% hematocrit were seeded onto a 96-well plate with an indicated range of purified anti-chimeric MSP and anti-chimeric InvP antibodies (either alone or in addition). This was done over two cycles of invasion (media change with the addition of antibodies). At the end of the second invasion, the plate was processed for lysis (100 mM Tris-Cl pH 7.5, 25 mM EDTA, 0.05% Saponin, 0.5% TritonX-100, and 1X sybr green dye) for 40 minutes in room temperature/dark conditions. The fluorescence readings were taken at 497 nm excitation and 520 nm emissions. Fluorescence intensity was normalized to the readings of uninfected RBCs and plotted using GraphPad Prism 8. The GIA

was done using active and inactive bleeds (data not shown) and purified antibodies in total N=9 times.

6.3 Results

6.3.1 Rabbit-generated antibodies recognize the parasite antigens

Similar to chimeric varB, we wanted to assess the neutralizing abilities of anti-chimeric MSP and InvP antigens. These two constructs contain the peptides of eight proteins that have a crucial role in merozoite's initial attachment to the new RBC, its reorientation to align the apical side, and finally, form a bridge for the invasion process. We generated polyclonal antibodies against these constructs in rabbits and further used them to assess their ability to block merozoites. The bleeds were purified using immobilized antigens as affinity columns and further validated using peptide blocking assay and immunofluorescence. Using purified antibodies, we observed multiple bands for chimeric MSP-specific antibodies precisely, three bands between size 135 to 180 (corresponding to MSP-1), a band near 68 kDa (AMA-1), and near 48 kDa. For chimeric InvP-specific antibodies, a strong band was observed near 135 kDa (GLURP), 100 kDa (SERA-5), and multiple bands between 63 and 75 kDa. However, all the bands observed were specific to antigens as they were efficiently blocked by adding native antigens during probing (Figure 6.1). Since both the constructs target the merozoite surface, we performed an immunofluorescence assay at the mature schizont stage. We observed the signal on the surface of developing merozoites for both antibodies (Figure 6.1). We used these antibodies to assess their growth inhibitory potential alone and in combination.

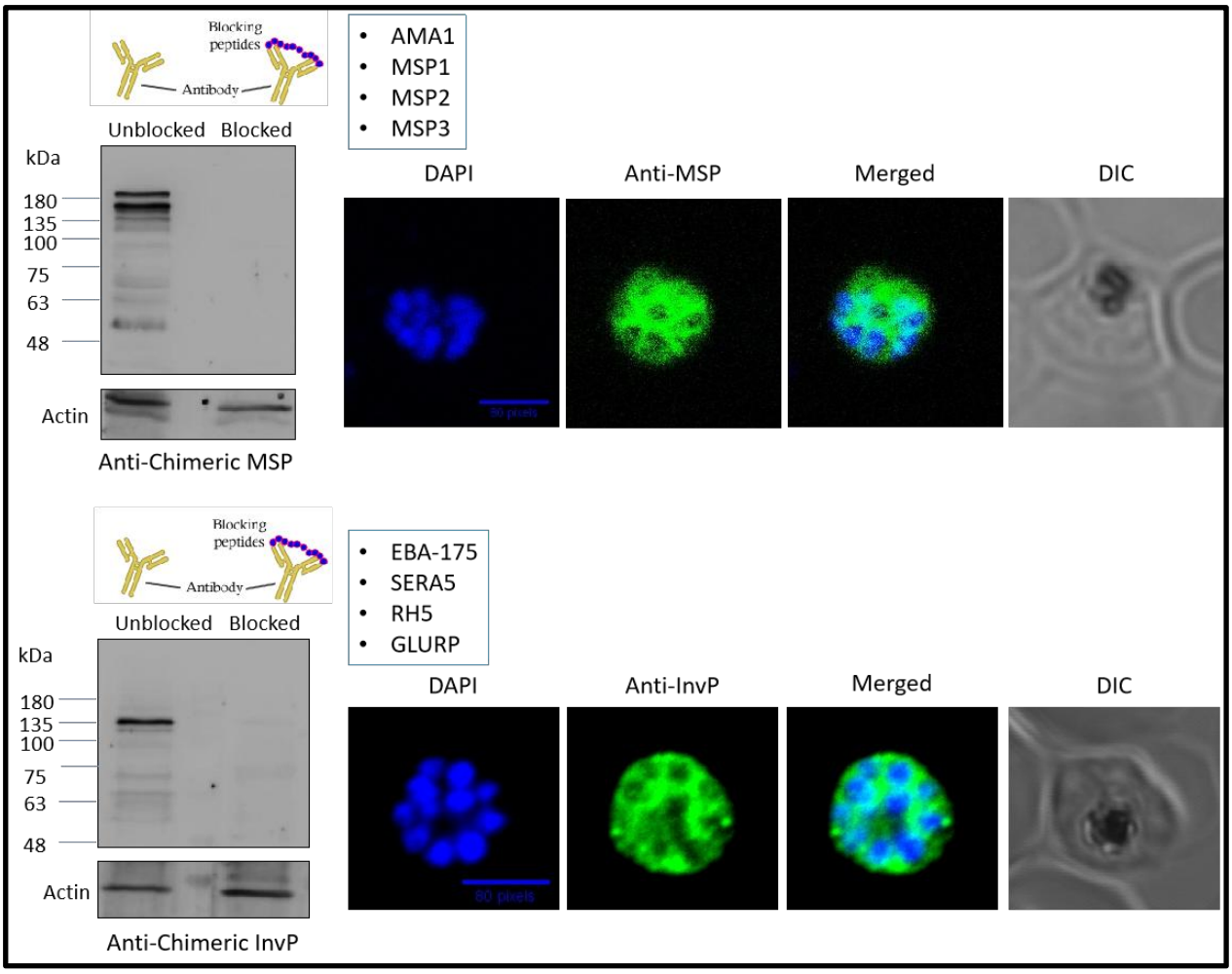


Figure 6.1. Validation of anti-chimeric MSP and InvP antibodies in parasite 3D7 line using peptide blocking assay and immunofluorescence. The top panel is anti-chimeric MSP, and the bottom is anti-chimeric InvP validation.

6.3.2 Anti-MSP and InvP antibodies inhibit the parasite growth

In single cycle GIA on the 3D7 strain, we used the antibodies in the final concentration range of 0.06 mg/ml (12.5 µg) to 0.5 mg/ml (100 µg) for both the chimeric antibodies. For chimeric MSP antibodies, 0.06 mg/ml concentration showed inhibition of around 35.7%, 0.125 mg/ml showed 62.41% inhibition, and 0.25 mg/ml concentration inhibited the parasite growth completely. For chimeric InvP antibodies, 0.06 mg/ml concentration showed inhibition of 36.45%, 0.125 mg/ml showed 57.82% inhibition, and complete inhibition at 0.25 mg/ml. When we added both the chimeric MSP and InvP antibodies in equivalent concentrations, the growth inhibition potential

was amplified—the 0.06 mg/ml mix concentration yielded the inhibition of 70.1%, and 0.125 mg/ml yielded 94.55% inhibition (Figure 6.2). The chimeric MSP and InvP constructs show complete inhibition with their additive effect. This shows a potent neutralizing effect of the generated antibodies in a combination.

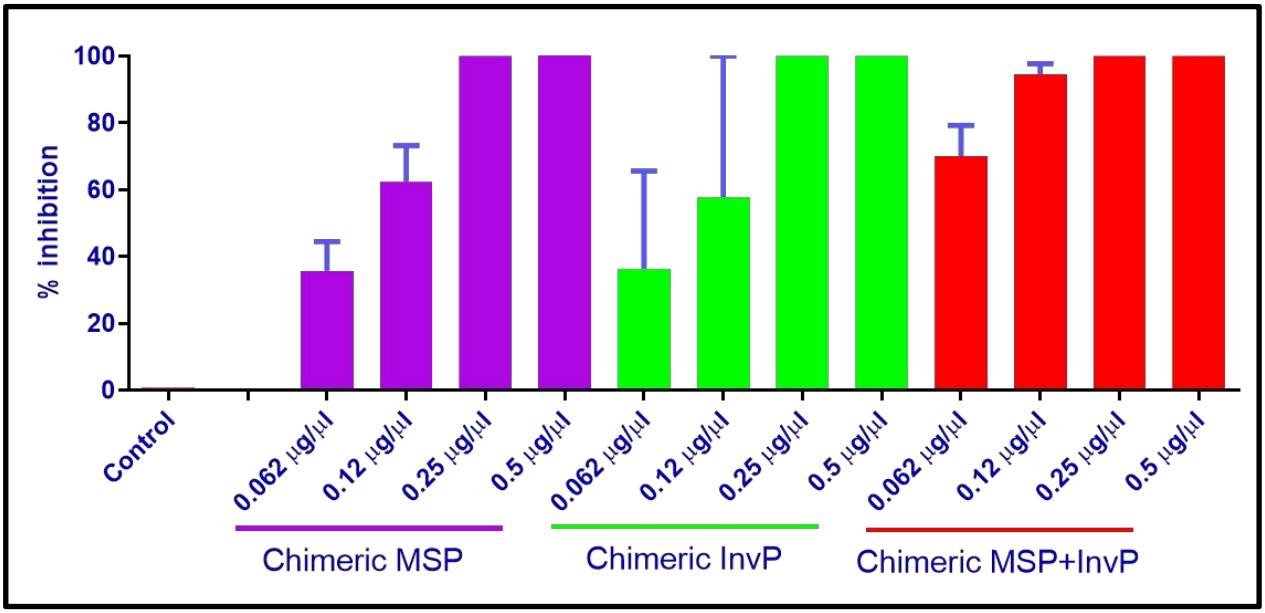


Figure 6.2. A Graph depicting the GIA values in % inhibition for chimeric MSP, chimeric InvP, and an equivalent mixture of both antibodies.

6.4 Discussion

The chimeric MSP and InvP antigens were designed to include AMA-1, MSP-1, MSP-2, MSP-3, and EBA-175, SERA-5, GLURP, RH5, respectively. This combination of proteins was considered based on the redundancy, polymorphism, and involvement in sialic acid-dependent and independent invasion pathways. The antibodies generated against the chimeric constructs were validated using peptide blocking assay and immunofluorescence assay on matured schizonts. We observed that the antibodies could identify native proteins, and the generated antibodies were chimera-specific. The antibodies showed inhibition of parasite invasion in GIA. As expected, the chimeric MSP and InvP construct antibodies had additive effects. Combining both the chimeric antigens yielded a 95% inhibition at 0.125 mg/ml– an antibody titer much lower than current vaccine candidates in the field.

The antigens gave much higher inhibitory concentrations when tested individually in different studies across different strains. The AMA-1 antibodies inhibited the 3D7 lab promisingly, but the efficacy during the phase 1/2a trial was disappointing as it did not translate into efficient protection (*139*). The MSP-1 immunization of either 3D7 or FVO strain in *Aotus nancymai* monkeys showed growth inhibition <30% when infected with *P. falciparum* FVO strain (*254*). Similarly, the EBA-175 and RH5-specific antibodies raised in mice showed 84% and 73% inhibition in GIA. Meanwhile, the combination of EBL-175 and RH-5 showed synergistic inhibition till a particular antibody concentration (*255*). The leading candidate, ChAd63-MVA RH-5, has the highest GIA of > 60% at 2.5 mg/ml concentration of antibodies in children aged 6-11 months (*256*). The attempts to make an antigen combination have always been limited to two combined antigens. In our study, for the first time, we show a combination of eight proteins in two different chimeric constructs showing a GIA inhibition of 95% at the concentration of 0.1 mg/ml– a concentration drastically lower than reported for any individual blood stage antigen. While immunization with an antigen can elicit an antibody titer range of 100-500 ug/ml, the antibody concentration required for complete inhibition using chimeric MSP and InvP antigens is within the physiological range of titer.

The journey of vaccine antigens from the bench to bed is always elaborate, often tricky, and sometimes not equivalently significant during clinical trials. We made the chimeric constructs specific to the *P. falciparum* 3D7 strain and tested them on the same homologous strain. The strain-transcending test, animal model studies, and safety and toxicity tests are the intuitive next steps before the efficiency in humans can be commented upon. However, given the protein selection, antigen combinations, and the promising amount of antibodies required, this combination is more likely to produce desirable clinical trial results.

Chapter 7: Conclusion and Prospects

Effectively targeting malaria infections remains a high-priority problem despite decade-long efforts. Research on other infectious diseases has attempted to construct a candidate with a broad antigen-targeting range. With a complex stage-specific disease, such as malaria, there is an urgent need for multi-target antigens. Here, we present a combined approach of multi-peptide, a multiprotein candidate for effectively targeting the blood stage of malaria. The selected proteins are well-known immunodominant targets verified in several seroepidemiological studies, CHMI experiments, and clinical trials (*89-91, 139, 142, 143, 145, 146, 254, 256*). Many infectious disease studies have used the chimeric design of multiple antigens with IEDB resources to select antigenic stretches (*203, 204, 206, 226, 227*). Our chimeric antigens were designed using six different parameters of IEDB resources to select B-cell epitope sequences confidently. They were successfully stitched, cloned, expressed, and validated. The human immune response recognized these chimeric antigens. The epitope mapping showed heterogeneous IgG and IgM responses that were expected in polymorphic genes and were present across all the peptides selected, validating our original antigen design. This further predicts that the chimeric antigens may successfully elicit an immune response in humans and can be sustained as circulating antibodies.

PfEMP1 proteins are known for their mutually exclusive expression, antigenic variation, and the vast number of endothelial receptors with which they interact (*103, 235*). Due to their epigenetic switching and endothelial receptor specificity, targeting any particular PfEMP1 protein is difficult. Acquired immunity in endemic regions is believed to occur in an orderly, starting from PfEMP1, causing cytoadhesion in vital organs with stronger receptor interaction. As the breadth of immunity increases, parasites are likely forced to express PfEMP1 proteins that interact comparatively weakly and sequester in non-vital organs (*167*). In some cases, multiple rounds of exposure to a sufficient antibody repertoire against PfEMP1 proteins are built to keep the disease asymptomatic (*107*). Sampling all PfEMP1 proteins in their epitope form, irrespective of the subclass, can theoretically protect against cytoadhesion. With antibodies specific to chimeric varB, we observed a reduction in the number of adhered RBCs in static assays and a further significant decrease in fluid-based dynamic cytoadherence assays. Our data emphasize the role

of flow dynamics in the process of cytoadhesion, as previously shown in other studies, and show that anti-PfEMP1 antibodies can inhibit the sequestration at physiological conditions. We also demonstrated using a fluid-based cytoadhesion assay in real-time and a quantification method to determine the binding of iRBCs per minute. This method is helpful for precisely assessing cytoadhesion and can be used with endothelial cell lines and receptors. The pan anti-PfEMP1 antibody pool, when used as a passive immunization in patients with severe malaria, will serve as an essential additional therapeutic in managing the malaria outcome. The field has yet to explore the tissue tropism in malaria infection comprehensively. Knowing the exact PfEMP1 domain organization and predicting the organ site of sequestration remains a topic of study, with a few reports suggesting a role of sub-type A with DC8 being majorly involved in cerebral malaria through ICAM-1 binding (*154*). Meanwhile, sub-type B is primarily seen in uncomplicated malaria (*158*). These reports vary in their results, and an intensive analysis of binding affinities has yet to be done. The knowledge of the PfEMP1 sub-type and their endothelial receptor affinities can further equip us with identifying the right pool of anti-PfEMP1 antibodies for passive immunization.

The blood-stage vaccine candidates in phase trials mainly target the merozoite surface proteins to either block entry into the new RBC or function by activating the Fc-mediated innate immune response (*199*). The current leading candidate, RH5, is shown to have neutralizing potential, while candidates such as MSP1 show clearance via activation of the complement pathway or opsonization (*88, 256*). Many of the blood-stage candidates have failed the phase trials for multiple reasons. The antigenic polymorphism and redundancy are the main bottlenecks for selecting antigens, along with a low time window of invasion and exponentially growing parasite count. Our study addresses it using a combination of multiple peptides from different proteins. It shows an additive effect in GIA imparted by the mixture of antibodies specific against chimeric MSP and InvP construct. In a single cycle GIA, the mixture of antibodies works much more efficiently at the concentration of 0.13 mg/ml compared to using antibodies separately. In a natural infection setting, having antibodies against multiple antigens belonging to important functional pathways may outweigh the effect of having a higher antibody titer against just one antigen.

Collectively, we show that, as a proof of principle, multi-protein candidates work more efficiently using multi-epitope than their single counterparts. An effective strategy against malaria will involve a combination of interventions against multiple stages with antimalarial drugs. Targeting the blood stage in a chimeric fashion will help reduce parasitemia, alleviate symptoms, inhibit or reverse cytoadhesion (making iRBCs more susceptible to immune clearance), and help reduce transmission to the next cycle.

Prospective experiments:

1. The epitope mapping microarray is a potent tool for identifying the antigenic epitope in synergy with the in-silico prediction. A comprehensive mapping of all surface exported antigens (irrespective of their known function) can be done to identify previously unknown, and putative vaccine targets.
2. The current project explores only the PfEMP1 subtype B through antigenic peptides of certain important binding domains. This can be expanded onto other PfEMP1 subtypes with more emphasis on antigenic stretches coming from domain cassettes and validated by large-scale patient sera microarray studies.
3. The cytoadhesion assay employed the use of HBEC-5i cells and showed a significant inhibition by anti-chimeric varB antibodies. This study can be further expanded to multiple other known receptors of human endothelial cells. A systematic study of various anti-PfEMP1 antibodies to endothelial receptor inhibition under physiological conditions can help design better therapeutics against cytoadhesion in *P. falciparum.*
4. We observed the anti-chimeric MSP and InvP antibodies to be highly potent with additive effect. It will be interesting to observe the strain transcending effect of these antibodies in sialic acid dependent strains and other heterologous strain inhibitions (especially in culture adapted lines of Indian isolates).
5. The formulation of chimeric antigens used here were in a protein form injected with an adjuvant. This can be further standardized with viral vector based techniques to ensure better peptide display to the humoral immune system.

APPENDIX

1. DNA sequence of chimeric genes used.

Chimeric Gene	Codon optimized sequence
Chimeric varB	ACCAGCGATAAAGGTAGTGAACCGACCGCACGCGGTCATAGCCATGTTG CCCGCAGCGCAGATGGTGCACCGAGCCCTAATGGTAATCCGCTGCCGCA GCCGGGCACCAATGGCACAAGCAATGAACCGATTAGCCAGTATCAGTAT GATAATACCACCGCAAGCGGTAATAATACCACCGCGAGCGGCAAAAAT ACCCCGAGTGATACCCAGAATGATATTCCGAGTACCAGCGGTAATAAGC ATAGCGATATTCCGTCAGGTAAACTGAGCGATACCCCGAGTGACAATAA TATTCATACCACCCAGGTGGAAACCCAGGCCAGCGGTGGTAATACCGAA ACCAGCCAGGTGAGTGGCGAAACCACCCCGCAGGGTCAGACCCCGAGT GAAAGCGAAGCACAGACCGCAAGCCAGGATACCAAACGCCAGAGCGTT CTGCCGCTGCTGGAACCGATTAATGGCGATACCATTAGTGATGATAATA ATCCGGAAAATACCACCGCTAGTGGTAATAATACAACCGCAAGCGATAC CCAGAACGATATTCAGAATGATGGCATTCCGAGCACCGAAGCCCAGGCA GGCGGCGATGAAGCAACCGAAGCAAGCGTGCCGCTGGGTGACGGCGTT AGTAAAAATCCGAAAGAAAAAGAAGAGCGCGAACGTGAAAATGCAGGC CTGGATCCGTTTGGCGGTAGCGTGGATGATGAAGCCAGTACCACCGCCA GCGGTAAAAATACCCCTAGTGATACCCAAAATGATATTCAGAGCGATGA TATTCCGAGCAGCAAGTTGATAGCAATCCGAATCAGGTTGATGATACCT ATGTGGATAGCAATCCTGATAATAGCAGTATGGATACCATTGAACAGGA AGAAGAAGAAAAAGGTGCCGGTGAAGATGAAGCCGCAAGTGAAGCAGA AGCCAGTGGTCCGAAAGTTACCAAACAGAATGATAGCGAAGGTAGTGA AGGTGGTCATCGCAGTAAACGCCATACCGAAAGTAGCGATAGCACCACC ACCGCCAGTGGCAATAATACCACAGCAAGTGGTAATAACACCACCGCCT CTGGCAAAAATACACCGAGTGATAAAAAAGCATACGGCAAAAATGGTA CCACCACCAAAGAAACCAGTAATGGCCCGATTAATAATCTGTATGTGGG TGGTGGCGGCAATACCGCCGCAAGCCAGGGCAGTGGCGAAGCCGCACA

	GCCGGTGACCGTGACCCAGCCTCAGGCCAGCGGCGGTAATACCCAGGTT GCCGTTAGCCCGGGCGGTGCAGCCAGTACCAGCACCACCGATTTTAAAA ATGTGAATAGTAGTAGCGGCAGCGGTGGCGGTGAAGGCAGCAATAAGA CCTTTAGCCATACCGAAGGCAATAGCGTGGTTAGTAGCAGTAGTGCACG TGGCAATGGCGCCAGCCGTGATAAAAATGGCGGTAGCGATAGCGATAAT ACCAATGGCGGCCCGCCGACCCAGGATGGTGAAGTTAAAAATGCACTGC TGGATGATAATAACAAACCGCGCAGCACCAGCGTTGAAATGAAAGCACT GAGCGGCGCAGGCGGCGGTCCGGAGTTAACCGGTAGCGGCAGCGATAA TACAACCGCGAGTGGTAATAATACGACCGCCAGCGGCAATAATACAACA GCCAGTGGTAATAATACTACCGCAGATATTCCGAATGATTATACCAGCG GCACCATTCCGACCAATACCAATATTACCACCACCAGCCGCCATAATGTT AATGATCTGTATAATGGTAAAAACAACCTGTATAGTGGTCAGAATAATG TGTATAGTGGTATTGATCCGACCAGTAAAGGCAGCAAAAGTCAGGAAAG TGGTAAAGCAGAAGGCACCAGTGAAAGCAGTGGCAGTGAAGCAAGTAG CCCGCTGGATGAAAAGAAAAAACAGCAGCGTGAAAGTGGCCTGGTGGG CGCACTGGATGGCAATAGTGGCAATGTTGATACCGCAAGCGGCAATAAC ACCACAGCAAGCGGCAACAATACCACCGCCTCAGGCAATAATACGACA GCAAGCGGTTATAATGGCAAAAATAATCTGTACAGTGGTCAGAACAATG TGTATTCAGGCATTGATCCG
Chimeric MSP	CTGCCTACCGGCGCATTCAAAGCCGATCGTTATAAAAGTCATGGTAAAG GTTATAACTGGGGTAATTATAATACCGATGAAATTATGAAGGAGATCGA ACGCGAAAGTAAACGTATTAAGCTGAATGATAACGATGATGAAGGCAAT AAGGGCAATGCAGAAAAATATGATAAGATGGATGAGCCGCAGGATTAT GGTAAAAGTAATAGCCGCAATGATGAAATGACCAAAGGCGCAAGTGCC CAGAGCGGCGCAAGTGCACAGAGCGGTGCCAGTGCACAGAGTGGCGCC AGTGCCCAGGCCCAGAGCGGTACAAGCGGTCCGAGCGGCCCGAGTGGC ACCTCACCTAGCAGTCGCAGCAATACCCTGCCGCGTGAAGATGGTGGCC ATAGTACCCATACCCTGAGTCAGAGTGGCGAAACCGAAGTTACCGAAGA

	AACCGAAGAAACAGAAGAACAGAAACAGATTACCGGCACCAGTAGCAC CAGCAGTCCGGGCAATACCACCGTTAATACCGCCCAGAGCGCAACCCAT AGTAATAGTCAGAATCAGCAGAGCAATGCCAGCAGCACCAATACCCAG AATGGTGTGGCCGTTAGTCATGATCCGCTGACCGTTCTGAGTATTAGCAA TGATCTGAAAGGTATTGTTAGCCTGCTGAATCTGGGTAATAAGGATGTTA CCCCGAGTCCGCTGAGTGTGCGCGTTAGTGGTAGCAGCGGTAGCACCAA AGAAGAAACCCAGATTCCGATTCGTCGTAGCATGGCCGAAAGCAAACCG AGCACCGGTGCCGGTGGTAGTGCCGGTGGTTCAGCCGGCGGTAGTGGTA GTGCCGGCGGCAGTGCAGGCGGTAGCGCTGGTAGCGGCGATGGCAATG GCGCAGATGCCGAAGGTAGTAGCACCACCAATGATGCAGAAGCAAGCA CCAGCACCAGCAGCGAAAATCCGAATCATAAAAATGCAGAAACCAATC CGAAAGGTAAAGGTGAAGTGCAGGAACCGAATCAGGCCAATAAGGAAA CCCAGAATAATAGCAATGTGCAGCAGGATCAGACCAAAAGTAATGTGCC GCCGACCCAGGATGCCGATACCAAAAGTCCGACCGCACAGCCGGAACA GGCAGAAAGCGCACCGACCGCCGAACAGACCGAAAGCCCGGAACTGCA GAGTGCCCCGGAAAATAAGGGCACCGGCCAGCATCATGGCAGTCGCAAT AATCATCCGCAGAATACCAGCGATAGTCAGAAAGAATGTACCGATGGTA ATAAGGAAAATCTGAATAATAACAGCCAGATTGAAAACGAAGAAAATG TTAATACCACCATTACCGGCAATGATTTTAGTGGCGGTAATGCATACGA AAAAGCAAAAAATGCCTATCAGAAAGCAAATCAGGCCGTGCTGAAAGC CAAAGAAGCAAGCAGTGAAGAAGAAAATGATAAAAAGAAAGAGCAGG AAAAGGAACAGAGCAATGAAAATAATGATCAGAAAAAGGACATG
Chimeric InvP	GATAGCCGTATTAATAACGGCCGCAATACCAGTAGCAATAATGAAGTTC TGAGTAATTGTCGTGAAAAACGCAAACTGGTGAAAAGCGTGCTGAATGG TAATGATAATACCATTAAGGAAAAGCGTGAACATATTGATCTGGATGAT TTTAATAACGAGCAGACCAGCCAGGAAGCAGTGCCGGAAGAAAGTACC GAAATTGCCCATCGTACCGAAACCCGCACCGATGAACGCAAAAATCAGG

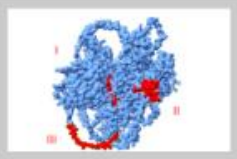
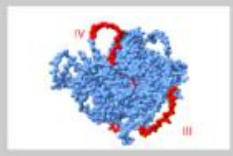
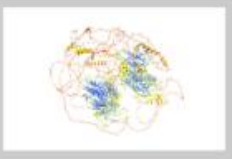
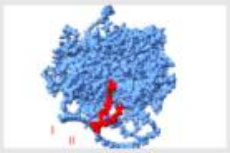
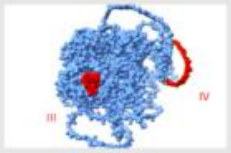
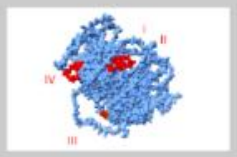
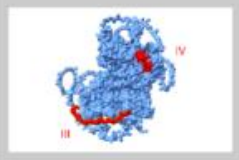
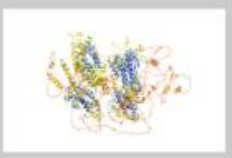
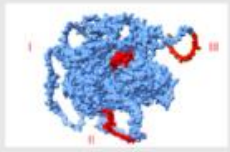
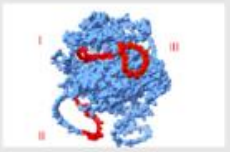
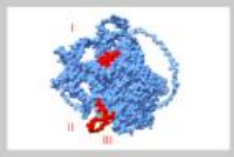
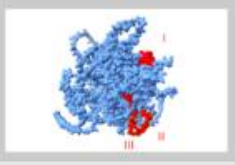
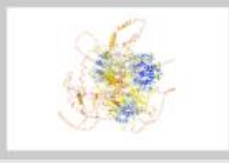
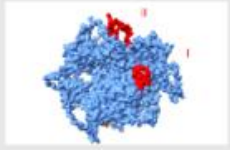
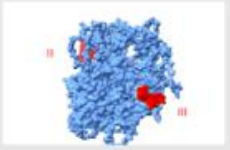
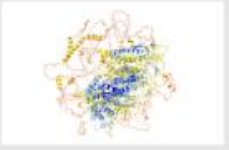
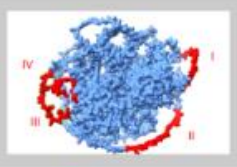
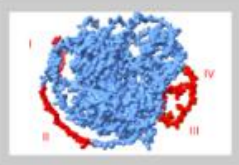
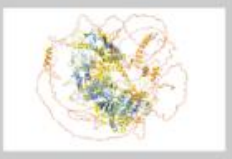
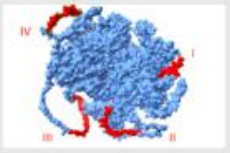
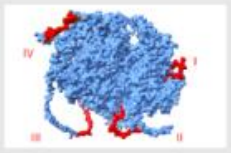
	AACCGGCAAATAAGGATCTGAAAAATCCGCAGCAGAGCGTTGGCGAAA ATGGTACCGGTGTGAATCATGGCATTCCGAAAGGTGAAGATCAGACCCT GGGCAAAAGCGATGCAATTCCGAATATTGGCGAACGTAGTCAGATTAAT CATAGTCATCATGGTAATCGCCAGGATCGTGGTGGCAATAGTGGTAATG TTCTGAATATGCGTAGTAATAATAACAACTTCAACAACATCCCGAGTCGT TATAATCTGTATGATAAAAAACTGGACCTGGATCTGAATACCGGTGGTG GCCAGGCAGGTAATACCGGCGGTGACCAGGCAGGTAGCACCGGTGGTA GCCCGCAGGGTAGTGTGAGCGTGAGTCAGACCAGCACCAGTAGCGAAA AACAGGATACCATTCAGGTTAAAAGCGCCCTGCTGAAAGATAGCAGTAG TAGTAGCAGCAGTAGTAGCTCAAGCAGCAGCAGTTCAAGCAGCTCAAGC AGTAGTTCAAGTAGCAGTCATGTTGATACCACCCTGGAAAAAGAAGATA CCCTGAGCTATGATAATAGCGATAATATGTTTTGCAACAAGGAAGAACA GTGTCCGAAAGTTGAAGATCATTGGATGAATCTGTGGGATAATGGTAAA ATTCTGCATAATAAGAACGAGTATTTCAAGAATTTCAACGTGGGCAAAA AGAATCTGTTTAGTGAAAAAGAAGACAACGAAAATAACAAGAAGCTGA ATTATATCATCTTCGGTCAGGATACCGCCGGCAGTGGTCAGAGCGGTAA AGAAAGCAATACCGCCCTGGAAAGTATTAAGAAAGAAATTGATAACGA CAAGGAGAATATCAAAACCAATAATGCCAAAGATCACAGCACCTATATT AAGGAACATCCGTATGATATTAACAACAAAAACGATGATAGCTACCGCT ATGATATTAGCGAAGAAATTGATGATAAGGATGAAACCGAAGAAGTTG AAGATAGCATTCAGGATACCGATAGCAATCATACCCCGAGTAATAAGAA AAAGAATAATGAAAGCAGCGACATTATCAGCGTTAATAATAAGAGCAAT AAGGTTCAGAACCATTTTGAAAGTCTGAGCGATACCCAGATTCATAAAG ATTATAAAGAGAAGAACCTGATCAACGAAGAAGATAGCGAACCGTTTCC GCGTCAGAAAGAACATATTGACCAGAGTCAGCATAATATTAATGTGCTG CAGGAAAATAACATCAATAATCATCAGCTGGAACCGACCGTGAGCCAGG AAAGCAATCCGGAAAAAGCCGATAATGATGGTAATGTGAGCCAGAATA GTAATAATGAACTGGAAAGCAGTCTGGAAGAAGGTCATCATGAAGAAA TTGTTCCGGAACAGAATAATGAAGAAAGCGGTGAAAGCAAAGAATTTG AACCGGATCAGAATGATAGCGAACTGAGCGAAAATGAACTGGTTGAAA

	GCGAAAAAAGTGTTAGTGAAGAAGTGAAAGAAAAGGAAAATGTTAGCG AAGTGGTTGAAGAAAAACAGAATAGTCAGGAAAGCGTTGAAGAAATT

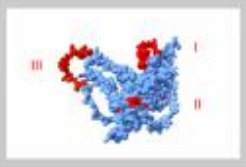
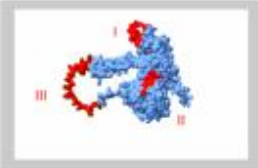
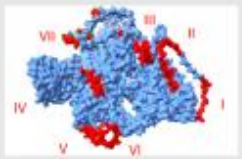
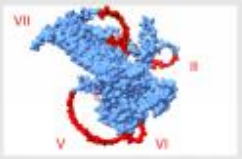
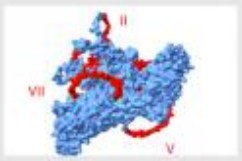
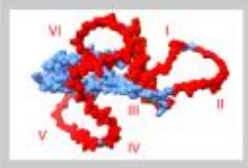
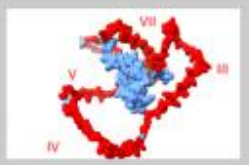
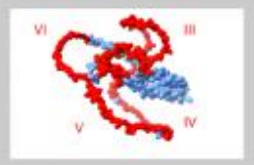
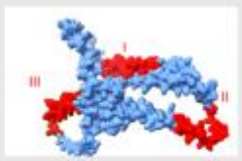
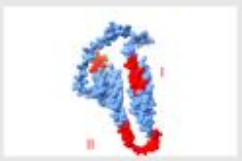
2. Alignment of antigenic peptides on their respective protein (3D structure)

For generation of chimeric varB antigen, peptides belonging to eight PfEMP1 proteins were selected (peptide stretches given in Table 1). The red colored stretch shows the location of these peptides in the 3D structure of selected PfEMP1. Similarly, the peptides taken for chimeric MSP (Table 2) and chimeric InvP (Table 3) are show in panel B and C respectively.

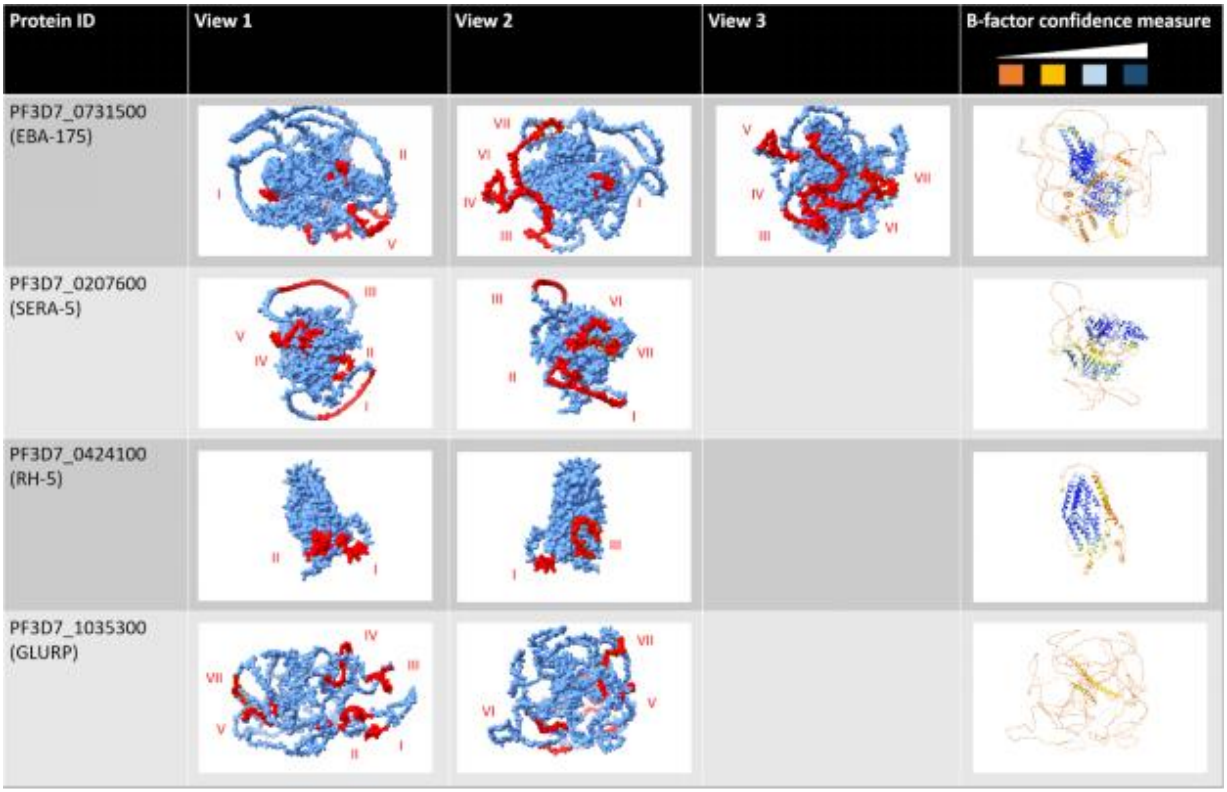
Alignment of peptides from chimeric varB on their respective proteins

Protein ID	View 1	View 2	B-factor confidence measure
PF3D7_1200100			
PF3D7_0500100			
PF3D7_1300100			
PF3D7_0324900			
PF3D7_0300100			
PF3D7_1100100			
PF3D7_0937800			
PF3D7_0400100			

Alignment of chimeric MSP peptides on their respective proteins

Protein ID	View 1	View 2	View 3	B-factor confidence measure
PF3D7_1133400 (AMA-1)				
PF3D7_0930300 (MSP-1)				
PF3D7_0206800 (MSP-2)				
PF3D7_1035400 (MSP-3)				

Alignment of chimeric InvP peptides on their respective proteins



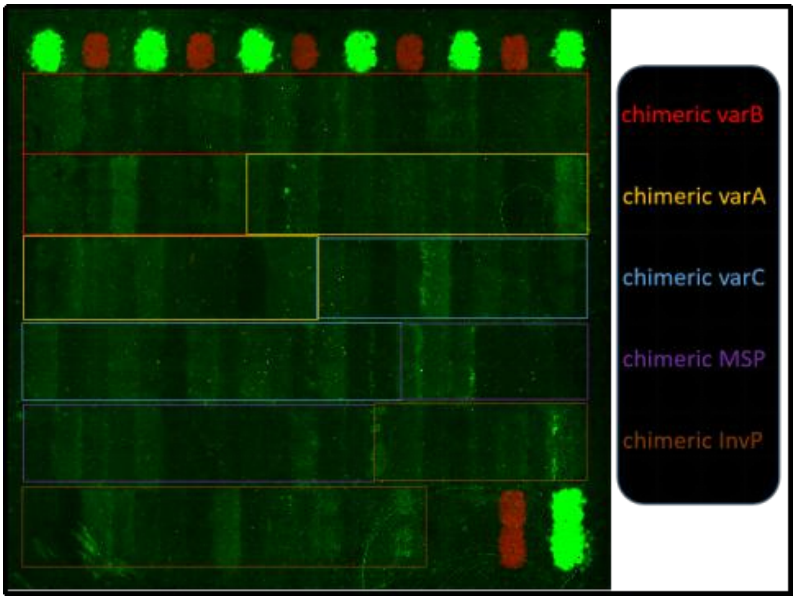
3. The codon-optimized DNA sequence of chimeric varB with linkers

ACCAGCGACAAGGGCAGCGAGCCGACCGCGCGTGGTCACAGCCATGTTGCGCGTAG
CGCGGACGGTGCGCCGAGCGGTGGTGGTAGCGGTGGCGGTAGCCCGAACGGTAACC
CGCTGCCGCAGCCGGGCACCAACGGCACCAGCAACGAGCCGATCAGCCAGTACCAA
TATGATGGCGGTGGCAGCGGTGGCGGTAGCAACACCACCGCGAGCGGCAACAACAC
CACCGCGAGCGGTAAAAACACCCCGAGCGACACCCAAAACGATATTCCGGGCGGTG
GCAGCGGTGGCGGTAGCAGCACCAGCGGTAACAAACACAGCGACATCCCGAGCGGT
AAGCTGAGCGACACCCCGAGCGATAACAACATTCACGGCGGTGGCAGCGGTGGCGG
TAGCACCACCCAGGTGGAGACCCAAGCGAGCGGCGGTAACACCGAAACCAGCCAG
GTTAGCGGCGGTGGCGGTAGCGGCGGTGGCAGCGAGACCACCCCGCAGGGTCAAAC

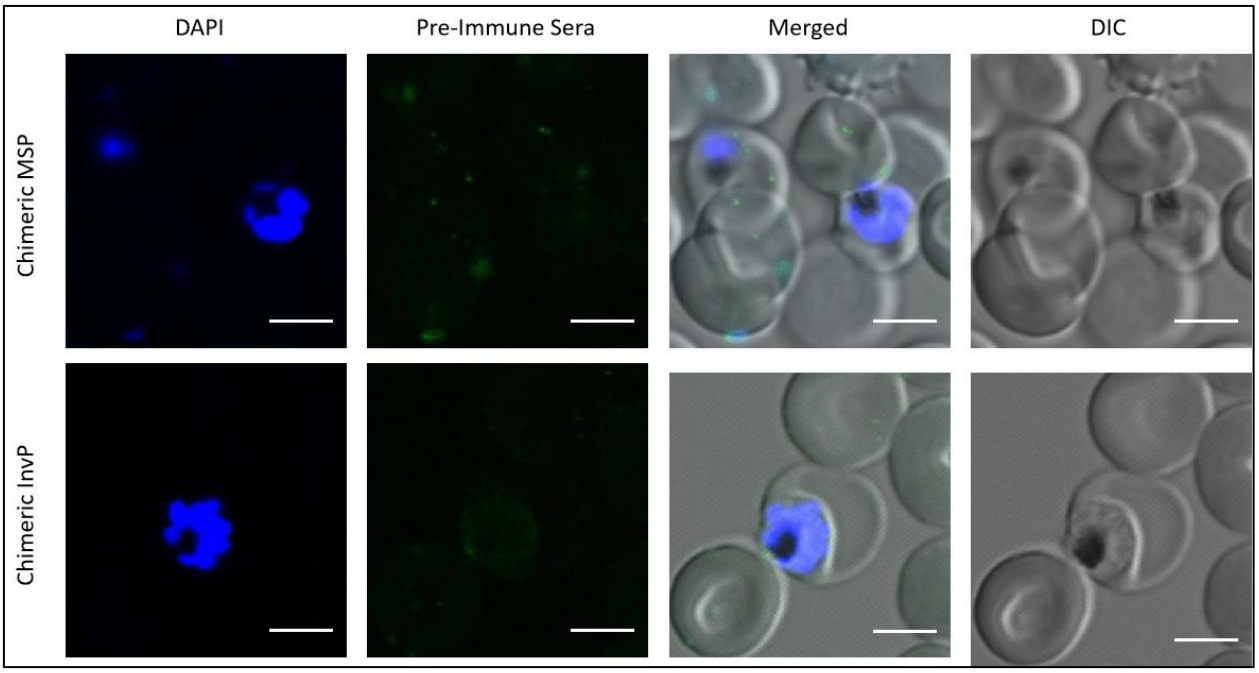
CCCGAGCGAGAGCGAAGCGCAGACCGCGAGCCAAGATGGTGGCGGTAGCGGCGGT
GGCAGCACCAAACGTCAAAGCGTGCTGCCGCTGCTGGAGCCGATCAACGGTGACAC
CATTAGCGACGATAACAACCCGGAAGGTGGCGGTAGCGGCGGTGGCAGCAACACCA
CCGCGAGCGGTAACAACACCACCGCGAGCGACACCCAGAACGACATCCAAAACGA
CGGTATTCCGAGCGGTGGCGGTAGCGGCGGTGGCAGCACCGAAGCGCAGGCGGGTG
GCGATGAGGCGACCGAAGCGAGCGTGCCGCTGGGCGACGGTGTTAGCAAGAATCCG
GGTGGCGGTAGCGGCGGTGGCAGCAAAGAGAAGGAGGAACGTGAGCGTGAAAACG
CGGGTCTGGACCCGTTCGGTGGCAGCGTGGACGATGAAGCGAGCGGTGGCGGTAGC
GGCGGTGGCAGCACCACCGCGAGCGGTAAAAACACCCCGAGCGATACCCAGAACG
ACATCCAAAGCGACGATATTCCGAGCAGCAAGGGTGGCGGTAGCGGCGGTGGCAGC
GTTGATAGCAACCCGAACCAGGTGGACGATACCTATGTTGATAGCAACCCGGACAA
CAGCAGCATGGACACCATCGGTGGCGGTAGCGGCGGTGGCAGCGAGCAAGAGGAA
GAGGAAAAGGGCGCGGGTGAGGATGAAGCGGCGAGCGAGGCGGAAGCGAGCGGTC
CGAAAGTTGGTGGCGGTAGCGGCGGTGGCAGCACCAAGCAGAACGATAGCGAGGG
TAGCGAAGGTGGCCACCGTAGCAAACGTCACACCGAAAGCAGCGACAGCACCGGTG
GCGGTAGCGGCGGTGGCAGCACCACCGCGAGCGGCAACAACACCACCGCGAGCGG
TAACAACACCACCGCGAGCGGCAAGAACACCCCGAGCGACGGTGGCGGTAGCGGC
GGTGGCAGCAAGAAAGCGTATGGCAAAAACGGCACCACCACCAAGGAGACCAGCA
ACGGTCCGATTAACAACCTGTACGTGGGTGGCGGTGGCAGCGGTGGCGGTAGCGGC
GGTGGCAACACCGCGGCGAGCCAGGGCAGCGGTGAAGCGGCGCAACCGGTGACCG
TTGGTGGCGGTAGCGGCGGTGGCAGCACCCAGCCGCAAGCGAGCGGTGGCAACACC
CAGGTGGCGGTTTCTCCGGGTGGCGCGGCGAGCACCAGCACCACCGGTGGCGGTAG
CGGCGGTGGCAGCGATTTCAAAAACGTGAACAGCAGCAGCGGCAGCGGTGGCGGTG
AGGGTAGCAACAAGACCTTTAGCCACACCGAAGGCGGTGGCAGCGGTGGCGGTAGC
GGTAACAGCGTGGTGAGCAGCAGCAGCGCGCGTGGCAACGGTGCGAGCCGTGATAA
AAACGGCGGTAGCGACAGCGGCGGTGGCAGCGGTGGCGGTAGCGATAACACCAAC
GGCGGTCCGCCGACCCAGGACGGTGAAGTGAAAAACGCGCTGCTGGACGATAACAA
CAAGCCGGGTGGTGGCAGCGGTGGCGGTAGCCGTAGCACCAGCGTTGAGATGAAGG
CGCTGAGCGGTGCGGGCGGTGGCCCGGAACTGACCGGCAGCGGTAGCGACGGTGGC
GGTAGCGGCGGTGGCAGCAACACCACCGCGAGCGGTAACAACACCACCGCGAGCG

GCAACAACACCACCGCGAGCGGTAACAACACCACCGCGGGTGGCGGTAGCGGCGGT
GGCAGCGACATCCCGAACGACTATACCAGCGGCACCATCCCGACCAACACCAACAT
TACCACCACCAGCCGTCACAACGTGGGTGGCGGTAGCGGCGGTGGCAGCAACGATC
TGTACAACGGCAAAAACAACCTGTATAGCGGTCAGAACAACGTTTACAGCGGTATT
GACCCGACCAGCGGTGGCGGTAGCGGCGGTGGCAGCAAAGGTAGCAAGAGCCAAG
AGAGCGGCAAGGCGGAGGGCACCAGCGAAAGCAGCGGTAGCGAGGCGAGCAGCCC
AGGTGGCGGTAGCGGCGGTGGCAGCCTGGACGAGAAGAAAAAGCAGCAACGTGAA
AGCGGCCTGGTGGGTGCGCTGGATGGCAACAGCGGTAACGTTGACGGTGGCGGTAG
CGGCGGTGGCAGCACCGCGAGCGGTAACAACACCACCGCGAGCGGTAACAACACC
ACCGCGAGCGGTAACAACACCACCGCGAGCGGTGGCGGTGGCAGCGGTGGCGGTA
GCTACAATGGTAAAAACAACCTGTATAGCGGCCAAAACAACGTGTATAGCGGTATT
GACCCGTAA

4. Epitope Mapping microarray peptide map



5 Immunofluorescence of late-stage schizont using pre immune sera (Control for chimeric MSP and InvP antibodies)



Addendum Video 1: A video depicting the cytoadhesion of iRBCs on HBEC-5i cells under 25 mbar pressure. (Video taken on Leica DM750 with Flexacam system using 10X magnification)

Publications

Bhagyashree Deshmukh, Dhruv Khatri, Sanjay Kumar Kochar, Chaitanya Athale, Krishanpal Karmodiya (2023). Multi-protein chimeric antigens, a novel combined approach for efficiently targeting and blocking the blood stage of *Plasmodium falciparum*. **BioRxiv**., DOI 10.1101/2023.11.22.568251 (Under revision- PLOS Pathogens)

Abhishek Kanyal, **Bhagyashree Deshmukh**, Heledd Davies, DV Mamatharani, Dilsha Farheen, Moritz Treeck, Krishanpal Karmodiya (2024). PfHDAC1 is an essential regulator of *P. falciparum* asexual proliferation and host cell invasion genes with a dynamic genomic occupancy responsive to artemisinin stress. **mBio**., (In Press).

Deepak Choubey, **Bhagyashree Deshmukh**, Anjani Gopal Rao, Abhishek Kanyal, Amiya Kumar Hati, Somenath Roy, Krishanpal Karmodiya (2023). Genomic Analysis of Indian isolates of *Plasmodium falciparum*: Implications for Drug Resistance and Virulence Factors. **International Journal for Parasitology: Drug and Drug Resistance**., Volume 52, pages 52-60.

Chhuttan L Meena, Tejashri Hingamire, Tanya Gupta, **Bhagyashree Deshmukh**, Krishanpal Karmodiya, Rakesh Joshi, Dhanasekaran Shanmugam, Gangadhar J Sanjayan (2023). Histidinal-Based Potent Antimalarial Agents. **ChemMedChem**., e202200709

Mukul Rawat, Abhishek Kanyal, Deepak Choubey, **Bhagyashree Deshmukh**, Rashim Malhotra, D V Mamatharani, Anjani Gopal Rao, Krishanpal Karmodiya (2022), Identification of co-existing mutations and gene expression trends associated with K13-mediated artemisinin resistance in *Plasmodium falciparum*. **Frontiers in genetics**., 13:824483.

REFERENCES

1. L. J. Bruce-Chwatt, History of malaria from prehistory to eradication. *Malaria: principles practice of malariology.* **Volume 1**, 1-59 (1988).
2. F. E. G. Cox, History of the discovery of the malaria parasites and their vectors. *Parasites & Vectors* **3**, 1-9 (2010).
3. C. Golgi, Intorno al preteso Bacillus malariae di Klebs, Tommasi-Crudeli e Schiavuzzi. *Archivio per le scienze mediche* **13**, 93 (1889).
4. E. Klebs, C. T. Crudeli, *Studi sulla natura della malaria*. (Coi tipi del Salviucci, 1879).
5. A. Laveran, Note sur un nouveau parasite trouvé dans le sang de plusieurs malades atteints de fièvre palustre. *Bull Acad Med* **9**, 1235-1236 (1880).
6. B. Danilewsky, *La parasitologie comparée du sang*. (Noms de l'éditeur variés, 1886).
7. C. Golgi, *Sul ciclo evolutivo dei parassiti malarici nella febbre terzana: diagnosi differenziale tra i parassiti endoglobulari malarici della terzana e quelli della quartana*. (Bona, 1889).
8. F. E. Cox, History of human parasitic diseases. *Infect Dis Clin North Am* **18**, 171-188, table of contents (2004).
9. R. Ross, *Memoirs: with a full account of the great malaria problem and its solution*. (J. Murray, 1923).
10. B. Grassi, *Studio di uno zoologo sulla malaria*. (R. Accademia dei lincei, 1900), vol. 3.
11. W. H. Organization, *WHO malaria policy advisory group (MPAG) meeting report, 18–20 April 2023*. (World Health Organization, 2023).
12. M. Rahi, A. Sharma, Malaria control initiatives that have the potential to be gamechangers in India's quest for malaria elimination. *The Lancet Regional Health-Southeast Asia* **2**, (2022).
13. P. Venkatesan, The 2023 WHO World malaria report. *Lancet Microbe* **5**, e214 (2024).
14. A. F. Cowman, J. Healer, D. Marapana, K. Marsh, Malaria: Biology and Disease. *Cell* **167**, 610-624 (2016).
15. M. S. Datoo, H. M. Natama, A. Some, D. Bellamy, O. Traore, T. Rouamba, M. C. Tahita, N. F. A. Ido, P. Yameogo, D. Valia, A. Millogo, F. Ouedraogo, R. Soma, S. Sawadogo, F. Sorgho, K. Derra, E. Rouamba, F. Ramos-Lopez, M. Cairns, S. Provstgaard-Morys, J. Aboagye, A. Lawrie, R. Roberts, I. Valea, H. Sorgho, N. Williams, G. Glenn, L. Fries, J. Reimer, K. J. Ewer, U. Shaligram, A. V. S. Hill, H. Tinto, Efficacy and immunogenicity of R21/Matrix-M vaccine against clinical malaria after 2 years' follow-up in children in Burkina Faso: a phase 1/2b randomised controlled trial. *Lancet Infect Dis* **22**, 1728-1736 (2022).
16. A. M. Samuels, D. Ansong, S. K. Kariuki, S. Adjei, A. Bollaerts, C. Ockenhouse, N. Westercamp, C. K. Lee, L. Schuerman, D. K. Bii, L. Osei-Tutu, M. Oneko, M. Lievens, M. A. Sarfo, C. Atieno, D. Morelle, A. Bakari, T. Sang, E. Jongert, M. F. Kotoh-Mortty, K. Otieno, F. Roman, P. B. Buabeng, Y. Ntiamoah, O. Ofori-Anyinam, T. Agbenyega, D. Sambian, A. A. Domudo, L. N. Badu, K. Akoi, E. Antwi, K. Onoka, K. K'Orimba, P. N. Oloo, E. Leakey, E. Gvozdenovic, C. Cravcenco, P. Vandoolaeghe, J. Vekemans, K. Ivinson, Efficacy of RTS, S/AS01E malaria vaccine administered according to different full, fractional, and delayed third or early fourth dose regimens in children aged 5–17 months in Ghana and Kenya: an open-label, phase 2b, randomised controlled trial. *Lancet Infect Dis* **22**, 1329-1342 (2022).
17. S. Baron, Medical microbiology. (1996).

18. L. J. Bruce-Chwatt, *Essential malariology*. (William Heinemann Medical Books Ltd, 1985).
19. N. J. White, Severe malaria. *Malaria journal* **21**, 284 (2022).
20. N. Day, A. M. Dondorp, The management of patients with severe malaria. *Am J Trop Med Hyg* **77**, 29-35 (2007).
21. L. Schofield, I. Mueller, Clinical immunity to malaria. *Curr Mol Med* **6**, 205-221 (2006).
22. A. N. Clements, *The biology of mosquitoes. Volume 2: sensory reception and behaviour*. (1999).
23. T. W. Scott, W. Takken, Feeding strategies of anthropophilic mosquitoes result in increased risk of pathogen transmission. *Trends Parasitol* **28**, 114-121 (2012).
24. Y. O. Zhao, S. Kurscheid, Y. Zhang, L. Liu, L. Zhang, K. Loeliger, E. Fikrig, Enhanced survival of Plasmodium-infected mosquitoes during starvation. *PLoS One* **7**, e40556 (2012).
25. C. M. Cirimotich, Y. Dong, L. S. Garver, S. Sim, G. Dimopoulos, Mosquito immune defenses against Plasmodium infection. *Dev Comp Immunol* **34**, 387-395 (2010).
26. J. C. Castillo, A. E. Robertson, M. R. Strand, Characterization of hemocytes from the mosquitoes Anopheles gambiae and Aedes aegypti. *Insect Biochem Mol Biol* **36**, 891-903 (2006).
27. J. A. Kengne-Ouafo, C. J. Sutherland, F. N. Binka, G. A. Awandare, B. C. Urban, B. Dinko, Immune Responses to the Sexual Stages of Plasmodium falciparum Parasites. *Front Immunol* **10**, 136 (2019).
28. T. M. Peterson, A. J. Gow, S. Luckhart, Nitric oxide metabolites induced in Anopheles stephensi control malaria parasite infection. *Free Radic Biol Med* **42**, 132-142 (2007).
29. J. W. K. Liew, M. Y. Fong, Y. L. Lau, Quantitative real-time PCR analysis of Anopheles dirus TEP1 and NOS during Plasmodium berghei infection, using three reference genes. *PeerJ* **5**, e3577 (2017).
30. M. L. Simões, Y. Dong, A. Hammond, A. Hall, A. Crisanti, T. Nolan, G. Dimopoulos, The Anopheles FBN9 immune factor mediates Plasmodium species-specific defense through transgenic fat body expression. *Developmental*
Comparative Immunology
67, 257-265 (2017).
31. C. Fouet, P. Atkinson, C. Kamdem, Human Interventions: Driving Forces of Mosquito Evolution. *Trends Parasitol* **34**, 127-139 (2018).
32. K. Raghavendra, P. S. Velamuri, V. Verma, N. Elamathi, T. K. Barik, R. M. Bhatt, A. P. Dash, Temporo-spatial distribution of insecticide-resistance in Indian malaria vectors in the last quarter-century: Need for regular resistance monitoring and management. *J Vector Borne Dis* **54**, 111-130 (2017).
33. S. S. Sahu, K. Gunasekaran, T. Vijayakumar, P. Jambulingam, Triple insecticide resistance in Anopheles culicifacies: A practical impediment for malaria control in Odisha State, India. *Indian J Med Res* **142 Suppl**, S59-63 (2015).
34. M. B. Markus, The hypnozoite concept, with particular reference to malaria. *Parasitol Res* **108**, 247-252 (2011).
35. N. J. White, P. L. Olliaro, Strategies for the prevention of antimalarial drug resistance: rationale for combination chemotherapy for malaria. *Parasitol Today* **12**, 399-401 (1996).
36. H. A. Babiker, S. J. Pringle, A. Abdel-Muhsin, M. Mackinnon, P. Hunt, D. Walliker, High-level chloroquine resistance in sudanese isolates of *Plasmodium falciparum* is associated with mutations in the chloroquine resistance transporter gene and the multidrug resistance gene. *Journal of Infectious Diseases* **183**, 1535-1538 (2001).
37. E. J. Phillips, J. S. Keystone, K. C. Kain, Failure of combined chloroquine and high-dose primaquine therapy for Plasmodium vivax malaria acquired in Guyana, South America. *Clin Infect Dis* **23**, 1171-1173 (1996).

38. V. Durrand, A. Berry, R. Sem, P. Glaziou, J. Beaudou, T. Fandeur, Variations in the sequence and expression of the *Plasmodium falciparum* chloroquine resistance transporter (Pfcrt) and their relationship to chloroquine resistance in vitro. *Molecular and Biochemical Parasitology* **136**, 273-285 (2004).
39. D. F. Clyde, G. T. Shute, Resistance of East African varieties of Plasmodium falciparum to pyrimethamine. *Trans R Soc Trop Med Hyg* **48**, 495-500 (1954).
40. S. Maberti, Development of Resistance to Pyrimethamine. Report of 15 Cases studied at Trujillo, Venezuela. *Arch Venez Med Trop Parasitol Med* **3**, 239-259 (1960).
41. D. S. Peterson, D. Walliker, T. E. Wellems, Evidence That a Point Mutation in Dihydrofolate-Reductase Thymidylate Synthase Confers Resistance to Pyrimethamine in Falciparum-Malaria. *Proceedings of the National Academy of Sciences of the United States of America* **85**, 9114-9118 (1988).
42. A. F. Cowman, D. Galatis, J. K. Thompson, Selection for Mefloquine Resistance in Plasmodium-Falciparum Is Linked to Amplification of the Pfmdr1 Gene and Cross-Resistance to Halofantrine and Quinine. *Proceedings of the National Academy of Sciences of the United States of America* **91**, 1143-1147 (1994).
43. O. Miotto, J. Almagro-Garcia, M. Manske, B. Macinnis, S. Campino, K. A. Rockett, C. Amaratunga, P. Lim, S. Suon, S. Sreng, J. M. Anderson, S. Duong, C. Nguon, C. M. Chuor, D. Saunders, Y. Se, C. Lon, M. M. Fukuda, L. Amenga-Etego, A. V. Hodgson, V. Asoala, M. Imwong, S. Takala-Harrison, F. Nosten, X. Z. Su, P. Ringwald, F. Ariey, C. Dolecek, T. T. Hien, M. F. Boni, C. Q. Thai, A. Amambua-Ngwa, D. J. Conway, A. A. Djimde, O. K. Doumbo, I. Zongo, J. B. Ouedraogo, D. Alcock, E. Drury, S. Auburn, O. Koch, M. Sanders, C. Hubbart, G. Maslen, V. Ruano-Rubio, D. Jyothi, A. Miles, J. O'Brien, C. Gamble, S. O. Oyola, J. C. Rayner, C. I. Newbold, M. Berriman, C. C. Spencer, G. McVean, N. P. Day, N. J. White, D. Bethell, A. M. Dondorp, C. V. Plowe, R. M. Fairhurst, D. P. Kwiatkowski, Multiple populations of artemisinin-resistant Plasmodium falciparum in Cambodia. *Nat Genet* **45**, 648-655 (2013).
44. H. Noedl, Y. Se, S. Sriwichai, K. Schaecher, P. Teja-Isavadharm, B. Smith, W. Rutvisuttinunt, D. Bethell, S. Surasri, M. M. Fukuda, D. Socheat, L. Chan Thap, Artemisinin resistance in Cambodia: a clinical trial designed to address an emerging problem in Southeast Asia. *Clin Infect Dis* **51**, e82-89 (2010).
45. S. Takala-Harrison, C. G. Jacob, C. Arze, M. P. Cummings, J. C. Silva, A. M. Dondorp, M. M. Fukuda, T. T. Hien, M. Mayxay, H. Noedl, F. Nosten, M. P. Kyaw, N. T. Nhien, M. Imwong, D. Bethell, Y. Se, C. Lon, S. D. Tyner, D. L. Saunders, F. Ariey, O. Mercereau-Puijalon, D. Menard, P. N. Newton, M. Khanthavong, B. Hongvanthong, P. Starzengruber, H. P. Fuehrer, P. Swoboda, W. A. Khan, A. P. Phyo, M. M. Nyunt, M. H. Nyunt, T. S. Brown, M. Adams, C. S. Pepin, J. Bailey, J. C. Tan, M. T. Ferdig, T. G. Clark, O. Miotto, B. MacInnis, D. P. Kwiatkowski, N. J. White, P. Ringwald, C. V. Plowe, Independent emergence of artemisinin resistance mutations among Plasmodium falciparum in Southeast Asia. *J Infect Dis* **211**, 670-679 (2015).
46. B. Balikagala, N. Fukuda, M. Ikeda, O. T. Katuro, S. I. Tachibana, M. Yamauchi, W. Opio, S. Emoto, D. A. Anywar, E. Kimura, N. M. Q. Palacpac, E. I. Odongo-Aginya, M. Ogwang, T. Horii, T. Mita, Evidence of Artemisinin-Resistant Malaria in Africa. *N Engl J Med* **385**, 1163-1171 (2021).
47. N. K. Kayiba, D. M. Yobi, E. Tshibangu-Kabamba, V. P. Tuan, Y. Yamaoka, B. Devleesschauwer, D. M. Mvumbi, E. Okitolonda Wemakoy, P. De Mol, G. L. Mvumbi, M. P. Hayette, A. Rosas-Aguirre, N. Speybroeck, Spatial and molecular mapping of Pfkelch13 gene polymorphism in Africa in the era of emerging Plasmodium falciparum resistance to artemisinin: a systematic review. *Lancet Infect Dis* **21**, e82-e92 (2021).
48. S. Mok, E. A. Ashley, P. E. Ferreira, L. Zhu, Z. Lin, T. Yeo, K. Chotivanich, M. Imwong, S. Pukrittayakamee, M. Dhorda, C. Nguon, P. Lim, C. Amaratunga, S. Suon, T. T. Hien, Y.

Htut, M. A. Faiz, M. A. Onyamboko, M. Mayxay, P. N. Newton, R. Tripura, C. J. Woodrow, O. Miotto, D. P. Kwiatkowski, F. Nosten, N. P. Day, P. R. Preiser, N. J. White, A. M. Dondorp, R. M. Fairhurst, Z. Bozdech, Drug resistance. Population transcriptomics of human malaria parasites reveals the mechanism of artemisinin resistance. *Science* **347**, 431-435 (2015).
49. F. Ariey, B. Witkowski, C. Amaratunga, J. Beghain, A. C. Langlois, N. Khim, S. Kim, V. Duru, C. Bouchier, L. Ma, P. Lim, R. Leang, S. Duong, S. Sreng, S. Suon, C. M. Chuor, D. M. Bout, S. Menard, W. O. Rogers, B. Genton, T. Fandeur, O. Miotto, P. Ringwald, J. Le Bras, A. Berry, J. C. Barale, R. M. Fairhurst, F. Benoit-Vical, O. Mercereau-Puijalon, D. Menard, A molecular marker of artemisinin-resistant Plasmodium falciparum malaria. *Nature* **505**, 50-55 (2014).
50. S. Bopp, P. Magistrado, W. Wong, S. F. Schaffner, A. Mukherjee, P. Lim, M. Dhorda, C. Amaratunga, C. J. Woodrow, E. A. Ashley, Plasmepsin II–III copy number accounts for bimodal piperaquine resistance among Cambodian Plasmodium falciparum. *Nature communications* **9**, 1769 (2018).
51. R. Chakrabarti, J. White, P. H. Babar, S. Kumar, D. G. Mudeppa, A. Mascarenhas, L. Pereira, R. Dash, J. N. Maki, A. Sharma, K. Gogoi, D. K. Sarma, I. Pal Bhowmick, S. K. Manoharan, E. Gomes, J. Mahanta, P. K. Mohapatra, L. Chery, P. K. Rathod, Decreased In Vitro Artemisinin Sensitivity of Plasmodium falciparum across India. *Antimicrob Agents Chemother* **63**, 10.1128/aac. 00101-00119 (2019).
52. N. Mishra, R. S. Bharti, P. Mallick, O. P. Singh, B. Srivastava, R. Rana, S. Phookan, H. P. Gupta, P. Ringwald, N. Valecha, Emerging polymorphisms in falciparum Kelch 13 gene in Northeastern region of India. *Malar J* **15**, 583 (2016).
53. S. Das, B. Saha, A. K. Hati, S. Roy, Evidence of Artemisinin-Resistant Plasmodium falciparum Malaria in Eastern India. *N Engl J Med* **379**, 1962-1964 (2018).
54. D. Choubey, B. Deshmukh, A. G. Rao, A. Kanyal, A. K. Hati, S. Roy, K. Karmodiya, Genomic analysis of Indian isolates of Plasmodium falciparum: Implications for drug resistance and virulence factors. *Int J Parasitol Drugs Drug Resist* **22**, 52-60 (2023).
55. M. Rawat, A. Kanyal, D. Choubey, B. Deshmukh, R. Malhotra, D. V. Mamatharani, A. G. Rao, K. Karmodiya, Identification of Co-Existing Mutations and Gene Expression Trends Associated With K13-Mediated Artemisinin Resistance in Plasmodium falciparum. *Front Genet* **13**, 824483 (2022).
56. A. Ray, M. Mathur, D. Choubey, K. Karmodiya, N. Surolia, Autophagy Underlies the Proteostasis Mechanisms of Artemisinin Resistance in P. falciparum Malaria. *mBio* **13**, e0063022 (2022).
57. S. Sato, The apicomplexan plastid and its evolution. *Cell Mol Life Sci* **68**, 1285-1296 (2011).
58. E. Siński, J. M. Behnke, Apicomplexan parasites: Environmental contamination and transmission. *Polish journal of microbiology* **53**, 67 (2004).
59. M. J. Shears, C. Y. Botte, G. I. McFadden, Fatty acid metabolism in the Plasmodium apicoplast: Drugs, doubts and knockouts. *Mol Biochem Parasitol* **199**, 34-50 (2015).
60. I. Landau, J. M. Chavatte, W. Peters, A. Chabaud, The sub-genera of avian Plasmodium. *Parasite* **17**, 3-7 (2010).
61. D. J. Harris, J. L. Santos, D. M. Borges-Nojosa, D. P. de Castro, Molecular Screening of Plasmodium (Haemosporidia: Plasmodiidae) Parasites from Reptiles in Brazil. *J Parasitol* **105**, 913-917 (2019).
62. W. H. Organization, *World malaria report 2022*. (World Health Organization, 2022).
63. A. R. Anvikar, N. Shah, A. C. Dhariwal, G. S. Sonal, M. M. Pradhan, S. K. Ghosh, N. Valecha, Epidemiology of Plasmodium vivax Malaria in India. *Am J Trop Med Hyg* **95**, 108-120 (2016).

64. I. K. Quaye, L. Aleksenko, C. Oeuvray, D. Yewhalaw, N. Duah, B. Gyan, D. H. Haiyambo, G. B. D. Dongho, R. A. Torgby, L. Amoah, M. A. Hamid, S. Worku, A. A. Bahiti, H. A. Pasquale, M. Bitshi, I. Troare, A. Diarra, E. Njunju, M. Cisse, I. Soulama, R. J. Savadogo, S. Issifou, A. Niangaly, L. Dembele, B. Greco, The Pan African Vivax and Ovale Network (PAVON): Refocusing on Plasmodium vivax, ovale and asymptomatic malaria in sub-Saharan Africa. *Parasitol Int* **84**, 102415 (2021).
65. J. X. D. Ang, K. A. Kadir, D. S. A. Mohamad, A. Matusop, P. C. S. Divis, K. Yaman, B. Singh, New vectors in northern Sarawak, Malaysian Borneo, for the zoonotic malaria parasite, Plasmodium knowlesi. *Parasit Vectors* **13**, 472 (2020).
66. B. Singh, L. Kim Sung, A. Matusop, A. Radhakrishnan, S. S. Shamsul, J. Cox-Singh, A. Thomas, D. J. Conway, A large focus of naturally acquired Plasmodium knowlesi infections in human beings. *Lancet* **363**, 1017-1024 (2004).
67. M. T. Zaw, Z. Lin, Human Plasmodium knowlesi infections in South-East Asian countries. *J Microbiol Immunol Infect* **52**, 679-684 (2019).
68. M. Enomoto, S. Kawazu, S. Kawai, W. Furuyama, T. Ikegami, J. Watanabe, K. Mikoshiba, Blockage of spontaneous Ca2+ oscillation causes cell death in intraerythrocitic Plasmodium falciparum. *PLoS One* **7**, e39499 (2012).
69. A. M. Vaughan, S. H. I. Kappe, Malaria Parasite Liver Infection and Exoerythrocytic Biology. *Cold Spring Harb Perspect Med* **7**, a025486 (2017).
70. V. Soulard, H. Bosson-Vanga, A. Lorthiois, C. Roucher, J. F. Franetich, G. Zanghi, M. Bordessoulles, M. Tefit, M. Thellier, S. Morosan, G. Le Naour, F. Capron, H. Suemizu, G. Snounou, A. Moreno-Sabater, D. Mazier, Plasmodium falciparum full life cycle and Plasmodium ovale liver stages in humanized mice. *Nat Commun* **6**, 7690 (2015).
71. D. A. Baker, Malaria gametocytogenesis. *Mol Biochem Parasitol* **172**, 57-65 (2010).
72. R. E. Sinden, E. U. Canning, R. S. Bray, M. E. Smalley, Gametocyte and gamete development in Plasmodium falciparum. *Proc R Soc Lond B Biol Sci* **201**, 375-399 (1978).
73. A. M. Talman, O. Domarle, F. E. McKenzie, F. Ariey, V. Robert, Gametocytogenesis: the puberty of Plasmodium falciparum. *Malar J* **3**, 24 (2004).
74. R. S. Osii, T. D. Otto, P. Garside, F. M. Ndungu, J. M. Brewer, The impact of malaria parasites on dendritic cell–T cell interaction. *Frontiers in Immunology* **11**, 529857 (2020).
75. M. J. Donovan, A. S. Messmore, D. A. Scrafford, D. L. Sacks, S. Kamhawi, M. A. McDowell, Uninfected mosquito bites confer protection against infection with malaria parasites. *Infect Immun* **75**, 2523-2530 (2007).
76. N. Villarino, N. W. Schmidt, CD8(+) T Cell Responses to Plasmodium and Intracellular Parasites. *Curr Immunol Rev* **9**, 169-178 (2013).
77. S. Chakravarty, I. A. Cockburn, S. Kuk, M. G. Overstreet, J. B. Sacci, F. Zavala, CD8+ T lymphocytes protective against malaria liver stages are primed in skin-draining lymph nodes. *Nat Med* **13**, 1035-1041 (2007).
78. L. Mac-Daniel, M. R. Buckwalter, M. Berthet, Y. Virk, K. Yui, M. L. Albert, P. Gueirard, R. Ménard, Local Immune Response to Injection of *Plasmodium falciparum* Sporozoites into the Skin. *Journal of Immunology* **193**, 1246-1257 (2014).
79. C. S. Hopp, P. Sinnis, The innate and adaptive response to mosquito saliva and Plasmodium sporozoites in the skin. *Ann N Y Acad Sci* **1342**, 37-43 (2015).
80. E. B. Belachew, Immune Response and Evasion Mechanisms of Plasmodium falciparum Parasites. *J Immunol Res* **2018**, 6529681 (2018).
81. G. Feng, B. D. Wines, L. Kurtovic, J.-A. Chan, P. Boeuf, V. Mollard, A. Cozijnsen, D. R. Drew, R. J. Center, D. L. Marshall, Mechanisms and targets of Fcγ-receptor mediated immunity to malaria sporozoites. *Nature communications* **12**, 1742 (2021).

82. J. L. Miller, B. K. Sack, M. Baldwin, A. M. Vaughan, S. H. I. Kappe, Interferon-mediated innate immune responses against malaria parasite liver stages. *Cell Rep* **7**, 436-447 (2014).
83. P. Liehl, V. Zuzarte-Luis, J. Chan, T. Zillinger, F. Baptista, D. Carapau, M. Konert, K. K. Hanson, C. Carret, C. Lassnig, M. Muller, U. Kalinke, M. Saeed, A. F. Chora, D. T. Golenbock, B. Strobl, M. Prudencio, L. P. Coelho, S. H. Kappe, G. Superti-Furga, A. Pichlmair, A. M. Vigario, C. M. Rice, K. A. Fitzgerald, W. Barchet, M. M. Mota, Host-cell sensors for Plasmodium activate innate immunity against liver-stage infection. *Nat Med* **20**, 47-53 (2014).
84. C. A. Ezema, I. U. Okagu, T. P. C. Ezeorba, Escaping the enemy's bullets: an update on how malaria parasites evade host immune response. *Parasitology research* **122**, 1715-1731 (2023).
85. S. Sharma, R. B. DeOliveira, P. Kalantari, P. Parroche, N. Goutagny, Z. Jiang, J. Chan, D. C. Bartholomeu, F. Lauw, J. P. Hall, G. N. Barber, R. T. Gazzinelli, K. A. Fitzgerald, D. T. Golenbock, Innate immune recognition of an AT-rich stem-loop DNA motif in the Plasmodium falciparum genome. *Immunity* **35**, 194-207 (2011).
86. R. Boonhok, N. Rachaphaew, A. Duangmanee, P. Chobson, S. Pattaradilokrat, P. Utaisincharoen, J. Sattabongkot, M. Ponpuak, LAP-like process as an immune mechanism downstream of IFN-γ in control of the human malaria Plasmodium vivax liver stage. *Proceedings of the National Academy of Sciences* **113**, E3519-E3528 (2016).
87. R. Adamou, C. Dechavanne, I. Sadissou, T. d'Almeida, A. Bouraima, P. Sonon, R. Amoussa, G. Cottrell, A. Le Port, M. Theisen, E. J. Remarque, S. Longacre, K. Moutairou, A. Massougbodji, A. J. F. Luty, G. Nuel, F. Migot-Nabias, A. Sanni, A. Garcia, J. Milet, D. Courtin, Plasmodium falciparum merozoite surface antigen-specific cytophilic IgG and control of malaria infection in a Beninese birth cohort. *Malar J* **18**, 194 (2019).
88. A. Jaschke, B. Coulibaly, E. J. Remarque, H. Bujard, C. Epp, Merozoite Surface Protein 1 from Plasmodium falciparum Is a Major Target of Opsonizing Antibodies in Individuals with Acquired Immunity against Malaria. *Clin Vaccine Immunol* **24**, e00155-00117 (2017).
89. F. H. Osier, G. Fegan, S. D. Polley, L. Murungi, F. Verra, K. K. Tetteh, B. Lowe, T. Mwangi, P. C. Bull, A. W. Thomas, D. R. Cavanagh, J. S. McBride, D. E. Lanar, M. J. Mackinnon, D. J. Conway, K. Marsh, Breadth and magnitude of antibody responses to multiple Plasmodium falciparum merozoite antigens are associated with protection from clinical malaria. *Infect Immun* **76**, 2240-2248 (2008).
90. F. H. Osier, M. J. Mackinnon, C. Crosnier, G. Fegan, G. Kamuyu, M. Wanaguru, E. Ogada, B. McDade, J. C. Rayner, G. J. Wright, K. Marsh, New antigens for a multicomponent blood-stage malaria vaccine. *Sci Transl Med* **6**, 247ra102 (2014).
91. S. B. Reddy, R. F. Anders, J. G. Beeson, A. Farnert, F. Kironde, S. K. Berenzon, M. Wahlgren, S. Linse, K. E. Persson, High affinity antibodies to Plasmodium falciparum merozoite antigens are associated with protection from malaria. *PLoS One* **7**, e32242 (2012).
92. A. N. Bucşan, K. C. Williamson, Setting the stage: The initial immune response to blood-stage parasites. *Virulence* **11**, 88-103 (2020).
93. M. Eberl, What you, too, should know about BTN2A1 Antigen recognition by human γδ T cells: one step closer to knowing. *Immunology and Cell Biology* **98**, 351-354 (2020).
94. T. Herrmann, A. S. Fichtner, M. M. Karunakaran, An update on the molecular basis of phosphoantigen recognition by Vγ9Vδ2 T cells. *Cells* **9**, 1433 (2020).
95. S. R. Elliott, T. P. Spurck, J. M. Dodin, A. G. Maier, T. S. Voss, F. Yosaatmadja, P. D. Payne, G. I. McFadden, A. F. Cowman, S. J. Rogerson, Inhibition of dendritic cell maturation by malaria is dose dependent and does not require Plasmodium falciparum erythrocyte membrane protein 1. *Infection immunity* **75**, 3621-3632 (2007).

96. M. Guenot, S. Loizon, J. Howard, G. Costa, D. A. Baker, S. Y. Mohabeer, M. Troye-Blomberg, J.-F. Moreau, J. Déchanet-Merville, O. J. I. Mercereau-Puijalon, immunity, Phosphoantigen burst upon Plasmodium falciparum schizont rupture can distantly activate Vγ9Vδ2 T cells. **83**, 3816-3824 (2015).
97. R. T. Gazzinelli, P. Kalantari, K. A. Fitzgerald, D. T. Golenbock, Innate sensing of malaria parasites. *Nat Rev Immunol* **14**, 744-757 (2014).
98. K. A. Babatunde, O. F. Adenuga, Neutrophils in malaria: A double-edged sword role. *Front Immunol* **13**, 922377 (2022).
99. S. Kho, G. Minigo, B. Andries, L. Leonardo, P. Prayoga, J. R. Poespoprodjo, E. Kenangalem, R. N. Price, T. Woodberry, N. M. Anstey, T. W. Yeo, Circulating Neutrophil Extracellular Traps and Neutrophil Activation Are Increased in Proportion to Disease Severity in Human Malaria. *J Infect Dis* **219**, 1994-2004 (2019).
100. S. M. Meinderts, P. A. Oldenborg, B. M. Beuger, T. R. L. Klei, J. Johansson, T. W. Kuijpers, T. Matozaki, E. J. Huisman, M. de Haas, T. K. van den Berg, R. van Bruggen, Human and murine splenic neutrophils are potent phagocytes of IgG-opsonized red blood cells. *Blood Adv* **1**, 875-886 (2017).
101. M. Depond, B. Henry, P. Buffet, P. A. Ndour, Methods to Investigate the Deformability of RBC During Malaria. *Front Physiol* **10**, 1613 (2019).
102. N. D. Pasternak, R. Dzikowski, PfEMP1: an antigen that plays a key role in the pathogenicity and immune evasion of the malaria parasite Plasmodium falciparum. *Int J Biochem Cell Biol* **41**, 1463-1466 (2009).
103. A. Scherf, J. J. Lopez-Rubio, L. Riviere, Antigenic variation in Plasmodium falciparum. *Annu Rev Microbiol* **62**, 445-470 (2008).
104. A. R. Jensen, Y. Adams, L. Hviid, Cerebral Plasmodium falciparum malaria: The role of PfEMP1 in its pathogenesis and immunity, and PfEMP1-based vaccines to prevent it. *Immunol Rev* **293**, 230-252 (2020).
105. R. W. Olsen, G. Ecklu-Mensah, A. Bengtsson, M. F. Ofori, J. P. A. Lusingu, F. C. Castberg, L. Hviid, Y. Adams, A. T. R. Jensen, Natural and Vaccine-Induced Acquisition of Cross-Reactive IgG-Inhibiting ICAM-1-Specific Binding of a Plasmodium falciparum PfEMP1 Subtype Associated Specifically with Cerebral Malaria. *Infect Immun* **86**, 10.1128/iai. 00622-00617 (2018).
106. Y. Fastman, R. Noble, M. Recker, R. Dzikowski, Erasing the epigenetic memory and beginning to switch--the onset of antigenic switching of var genes in Plasmodium falciparum. *PLoS One* **7**, e34168 (2012).
107. S. K. Tessema, R. Nakajima, A. Jasinskas, S. L. Monk, L. Lekieffre, E. Lin, B. Kiniboro, C. Proietti, P. Siba, P. L. Felgner, D. L. Doolan, I. Mueller, A. E. Barry, Protective Immunity against Severe Malaria in Children Is Associated with a Limited Repertoire of Antibodies to Conserved PfEMP1 Variants. *Cell Host Microbe* **26**, 579-590 e575 (2019).
108. J. Dunst, F. Kamena, K. Matuschewski, Cytokines and Chemokines in Cerebral Malaria Pathogenesis. *Front Cell Infect Microbiol* **7**, 324 (2017).
109. V. Lorenz, P. Karanis, Malaria vaccines: looking back and lessons learnt. *Asian Pac J Trop Biomed* **1**, 74-78 (2011).
110. S. L. Hoffman, P. F. Billingsley, E. James, A. Richman, M. Loyevsky, T. Li, S. Chakravarty, A. Gunasekera, R. Chattopadhyay, M. Li, R. Stafford, A. Ahumada, J. E. Epstein, M. Sedegah, S. Reyes, T. L. Richie, K. E. Lyke, R. Edelman, M. B. Laurens, C. V. Plowe, B. K. Sim, Development of a metabolically active, non-replicating sporozoite vaccine to prevent Plasmodium falciparum malaria. *Hum Vaccin* **6**, 97-106 (2010).
111. L. Rénia, Y. S. Goh, Malaria parasites: the great escape. *Frontiers in immunology* **7**, 226450 (2016).
112. V. Nussenzweig, R. S. Nussenzweig, Recent advances in the development of a sporozoite vaccine for malaria. *Asian Pac J Allergy Immunol* **2**, 289-292 (1984).

113. D. F. Clyde, Immunization of man against falciparum and vivax malaria by use of attenuated sporozoites. *Am J Trop Med Hyg* **24**, 397-401 (1975).
114. D. F. Clyde, H. Most, V. C. Mccarthy, J. P. Vanderberg, Immunization of man against sporozoite-induced falciparum malaria. *American journal of medical sciences* **266**, 169-177 (1973).
115. R. F. Anders, C. G. Adda, M. Foley, R. S. Norton, Recombinant protein vaccines against the asexual blood stages of Plasmodium falciparum. *Hum Vaccin* **6**, 39-53 (2010).
116. J. B. Dame, J. L. Williams, T. F. McCutchan, J. L. Weber, R. A. Wirtz, W. T. Hockmeyer, W. L. Maloy, J. D. Haynes, I. Schneider, D. Roberts, et al., Structure of the gene encoding the immunodominant surface antigen on the sporozoite of the human malaria parasite Plasmodium falciparum. *Science* **225**, 593-599 (1984).
117. S. Mian-McCarthy, S. T. Agnandji, B. Lell, J. F. Fernandes, B. P. Abossolo, B. G. N. O. Methogo, A. L. Kabwende, A. A. Adegnika, B. Mordmüller, S. Issifou, P. G. Kremsner, J. Sacarlal, P. Aide, M. Lanaspa, J. J. Aponte, S. Machevo, S. Acacio, H. Bulo, B. Sigauque, E. Macete, P. Alonso, S. Abdulla, N. Salim, R. Minja, M. Mpina, S. Ahmed, A. M. Ali, A. T. Mtoro, A. S. Hamad, P. Mutani, M. Tanner, H. Tinto, U. D'Alessandro, H. Sorgho, I. Valea, B. Bihoun, I. Guiraud, B. Kaboré, O. Sombié, R. T. Guiguemdé, J. B. Ouédraogo, M. J. Hamel, S. Kariuki, M. Oneko, C. Odero, K. Otieno, N. Awino, M. McMorrow, V. Muturi-Kioi, K. F. Laserson, L. Slutsker, W. Otieno, L. Otieno, N. Otsyula, S. Gondi, A. Otieno, V. Owira, E. Oguk, G. Odongo, J. Ben Woods, B. Ogutu, P. Njuguna, R. Chilengi, P. Akoo, C. Kerubo, C. Maingi, T. Lang, A. Olotu, P. Bejon, K. Marsh, G. Mwanbingu, S. Owusu-Agyei, K. P. Asante, K. Osei-Kwakye, O. Boahen, D. Dosoo, I. Asante, G. Adjei, E. Kwara, D. Chandramohan, B. Greenwood, J. Lusingu, S. Gesase, A. Malabeja, O. Abdul, C. Mahende, E. Liheluka, L. Malle, M. Lemnge, T. G. Theander, C. Drakeley, D. Ansong, T. Agbenyega, S. Adjei, H. O. Boateng, T. Rettig, J. Bawa, J. Sylverken, D. Sambian, A. Sarfo, A. Agyekum, F. Martinson, I. Hoffman, T. Mvalo, P. Kamthunzi, R. Nkomo, T. Tembo, G. Tegha, M. Tsidya, J. Kilembe, C. Chawinga, W. R. Ballou, J. Cohen, Y. Guerra, E. Jongert, D. Lapierre, A. Leach, M. Lievens, O. Ofori-Anyinam, A. Olivier, J. Vekemans, T. Carter, D. Kaslow, D. Leboulleux, C. Loucq, A. Radford, B. Savarese, D. Schellenberg, M. Sillman, P. Vansadia, R. S. C. T. Partnership, A Phase 3 Trial of RTS,S/AS01 Malaria Vaccine in African Infants. *New England Journal of Medicine* **367**, 2284-2295 (2012).
118. P. A. Minsoko, B. Lell, J. F. Fernandes, B. P. Abossolo, A. L. Kabwende, A. A. Adegnika, B. Mordmüller, S. Issifou, P. G. Kremsner, M. M. Loembe, J. Sacarlal, P. Aide, L. Madrid, M. Lanaspa, S. Mandjate, J. J. Aponte, H. Bulo, A. Nhama, E. Macete, P. Alonso, S. Abdulla, N. Salim, A. T. Mtoro, P. Mutani, M. Tanner, C. Mavere, G. Mwangoka, O. Lweno, O. A. Juma, S. Shekalaghe, H. Tinto, U. D'Alessandro, H. Sorgho, I. Valea, J. B. Ouédraogo, P. Lompo, S. Diallo, O. Traore, A. Bassole, E. Dao, M. J. Hamel, S. Kariuki, M. Oneko, C. Odero, K. Otieno, N. Awino, V. Muturi-Kioi, J. Omoto, K. F. Laserson, L. Slutsker, W. Otieno, L. Otieno, N. Otsyula, S. Gondi, A. Otieno, B. Ogutu, J. Ochola, I. Onyango, J. Oyieko, P. Njuguna, R. Chilengi, P. Akoo, C. Kerubo, C. Maingi, A. Olotu, P. Bejon, K. Marsh, G. Mwabingu, J. Gitaka, S. Owusu-Agyei, K. P. Asante, O. Boahen, D. Dosoo, G. Adjei, E. Adeniji, A. K. Yawson, K. Kayan, D. Chandramohan, B. Greenwood, J. Lusingu, S. Gesase, A. Malabeja, O. Abdul, C. Mahende, E. Liheluka, M. Lemnge, T. G. Theander, C. Drakeley, J. Mbwana, D. Ansong, T. Agbenyega, S. Adjei, H. O. Boateng, T. Rettig, J. Bawa, J. Sylverken, D. Sambian, A. Sarfo, A. Agyekum, F. Martinson, I. Hoffman, T. Mvalo, P. Kamthunzi, R. Nkomo, T. Tembo, G. T. M. Tsidya, J. Kilembe, C. Chawinga, W. R. Ballou, J. Cohen, Y. Guerra, E. Jongert, D. Lapierre, A. Leach, M. Lievens, O. Ofori-Anyinam, A. Olivier, J. Vekemans, D. Kaslow, D. Leboulleux, B. Savarese, D. Schellenberg, R. S. C. T. Partnership, Efficacy and Safety of the RTS,S/AS01 Malaria Vaccine during 18 Months after Vaccination: A Phase 3

Randomized, Controlled Trial in Children and Young Infants at 11 African Sites. *Plos Medicine* **11**, e1001685 (2014).
119. H. Tinto, U. D'Alessandro, H. Sorgho, I. Valea, M. C. Tahita, W. Kabore, F. Kiemde, P. Lompo, S. Ouédraogo, K. Derra, F. Ouédraogo, J. B. Ouédraogo, W. R. Ballou, J. Cohen, Y. Guerra, D. Heerwegh, E. Jongert, D. Lapierre, A. Leach, M. Lievens, O. Ofori-Anyinam, A. Olivier, J. Vekemans, S. T. Agnandji, B. Lell, J. F. Fernandes, B. P. Abossolo, A. L. Kabwende, A. A. Adegnika, B. Mordmüller, S. Issifou, P. G. Kremsner, M. M. Loembe, E. Bache, A. Alabi, S. Owusu-Agyei, K. P. Asante, O. Boahen, D. Dosoo, I. Asante, Z. Yidana, J. Anim, E. Adeniji, A. K. Yawson, K. Kayan, D. Chandramohan, B. Greenwood, D. Ansong, T. Agbenyega, S. Adjei, H. O. Boateng, T. Rettig, J. Sylverken, D. Sambian, A. Badu-Prepah, A. Kotey, P. Buabeng, V. Paintsil, A. Enimil, M. J. Hamel, S. Kariuki, M. Oneko, C. Odero, K. Otieno, N. Awino, V. Muturi-Kioi, J. Omoto, T. Sang, S. Odhiambo, K. F. Laserson, L. Slutsker, W. Otieno, L. Otieno, N. Otsyula, S. Gondi, J. Ochola, G. Okoth, D. C. Mabunde, A. Wangwe, A. Otieno, J. Oyieko, J. Cowden, B. Ogutu, P. Njuguna, K. Marsh, P. Akoo, C. Kerubo, C. Maingi, P. Bejon, A. Olotu, R. Chilengi, B. Tsofa, T. Lang, J. Gitaka, K. Awuondo, F. Martinson, I. Hoffman, T. Mvalo, P. Kamthunzi, R. Nkomo, T. Tembo, G. Tegha, C. Chawinga, T. Banda, S. Khan, S. Mwambakulu, E. Mzembe, J. Sacarlal, P. Aide, L. Madrid, S. Mandjate, J. J. Aponte, H. Bulo, S. Massora, E. Varela, E. Macete, P. Alonso, J. Lusingu, S. Gesase, A. Malabeja, O. Abdul, C. Mahende, E. Liheluka, M. Lemnge, T. G. Theander, C. Drakeley, J. Mbwana, R. Olomi, B. Mmbando, S. Abdulla, N. Salim, A. Mtoro, S. Ahmed, A. Hamad, S. Kafuruki, R. Minja, M. Tanner, M. Maganga, A. Mdemu, C. Gwandu, A. Mohammed, D. Kaslow, D. Leboulleux, B. Savarese, D. Schellenberg, R. S. C. T. Partnership, Efficacy and safety of RTS,S/AS01 malaria vaccine with or without a booster dose in infants and children in Africa: final results of a phase 3, individually randomised, controlled trial. *Lancet* **386**, 31-45 (2015).
120. M. S. Datoo, M. H. Natama, A. Some, O. Traore, T. Rouamba, D. Bellamy, P. Yameogo, D. Valia, M. Tegneri, F. Ouedraogo, R. Soma, S. Sawadogo, F. Sorgho, K. Derra, E. Rouamba, B. Orindi, F. Ramos Lopez, A. Flaxman, F. Cappuccini, R. Kailath, S. Elias, E. Mukhopadhyay, A. Noe, M. Cairns, A. Lawrie, R. Roberts, I. Valea, H. Sorgho, N. Williams, G. Glenn, L. Fries, J. Reimer, K. J. Ewer, U. Shaligram, A. V. S. Hill, H. Tinto, Efficacy of a low-dose candidate malaria vaccine, R21 in adjuvant Matrix-M, with seasonal administration to children in Burkina Faso: a randomised controlled trial. *Lancet* **397**, 1809-1818 (2021).
121. A. Verma, A. Anand, V. A. Patel, M. W. Nazar, A. Mukherjee, K. A. Karim, M. O. Oduoye, P. Satapathy, S. Rustagi, Breaking the malaria barrier: the WHO-approved R21/Matrix-M vaccine and its global impact–an editorial. *Annals of Medicine Surgery* **86**, 1824-1827 (2024).
122. P. E. Duffy, J. Patrick Gorres, Malaria vaccines since 2000: progress, priorities, products. *NPJ Vaccines* **5**, 48 (2020).
123. J. C. Dejon-Agobe, U. Ateba-Ngoa, A. Lalremruata, A. Homoet, J. Engelhorn, O. P. Nouatin, J. R. Edoa, J. F. Fernandes, M. Esen, Y. D. Mouwenda, E. M. Betouke Ongwe, M. Massinga-Loembe, S. L. Hoffman, B. K. L. Sim, M. Theisen, P. G. Kremsner, A. A. Adegnika, B. Lell, B. Mordmuller, Controlled Human Malaria Infection of Healthy Adults With Lifelong Malaria Exposure to Assess Safety, Immunogenicity, and Efficacy of the Asexual Blood Stage Malaria Vaccine Candidate GMZ2. *Clin Infect Dis* **69**, 1377-1384 (2019).
124. B. Mordmüller, G. Surat, H. Lagler, S. Chakravarty, A. S. Ishizuka, A. Lalremruata, M. Gmeiner, J. J. Campo, M. Esen, A. J. Ruben, Sterile protection against human malaria by chemoattenuated PfSPZ vaccine. *Nature* **542**, 445-449 (2017).

125. T. L. Richie, P. F. Billingsley, B. K. Sim, E. R. James, S. Chakravarty, J. E. Epstein, K. E. Lyke, B. Mordmuller, P. Alonso, P. E. Duffy, O. K. Doumbo, R. W. Sauerwein, M. Tanner, S. Abdulla, P. G. Kremsner, R. A. Seder, S. L. Hoffman, Progress with Plasmodium falciparum sporozoite (PfSPZ)-based malaria vaccines. *Vaccine* **33**, 7452-7461 (2015).
126. M. S. Sissoko, S. A. Healy, A. Katile, F. Omaswa, I. Zaidi, E. E. Gabriel, B. Kamate, Y. Samake, M. A. Guindo, A. Dolo, A. Niangaly, K. Niare, A. Zeguime, K. Sissoko, H. Diallo, I. Thera, K. Ding, M. P. Fay, E. M. O'Connell, T. B. Nutman, S. Wong-Madden, T. Murshedkar, A. J. Ruben, M. Li, Y. Abebe, A. Manoj, A. Gunasekera, S. Chakravarty, B. K. L. Sim, P. F. Billingsley, E. R. James, M. Walther, T. L. Richie, S. L. Hoffman, O. Doumbo, P. E. Duffy, Safety and efficacy of PfSPZ Vaccine against Plasmodium falciparum via direct venous inoculation in healthy malaria-exposed adults in Mali: a randomised, double-blind phase 1 trial. *Lancet Infect Dis* **17**, 498-509 (2017).
127. J. Walk, I. J. Reuling, M. C. Behet, L. Meerstein-Kessel, W. Graumans, G. J. van Gemert, R. Siebelink-Stoter, M. van de Vegte-Bolmer, T. Janssen, K. Teelen, J. H. W. de Wilt, Q. de Mast, A. J. van der Ven, E. Diez Benavente, S. Campino, T. G. Clark, M. A. Huynen, C. C. Hermsen, E. M. Bijker, A. Scholzen, R. W. Sauerwein, Modest heterologous protection after Plasmodium falciparum sporozoite immunization: a double-blind randomized controlled clinical trial. *BMC Med* **15**, 168 (2017).
128. E. S. Bergmann-Leitner, R. M. Mease, P. De La Vega, T. Savranskaya, M. Polhemus, C. Ockenhouse, E. Angov, Immunization with pre-erythrocytic antigen CelTOS from Plasmodium falciparum elicits cross-species protection against heterologous challenge with Plasmodium berghei. *PLoS One* **5**, e12294 (2010).
129. R. Carter, D. H. Chen, Malaria transmission blocked by immunisation with gametes of the malaria parasite. *Nature* **263**, 57-60 (1976).
130. C. A. Grotendorst, N. Kumar, R. Carter, D. C. Kaushal, A Surface Protein Expressed during the Transformation of Zygotes of Plasmodium-Gallinaceum Is a Target of Transmission-Blocking Antibodies. *Infection and Immunity* **45**, 775-777 (1984).
131. D. Read, A. Lensen, S. Begarnie, S. Haley, A. Raza, R. Carter, Transmission-blocking antibodies against multiple, non-variant target epitopes of the Plasmodium falciparum gamete surface antigen Pfs230 are all complement-fixing. *Parasite immunology* **16**, 511-519 (1994).
132. P. E. Duffy, P. Pimenta, D. C. Kaslow, Pgs28 Belongs to a Family of Epidermal Growth-Factor Like Antigens That Are Targets of Malaria Transmission-Blocking Antibodies. *Journal of Experimental Medicine* **177**, 505-510 (1993).
133. M. C. Kapulu, D. F. Da, K. Miura, Y. Li, A. M. Blagborough, T. S. Churcher, D. Nikolaeva, A. R. Williams, A. L. Goodman, I. Sangare, A. V. Turner, M. G. Cottingham, A. Nicosia, U. Straschil, T. Tsuboi, S. C. Gilbert, C. A. Long, R. E. Sinden, S. J. Draper, A. V. Hill, A. Cohuet, S. Biswas, Comparative assessment of transmission-blocking vaccine candidates against Plasmodium falciparum. *Sci Rep* **5**, 11193 (2015).
134. V. Menon, M. C. Kapulu, I. Taylor, K. Jewell, Y. Li, F. Hill, C. A. Long, K. Miura, S. Biswas, Assessment of Antibodies Induced by Multivalent Transmission-Blocking Malaria Vaccines. *Front Immunol* **8**, 1998 (2017).
135. J. S. Richards, J. G. Beeson, The future for blood-stage vaccines against malaria. *Immunol Cell Biol* **87**, 377-390 (2009).
136. S. Cohen, G. I. Mc, S. Carrington, Gamma-globulin and acquired immunity to human malaria. *Nature* **192**, 733-737 (1961).
137. I. McGregor, S. Carrington, S. Cohen, Treatment of East African P. falciparum malaria with West African human γ-globulin. *Trans R Soc Trop Med Hyg* **57**, 170-175 (1963).
138. W. A. Siddiqui, An effective immunization of experimental monkeys against a human malaria parasite, Plasmodium falciparum. *Science* **197**, 388-389 (1977).

139. M. D. Spring, J. F. Cummings, C. F. Ockenhouse, S. Dutta, R. Reidler, E. Angov, E. Bergmann-Leitner, V. A. Stewart, S. Bittner, L. Juompan, M. G. Kortepeter, R. Nielsen, U. Krzych, E. Tierney, L. A. Ware, M. Dowler, C. C. Hermsen, R. W. Sauerwein, S. J. de Vlas, O. Ofori-Anyinam, D. E. Lanar, J. L. Williams, K. E. Kester, K. Tucker, M. Shi, E. Malkin, C. Long, C. L. Diggs, L. Soisson, M. C. Dubois, W. R. Ballou, J. Cohen, D. G. Heppner, Jr., Phase 1/2a study of the malaria vaccine candidate apical membrane antigen-1 (AMA-1) administered in adjuvant system AS01B or AS02A. *PLoS One* **4**, e5254 (2009).
140. J. Healer, W. Wong, J. K. Thompson, W. He, R. W. Birkinshaw, K. Miura, C. A. Long, V. Soroka, T. M. M. Sogaard, T. Jorgensen, W. A. de Jongh, C. Weir, E. Svahn, P. E. Czabotar, W. H. Tham, I. Mueller, P. N. Barlow, A. F. Cowman, Neutralising antibodies block the function of Rh5/Ripr/CyRPA complex during invasion of Plasmodium falciparum into human erythrocytes. *Cell Microbiol* **21**, e13030 (2019).
141. A. M. Minassian, S. E. Silk, J. R. Barrett, C. M. Nielsen, K. Miura, A. Diouf, C. Loos, J. K. Fallon, A. R. Michell, M. T. White, N. J. Edwards, I. D. Poulton, C. H. Mitton, R. O. Payne, M. Marks, H. Maxwell-Scott, A. Querol-Rubiera, K. Bisnauthsing, R. Batra, T. Ogrina, N. J. Brendish, Y. Themistocleous, T. A. Rawlinson, K. J. Ellis, D. Quinkert, M. Baker, R. Lopez Ramon, F. Ramos Lopez, L. Barfod, P. M. Folegatti, D. Silman, M. Datoo, I. J. Taylor, J. Jin, D. Pulido, A. D. Douglas, W. A. de Jongh, R. Smith, E. Berrie, A. R. Noe, C. L. Diggs, L. A. Soisson, R. Ashfield, S. N. Faust, A. L. Goodman, A. M. Lawrie, F. L. Nugent, G. Alter, C. A. Long, S. J. Draper, Reduced blood-stage malaria growth and immune correlates in humans following RH5 vaccination. *Med* **2**, 701-719 e719 (2021).
142. B. O. Baptista, A. B. L. de Souza, E. K. P. Riccio, C. Bianco-Junior, P. R. R. Totino, J. H. Martins da Silva, M. Theisen, S. K. Singh, L. E. Amoah, M. Ribeiro-Alves, R. M. Souza, J. C. Lima-Junior, C. T. Daniel-Ribeiro, L. R. Pratt-Riccio, Naturally acquired antibody response to a Plasmodium falciparum chimeric vaccine candidate GMZ2.6c and its components (MSP-3, GLURP, and Pfs48/45) in individuals living in Brazilian malaria-endemic areas. *Malar J* **21**, 6 (2022).
143. V. Meraldi, I. Nebie, A. B. Tiono, D. Diallo, E. Sanogo, M. Theisen, P. Druilhe, G. Corradin, R. Moret, B. S. Sirima, Natural antibody response to Plasmodium falciparum Exp-1, MSP-3 and GLURP long synthetic peptides and association with protection. *Parasite Immunol* **26**, 265-272 (2004).
144. S. H. Qari, Y. P. Shi, I. F. Goldman, B. L. Nahlen, M. Tibayrenc, A. A. Lal, Predicted and observed alleles of Plasmodium falciparum merozoite surface protein-1 (MSP-1), a potential malaria vaccine antigen. *Mol Biochem Parasitol* **92**, 241-252 (1998).
145. S. B. Sirima, S. Cousens, P. Druilhe, Protection against malaria by MSP3 candidate vaccine. *N Engl J Med* **365**, 1062-1064 (2011).
146. R. O. Payne, K. H. Milne, S. C. Elias, N. J. Edwards, A. D. Douglas, R. E. Brown, S. E. Silk, S. Biswas, K. Miura, R. Roberts, T. W. Rampling, N. Venkatraman, S. H. Hodgson, G. M. Labbe, F. D. Halstead, I. D. Poulton, F. L. Nugent, H. de Graaf, P. Sukhtankar, N. C. Williams, C. F. Ockenhouse, A. K. Kathcart, A. N. Qabar, N. C. Waters, L. A. Soisson, A. J. Birkett, G. S. Cooke, S. N. Faust, C. Woods, K. Ivinson, J. S. McCarthy, C. L. Diggs, J. Vekemans, C. A. Long, A. V. Hill, A. M. Lawrie, S. Dutta, S. J. Draper, Demonstration of the Blood-Stage Plasmodium falciparum Controlled Human Malaria Infection Model to Assess Efficacy of the P. falciparum Apical Membrane Antigen 1 Vaccine, FMP2.1/AS01. *J Infect Dis* **213**, 1743-1751 (2016).
147. J. A. Chan, F. J. Fowkes, J. G. Beeson, Surface antigens of Plasmodium falciparum-infected erythrocytes as immune targets and malaria vaccine candidates. *Cell Mol Life Sci* **71**, 3633-3657 (2014).

148. I. J. Udeinya, J. A. Schmidt, M. Aikawa, L. H. Miller, I. Green, Falciparum malaria-infected erythrocytes specifically bind to cultured human endothelial cells. *Science* **213**, 555-557 (1981).
149. R. Udomsangpetch, B. Wahlin, J. Carlson, K. Berzins, M. Torii, M. Aikawa, P. Perlmann, M. Wahlgren, Plasmodium falciparum-infected erythrocytes form spontaneous erythrocyte rosettes. *J Exp Med* **169**, 1835-1840 (1989).
150. A. Pain, D. J. Ferguson, O. Kai, B. C. Urban, B. Lowe, K. Marsh, D. J. Roberts, Platelet-mediated clumping of Plasmodium falciparum-infected erythrocytes is a common adhesive phenotype and is associated with severe malaria. *Proceedings of the National Academy of Sciences* **98**, 1805-1810 (2001).
151. R. S. Bray, R. E. Sinden, The sequestration of Plasmodium falciparum infected erythrocytes in the placenta. *Trans R Soc Trop Med Hyg* **73**, 716-719 (1979).
152. S. M. Kraemer, J. D. Smith, A family affair: var genes, PfEMP1 binding, and malaria disease. *Curr Opin Microbiol* **9**, 374-380 (2006).
153. A. T. Jensen, P. Magistrado, S. Sharp, L. Joergensen, T. Lavstsen, A. Chiucchiuini, A. Salanti, L. S. Vestergaard, J. P. Lusingu, R. Hermsen, R. Sauerwein, J. Christensen, M. A. Nielsen, L. Hviid, C. Sutherland, T. Staalsoe, T. G. Theander, Plasmodium falciparum associated with severe childhood malaria preferentially expresses PfEMP1 encoded by group A var genes. *J Exp Med* **199**, 1179-1190 (2004).
154. L. S. Ortolan, M. Avril, J. Xue, K. B. Seydel, Y. Zheng, J. D. Smith, Plasmodium falciparum Parasite Lines Expressing DC8 and Group A PfEMP1 Bind to Brain, Intestinal, and Kidney Endothelial Cells. *Front Cell Infect Microbiol* **12**, 813011 (2022).
155. J. A. Rowe, A. Claessens, R. A. Corrigan, M. Arman, Adhesion of Plasmodium falciparum-infected erythrocytes to human cells: molecular mechanisms and therapeutic implications. *Expert Rev Mol Med* **11**, e16 (2009).
156. Q. Chen, A. Heddini, A. Barragan, V. Fernandez, S. F. Pearce, M. Wahlgren, The semiconserved head structure of Plasmodium falciparum erythrocyte membrane protein 1 mediates binding to multiple independent host receptors. *J Exp Med* **192**, 1-10 (2000).
157. B. A. Robinson, T. L. Welch, J. D. Smith, Widespread functional specialization of Plasmodium falciparum erythrocyte membrane protein 1 family members to bind CD36 analysed across a parasite genome. *Mol Microbiol* **47**, 1265-1278 (2003).
158. F. L. Hsieh, L. Turner, J. R. Bolla, C. V. Robinson, T. Lavstsen, M. K. Higgins, The structural basis for CD36 binding by the malaria parasite. *Nat Commun* **7**, 12837 (2016).
159. L. Turner, T. Lavstsen, S. S. Berger, C. W. Wang, J. E. V. Petersen, M. Avril, A. J. Brazier, J. Freeth, J. S. Jespersen, M. A. Nielsen, P. Magistrado, J. Lusingu, J. D. Smith, M. K. Higgins, T. G. Theander, Severe malaria is associated with parasite binding to endothelial protein C receptor. *Nature* **498**, 502-+ (2013).
160. M. Avril, M. Bernabeu, M. Benjamin, A. J. Brazier, J. D. Smith, Interaction between Endothelial Protein C Receptor and Intercellular Adhesion Molecule 1 to Mediate Binding of
-Infected Erythrocytes to Endothelial Cells. *Mbio* **7**, 10.1128/mbio. 00615-00616 (2016).
161. A. L. Springer, L. M. Smith, D. Q. Mackay, S. O. Nelson, J. D. Smith, Functional interdependence of the DBLβ domain and c2 region for binding of the Plasmodium falciparum variant antigen to ICAM-1. *Molecular biochemical parasitology* **137**, 55-64 (2004).
162. A. V. Oleinikov, E. Amos, I. T. Frye, E. Rossnagle, T. K. Mutabingwa, M. Fried, P. E. Duffy, High Throughput Functional Assays of the Variant Antigen PfEMP1 Reveal a Single Domain in the 3D7
Genome that Binds ICAM1 with High Affinity and Is Targeted by Naturally Acquired Neutralizing Antibodies. *Plos Pathog* **5**, e1000386 (2009).

163. F. Lennartz, Y. Adams, A. Bengtsson, R. W. Olsen, L. Turner, N. T. Ndam, G. Ecklu-Mensah, A. Moussiliou, M. F. Ofori, B. Gamain, J. P. Lusingu, J. E. V. Petersen, C. W. Wang, S. Nunes-Silva, J. S. Jespersen, C. K. Y. Lau, T. G. Theander, T. Lavstsen, L. Hviid, M. K. Higgins, A. T. R. Jensen, Structure-Guided Identification of a Family of Dual Receptor-Binding PfEMP1 that Is Associated with Cerebral Malaria. *Cell Host & Microbe* **21**, 403-414 (2017).
164. L. B. Ochola, B. R. Siddondo, H. Ocholla, S. Nkya, E. N. Kimani, T. N. Williams, J. O. Makale, A. Liljander, B. C. Urban, P. C. Bull, T. Szestak, K. Marsh, A. G. Craig, Specific Receptor Usage in
Cytoadherence Is Associated with Disease Outcome. *Plos One* **6**, e14741 (2011).
165. J. Montgomery, F. A. Mphande, M. Berriman, A. Pain, S. J. Rogerson, T. E. Taylor, M. E. Molyneux, A. Craig, Differential var gene expression in the organs of patients dying of falciparum malaria. *Mol Microbiol* **65**, 959-967 (2007).
166. D. L. Doolan, C. Dobano, J. K. Baird, Acquired immunity to malaria. *Clin Microbiol Rev* **22**, 13-36, Table of Contents (2009).
167. G. K. Cham, L. Turner, J. Lusingu, L. Vestergaard, B. P. Mmbando, J. D. Kurtis, A. T. Jensen, A. Salanti, T. Lavstsen, T. G. Theander, Sequential, ordered acquisition of antibodies to Plasmodium falciparum erythrocyte membrane protein 1 domains. *J Immunol* **183**, 3356-3363 (2009).
168. N. Obeng-Adjei, D. B. Larremore, L. Turner, A. Ongoiba, S. Li, S. Doumbo, T. B. Yazew, K. Kayentao, L. H. Miller, B. Traore, S. K. Pierce, C. O. Buckee, T. Lavstsen, P. D. Crompton, T. M. Tran, Longitudinal analysis of naturally acquired PfEMP1 CIDR domain variant antibodies identifies associations with malaria protection. *JCI Insight* **5**, (2020).
169. A. Bengtsson, L. Joergensen, T. S. Rask, R. W. Olsen, M. A. Andersen, L. Turner, T. G. Theander, L. Hviid, M. K. Higgins, A. Craig, A. Brown, A. T. R. Jensen, A Novel Domain Cassette Identifies
PfEMP1 Proteins Binding ICAM-1 and Is a Target of Cross-Reactive, Adhesion-Inhibitory Antibodies. *Journal of Immunology* **190**, 240-249 (2013).
170. Q. Chen, F. Pettersson, A. M. Vogt, B. Schmidt, S. Ahuja, P. Liljeström, M. Wahlgren, Immunization with PfEMP1-DBL1α generates antibodies that disrupt rosettes and protect against the sequestration of Plasmodium falciparum-infected erythrocytes. *Vaccine* **22**, 2701-2712 (2004).
171. J. Y. A. Doritchamou, J. Suurbaar, N. Tuikue Ndam, Progress and new horizons toward a VAR2CSA-based placental malaria vaccine. *Expert Rev Vaccines* **20**, 215-226 (2021).
172. D. Waller, S. Krishna, J. Crawley, K. Miller, F. Nosten, D. Chapman, F. O. ter Kuile, C. Craddock, C. Berry, P. A. Holloway, et al., Clinical features and outcome of severe malaria in Gambian children. *Clin Infect Dis* **21**, 577-587 (1995).
173. R. Idro, N. E. Jenkins, C. R. Newton, Pathogenesis, clinical features, and neurological outcome of cerebral malaria. *Lancet Neurol* **4**, 827-840 (2005).
174. C. R. Newton, F. J. Kirkham, P. A. Winstanley, G. Pasvol, N. Peshu, D. A. Warrell, K. Marsh, Intracranial pressure in African children with cerebral malaria. *Lancet* **337**, 573-576 (1991).
175. C. R. Newton, D. A. Warrell, Neurological manifestations of falciparum malaria. *Ann Neurol* **43**, 695-702 (1998).
176. S. C. Wassmer, T. E. Taylor, P. K. Rathod, S. K. Mishra, S. Mohanty, M. Arevalo-Herrera, M. T. Duraisingh, J. D. Smith, Investigating the Pathogenesis of Severe Malaria: A Multidisciplinary and Cross-Geographical Approach. *Am J Trop Med Hyg* **93**, 42-56 (2015).
177. S. Mishra, S. Mohanty, S. Satpathy, D. Mohapatra, Cerebral malaria in adults—a description of 526 cases admitted to Ispat General Hospital in Rourkela, India. *Annals of Tropical Medicine Parasitology* **101**, 187-193 (2007).

178. K. Silamut, N. H. Phu, C. Whitty, G. D. Turner, K. Louwrier, N. T. Mai, J. A. Simpson, T. T. Hien, N. J. White, A quantitative analysis of the microvascular sequestration of malaria parasites in the human brain. *Am J Pathol* **155**, 395-410 (1999).
179. T. N. Ramos, D. C. Bullard, M. M. Darley, K. McDonald, D. F. Crawford, S. R. Barnum, Experimental cerebral malaria develops independently of endothelial expression of intercellular adhesion molecule-1 (icam-1). *J Biol Chem* **288**, 10962-10966 (2013).
180. A. Kessler, S. Dankwa, M. Bernabeu, V. Harawa, S. A. Danziger, F. Duffy, S. D. Kampondeni, M. J. Potchen, N. Dambrauskas, V. Vigdorovich, B. G. Oliver, S. E. Hochman, W. B. Mowrey, I. J. C. MacCormick, W. L. Mandala, S. J. Rogerson, D. N. Sather, J. D. Aitchison, T. E. Taylor, K. B. Seydel, J. D. Smith, K. Kim, Linking EPCR-Binding PfEMP1 to Brain Swelling in Pediatric Cerebral Malaria. *Cell Host Microbe* **22**, 601-614 e605 (2017).
181. M. Bernabeu, C. Howard, Y. Zheng, J. D. Smith, Bioengineered 3D Microvessels for Investigating Plasmodium falciparum Pathogenesis. *Trends Parasitol* **37**, 401-413 (2021).
182. G. Nishanth, D. Schlüter, Blood–brain barrier in cerebral malaria: pathogenesis and therapeutic intervention. *Trends in parasitology* **35**, 516-528 (2019).
183. L. V. Mohan Rao, C. T. Esmon, U. R. Pendurthi, Endothelial cell protein C receptor: a multiliganded and multifunctional receptor. *Blood* **124**, 1553-1562 (2014).
184. A. L. Conroy, S. J. Glover, M. Hawkes, L. K. Erdman, K. B. Seydel, T. E. Taylor, M. E. Molyneux, K. C. Kain, Angiopoietin-2 levels are associated with retinopathy and predict mortality in Malawian children with cerebral malaria: a retrospective case–control study. *Critical care medicine* **40**, 952-959 (2012).
185. M. Eisenhut, Low angiopoietin-1 as a predisposing factor for cerebral vasospasm in cerebral malaria. *Critical Care Medicine* **40**, 3333-3334 (2012).
186. S. Ghosh, A. Sengupta, S. Sharma, H. M. Sonawat, Metabolic fingerprints of serum, brain, and liver are distinct for mice with cerebral and noncerebral malaria: a (1)H NMR spectroscopy-based metabonomic study. *J Proteome Res* **11**, 4992-5004 (2012).
187. M. Salomao, X. Zhang, Y. Yang, S. Lee, J. H. Hartwig, J. A. Chasis, N. Mohandas, X. An, Protein 4.1 R-dependent multiprotein complex: new insights into the structural organization of the red blood cell membrane. *Proceedings of the National Academy of Sciences* **105**, 8026-8031 (2008).
188. T. K. Jonsdottir, M. Gabriela, B. S. Crabb, F. d. K.-W. T, P. R. Gilson, Defining the Essential Exportome of the Malaria Parasite. *Trends Parasitol* **37**, 664-675 (2021).
189. G. E. Weiss, P. R. Gilson, T. Taechalertpaisarn, W. H. Tham, N. W. de Jong, K. L. Harvey, F. J. Fowkes, P. N. Barlow, J. C. Rayner, G. J. Wright, A. F. Cowman, B. S. Crabb, Revealing the sequence and resulting cellular morphology of receptor-ligand interactions during Plasmodium falciparum invasion of erythrocytes. *Plos Pathog* **11**, e1004670 (2015).
190. M. R. Baldwin, X. Li, T. Hanada, S. C. Liu, A. H. Chishti, Merozoite surface protein 1 recognition of host glycophorin A mediates malaria parasite invasion of red blood cells. *Blood* **125**, 2704-2711 (2015).
191. M. J. Boyle, D. W. Wilson, J. G. Beeson, New approaches to studying Plasmodium falciparum merozoite invasion and insights into invasion biology. *Int J Parasitol* **43**, 1-10 (2013).
192. G. E. Weiss, B. S. Crabb, P. R. Gilson, Overlaying Molecular and Temporal Aspects of Malaria Parasite Invasion. *Trends Parasitol* **32**, 284-295 (2016).
193. W. H. Tham, J. Healer, A. F. Cowman, Erythrocyte and reticulocyte binding-like proteins of Plasmodium falciparum. *Trends Parasitol* **28**, 23-30 (2012).
194. A. F. Cowman, C. J. Tonkin, W. H. Tham, M. T. Duraisingh, The Molecular Basis of Erythrocyte Invasion by Malaria Parasites. *Cell Host Microbe* **22**, 232-245 (2017).

195. R. L. Ord, M. Rodriguez, C. A. Lobo, Malaria invasion ligand RH5 and its prime candidacy in blood-stage malaria vaccine design. *Hum Vaccin Immunother* **11**, 1465-1473 (2015).
196. K. E. Wright, K. A. Hjerrild, J. Bartlett, A. D. Douglas, J. Jin, R. E. Brown, J. J. Illingworth, R. Ashfield, S. B. Clemmensen, W. A. de Jongh, S. J. Draper, M. K. Higgins, Structure of malaria invasion protein RH5 with erythrocyte basigin and blocking antibodies. *Nature* **515**, 427-430 (2014).
197. S. Singh, M. M. Alam, I. Pal-Bhowmick, J. A. Brzostowski, C. E. Chitnis, Distinct external signals trigger sequential release of apical organelles during erythrocyte invasion by malaria parasites. *Plos Pathog* **6**, e1000746 (2010).
198. M. J. Boyle, J. S. Richards, P. R. Gilson, W. Chai, J. G. Beeson, Interactions with heparin-like molecules during erythrocyte invasion by Plasmodium falciparum merozoites. *Blood* **115**, 4559-4568 (2010).
199. J. G. Beeson, D. R. Drew, M. J. Boyle, G. Feng, F. J. Fowkes, J. S. Richards, Merozoite surface proteins in red blood cell invasion, immunity and vaccines against malaria. *FEMS Microbiol Rev* **40**, 343-372 (2016).
200. I. C. A. Batista, B. R. Quinan, É. A. R. Alves, S. T. G. Jangola, E. S. Oliveira, S. G. Colombarolli, J. G. G. Ferreira, E. S. de Oliveira Rocha, E. G. Kroon, R. R. J. V. de Assis, Design and production of dengue virus chimeric proteins useful for developing tetravalent vaccines. **38**, 2005-2015 (2020).
201. W.-X. Chin, R. C. H. Lee, P. Kaur, T. S. Lew, T. Yogarajah, H. Y. Kong, Z.-Y. Teo, C. K. Salim, R.-R. Zhang, X.-F. J. n. V. Li, A single-dose live attenuated chimeric vaccine candidate against Zika virus. **6**, 20 (2021).
202. T. R. Fuerst, B. G. Pierce, Z. Y. Keck, S. K. H. Foung, Designing a B Cell-Based Vaccine against a Highly Variable Hepatitis C Virus. *Front Microbiol* **8**, 2692 (2017).
203. R. Kaur, N. Arora, S. S. Rawat, A. K. Keshri, N. Singh, S. K. Show, P. Kumar, A. Mishra, A. Prasad, Immunoinformatics driven construction of multi-epitope vaccine candidate against Ascaris lumbricoides using its entire immunogenic epitopes. *Expert Rev Vaccines* **20**, 1637-1649 (2021).
204. D. S. Dias, P. A. F. Ribeiro, V. T. Martins, D. P. Lage, L. E. Costa, M. A. Chavez-Fumagalli, F. F. Ramos, T. T. O. Santos, F. Ludolf, J. S. Oliveira, T. A. O. Mendes, E. S. Silva, A. S. Galdino, M. C. Duarte, B. M. Roatt, D. Menezes-Souza, A. L. Teixeira, E. A. F. Coelho, Vaccination with a CD4(+) and CD8(+) T-cell epitopes-based recombinant chimeric protein derived from Leishmania infantum proteins confers protective immunity against visceral leishmaniasis. *Transl Res* **200**, 18-34 (2018).
205. A. Asghari, H. Nourmohammadi, H. Majidiani, S. A. Shariatzadeh, M. Shams, F. Montazeri, In silico analysis and prediction of immunogenic epitopes for pre-erythrocytic proteins of the deadly Plasmodium falciparum. *Infect Genet Evol* **93**, 104985 (2021).
206. K. Hajissa, R. Zakaria, R. Suppian, Z. Mohamed, Epitope-based vaccine as a universal vaccination strategy against Toxoplasma gondii infection: A mini-review. *J. Adv. Vet. Res* **6**, 174 (2019).
207. S. B. Sirima, B. Mordmuller, P. Milligan, U. A. Ngoa, F. Kironde, F. Atuguba, A. B. Tiono, S. Issifou, M. Kaddumukasa, O. Bangre, C. Flach, M. Christiansen, P. Bang, R. Chilengi, S. Jepsen, P. G. Kremsner, M. Theisen, G. M. Z. T. S. Group, A phase 2b randomized, controlled trial of the efficacy of the GMZ2 malaria vaccine in African children. *Vaccine* **34**, 4536-4542 (2016).
208. A. J. Pollard, E. M. Bijker, A guide to vaccinology: from basic principles to new developments (Dec, 10.1038/s41577-020-00479-7, 2020). *Nature Reviews Immunology* **21**, 129-129 (2021).
209. A. S. Kolaskar, P. C. Tongaonkar, A semi-empirical method for prediction of antigenic determinants on protein antigens. *FEBS Lett* **276**, 172-174 (1990).

210. Q. Zhang, P. Wang, Y. Kim, P. Haste-Andersen, J. Beaver, P. E. Bourne, H. H. Bui, S. Buus, S. Frankild, J. Greenbaum, O. Lund, C. Lundegaard, M. Nielsen, J. Ponomarenko, A. Sette, Z. Zhu, B. Peters, Immune epitope database analysis resource (IEDB-AR). *Nucleic Acids Res* **36**, W513-518 (2008).
211. M. C. Jespersen, B. Peters, M. Nielsen, P. Marcatili, BepiPred-2.0: improving sequence-based B-cell epitope prediction using conformational epitopes. *Nucleic Acids Res* **45**, W24-W29 (2017).
212. P. Y. Chou, G. D. Fasman, Prediction of beta-turns. *Biophys J* **26**, 367-383 (1979).
213. E. A. Emini, J. V. Hughes, D. S. Perlow, J. Boger, Induction of hepatitis A virus-neutralizing antibody by a virus-specific synthetic peptide. *J Virol* **55**, 836-839 (1985).
214. P. A. Karplus, G. E. Schulz, Prediction of Chain Flexibility in Proteins - a Tool for the Selection of Peptide Antigens. *Naturwissenschaften* **72**, 212-213 (1985).
215. J. M. Parker, D. Guo, R. S. Hodges, New hydrophilicity scale derived from high-performance liquid chromatography peptide retention data: correlation of predicted surface residues with antigenicity and X-ray-derived accessible sites. *Biochemistry* **25**, 5425-5432 (1986).
216. M. Rawat, A. Srivastava, S. Johri, I. Gupta, K. Karmodiya, Single-Cell RNA Sequencing Reveals Cellular Heterogeneity and Stage Transition under Temperature Stress in Synchronized Plasmodium falciparum Cells. *Microbiol Spectr* **9**, e0000821 (2021).
217. R. F. Anders, P. E. Crewther, S. Edwards, M. Margetts, M. L. Matthew, B. Pollock, D. Pye, Immunisation with recombinant AMA-1 protects mice against infection with Plasmodium chabaudi. *Vaccine* **16**, 240-247 (1998).
218. C. H. Kocken, M. A. Dubbeld, A. Van Der Wel, J. T. Pronk, A. P. Waters, J. A. Langermans, A. W. Thomas, High-level expression of Plasmodium vivax apical membrane antigen 1 (AMA-1) in Pichia pastoris: strong immunogenicity in Macaca mulatta immunized with P. vivax AMA-1 and adjuvant SBAS2. *Infect Immun* **67**, 43-49 (1999).
219. S. Aoki, J. Li, S. Itagaki, B. A. Okech, T. G. Egwang, H. Matsuoka, N. M. Palacpac, T. Mitamura, T. Horii, Serine repeat antigen (SERA5) is predominantly expressed among the SERA multigene family of Plasmodium falciparum, and the acquired antibody titers correlate with serum inhibition of the parasite growth. *J Biol Chem* **277**, 47533-47540 (2002).
220. S. K. Miller, R. T. Good, D. R. Drew, M. Delorenzi, P. R. Sanders, A. N. Hodder, T. P. Speed, A. F. Cowman, T. F. de Koning-Ward, B. S. Crabb, A subset of Plasmodium falciparum SERA genes are expressed and appear to play an important role in the erythrocytic cycle. *J Biol Chem* **277**, 47524-47532 (2002).
221. R. Stallmach, M. Kavishwar, C. Withers-Martinez, F. Hackett, C. R. Collins, S. A. Howell, S. Yeoh, E. Knuepfer, A. J. Atid, A. A. Holder, Plasmodium falciparum SERA 5 plays a non-enzymatic role in the malarial asexual blood-stage lifecycle. *Molecular microbiology* **96**, 368-387 (2015).
222. C. C. Hermsen, D. E. Verhage, D. S. C. Telgt, K. Teelen, J. T. Bousema, M. Roestenberg, A. Bolad, K. Berzins, G. Corradin, O. Leroy, M. Theisen, R. W. Sauerwein, Glutamate-rich protein (GLURP) induces antibodies that inhibit
growth of
in a phase 1 malaria vaccine trial. *Vaccine* **25**, 2930-2940 (2007).
223. X. Chen, J. L. Zaro, W. C. Shen, Fusion protein linkers: property, design and functionality. *Adv Drug Deliv Rev* **65**, 1357-1369 (2013).
224. S. Parvizpour, M. M. Pourseif, J. Razmara, M. A. Rafi, Y. Omidi, Epitope-based vaccine design: a comprehensive overview of bioinformatics approaches. *Drug Discov Today* **25**, 1034-1042 (2020).

225. L. C. Yen, H. W. Chen, C. L. Ho, C. C. Lin, Y. L. Lin, Q. W. Yang, K. C. Chiu, S. P. Lien, R. J. Lin, C. L. Liao, Neutralizing antibodies targeting a novel epitope on envelope protein exhibited broad protection against flavivirus without risk of disease enhancement. *Journal of Biomedical Science* **30**, 41 (2023).
226. S. Sanami, M. Rafieian-Kopaei, K. A. Dehkordi, H. Pazoki-Toroudi, F. Azadegan-Dehkordi, G. R. Mobini, M. Alizadeh, M. S. Nezhad, M. Ghasemi-Dehnoo, N. Bagheri, In silico design of a multi-epitope vaccine against HPV16/18. *BMC Bioinformatics* **23**, 311 (2022).
227. S. Sanami, S. Nazarian, S. Ahmad, E. Raeisi, M. Tahir Ul Qamar, S. Tahmasebian, H. Pazoki-Toroudi, M. Fazeli, M. Ghatreh Samani, In silico design and immunoinformatics analysis of a universal multi-epitope vaccine against monkeypox virus. *PLoS One* **18**, e0286224 (2023).
228. S. Gorai, N. C. Das, P. S. S. Gupta, S. K. Panda, M. K. Rana, S. Mukherjee, Designing efficient multi-epitope peptide-based vaccine by targeting the antioxidant thioredoxin of bancroftian filarial parasite. *Infect Genet Evol* **98**, 105237 (2022).
229. M. Azimi-Resketi, S. Heydaryan, N. Kumar, A. Takalou, R. E. Dizaji, B. N. Gorgani, M. Shams, Computational Clues of Immunogenic Hotspots in Plasmodium falciparum Erythrocytic Stage Vaccine Candidate Antigens: In Silico Approach. *Biomed Res Int* **2022**, 5886687 (2022).
230. P. M. Folegatti, A. M. Siqueira, W. M. Monteiro, M. V. G. Lacerda, C. J. Drakeley, E. M. Braga, A systematic review on malaria sero-epidemiology studies in the Brazilian Amazon: insights into immunological markers for exposure and protection. *Malaria Journal* **16**, 1-15 (2017).
231. L. Wu, T. Hall, I. Ssewanyana, T. Oulton, C. Patterson, H. Vasileva, S. Singh, M. Affara, J. Mwesigwa, S. Correa, M. Bah, U. D'Alessandro, N. Sepulveda, C. Drakeley, K. K. A. Tetteh, Optimisation and standardisation of a multiplex immunoassay of diverse Plasmodium falciparum antigens to assess changes in malaria transmission using sero-epidemiology. *Wellcome Open Res* **4**, 26 (2019).
232. I. H. Kana, A. Garcia-Senosiain, S. K. Singh, R. W. Tiendrebeogo, B. K. Chourasia, P. Malhotra, S. K. Sharma, M. K. Das, S. Singh, B. Adu, M. Theisen, Cytophilic Antibodies Against Key Plasmodium falciparum Blood Stage Antigens Contribute to Protection Against Clinical Malaria in a High Transmission Region of Eastern India. *J Infect Dis* **218**, 956-965 (2018).
233. M. J. Boyle, J. A. Chan, I. Handayuni, L. Reiling, G. Feng, A. Hilton, L. Kurtovic, D. Oyong, K. A. Piera, B. E. Barber, T. William, D. P. Eisen, G. Minigo, C. Langer, D. R. Drew, F. de Labastida Rivera, F. H. Amante, T. N. Williams, S. Kinyanjui, K. Marsh, D. L. Doolan, C. Engwerda, F. J. I. Fowkes, M. J. Grigg, I. Mueller, J. S. McCarthy, N. M. Anstey, J. G. Beeson, IgM in human immunity to Plasmodium falciparum malaria. *Sci Adv* **5**, eaax4489 (2019).
234. E. Nagao, O. Kaneko, J. A. Dvorak, Plasmodium falciparum-infected erythrocytes: qualitative and quantitative analyses of parasite-induced knobs by atomic force microscopy. *J Struct Biol* **130**, 34-44 (2000).
235. K. W. Deitsch, R. Dzikowski, Variant Gene Expression and Antigenic Variation by Malaria Parasites. *Annu Rev Microbiol* **71**, 625-641 (2017).
236. S. M. Kraemer, J. D. Smith, Evidence for the importance of genetic structuring to the structural and functional specialization of the Plasmodium falciparum var gene family. *Mol Microbiol* **50**, 1527-1538 (2003).
237. S. A. Kyes, S. M. Kraemer, J. D. Smith, Antigenic variation in Plasmodium falciparum: gene organization and regulation of the var multigene family. *Eukaryot Cell* **6**, 1511-1520 (2007).

238. M. Rug, M. Cyrklaff, A. Mikkonen, L. Lemgruber, S. Kuelzer, C. P. Sanchez, J. Thompson, E. Hanssen, M. O'Neill, C. Langer, M. Lanzer, F. Frischknecht, A. G. Maier, A. F. Cowman, Export of virulence proteins by malaria-infected erythrocytes involves remodeling of host actin cytoskeleton. *Blood* **124**, 3459-3468 (2014).
239. A. van de Stolpe, P. T. van der Saag, Intercellular adhesion molecule-1. *J Mol Med (Berl)* **74**, 13-33 (1996).
240. C. I. Newbold, A. G. Craig, S. Kyes, A. R. Berendt, R. W. Snow, N. Peshu, K. Marsh, PfEMP1, polymorphism and pathogenesis. *Ann Trop Med Parasitol* **91**, 551-557 (1997).
241. G. D. Turner, H. Morrison, M. Jones, T. M. Davis, S. Looareesuwan, I. D. Buley, K. C. Gatter, C. I. Newbold, S. Pukritayakamee, B. Nagachinta, et al., An immunohistochemical study of the pathology of fatal malaria. Evidence for widespread endothelial activation and a potential role for intercellular adhesion molecule-1 in cerebral sequestration. *Am J Pathol* **145**, 1057-1069 (1994).
242. N. Horata, K. Choowongkomon, S. Ratanabunyong, J. Tongshoob, S. Khusmith, Acquisition of naturally acquired antibody response to Plasmodium falciparum erythrocyte membrane protein 1-DBLα and differential regulation of IgG subclasses in severe and uncomplicated malaria. *Asian Pac. J. Trop. Biomed.* **7**, 1055-1061 (2017).
243. A. Radfar, D. Méndez, C. Moneriz, M. Linares, P. Marín-García, A. Puyet, A. Diez, J. M. Bautista, Synchronous culture of
at high parasitemia levels. *Nature Protocols* **4**, 1899-1915 (2009).
244. M. d. P. Quintana, J.-H. Ch'ng, in *Malaria Immunology: Targeting the Surface of Infected Erythrocytes*. (Springer, 2022), pp. 493-503.
245. M. Tibúrcio, M. Niang, G. Deplaine, S. Perrot, E. Bischoff, P. A. Ndour, F. Silvestrini, A. Khattab, G. Milon, P. H. David, A switch in infected erythrocyte deformability at the maturation and blood circulation of Plasmodium falciparum transmission stages. *Blood, The Journal of the American Society of Hematology* **119**, e172-e180 (2012).
246. G. I. Bertin, T. Lavstsen, F. Guillonneau, J. Doritchamou, C. W. Wang, J. S. Jespersen, S. Ezimegnon, N. Fievet, M. J. Alao, F. Lalya, A. Massougbodji, N. T. Ndam, T. G. Theander, P. Deloron, Expression of the domain cassette 8 Plasmodium falciparum erythrocyte membrane protein 1 is associated with cerebral malaria in Benin. *PLoS One* **8**, e68368 (2013).
247. M. R. Gillrie, M. Ho, Dynamic interactions of Plasmodium spp. with vascular endothelium. *Tissue Barriers* **5**, e1268667 (2017).
248. J. S. Pober, W. C. Sessa, Inflammation and the Blood Microvascular System. *Cold Spring Harbor Perspectives in Biology* **7**, a016345 (2015).
249. J. N. Topper, M. A. Gimbrone, Blood flow and vascular gene expression: fluid shear stress as a modulator of endothelial phenotype. *Molecular Medicine Today* **5**, 40-46 (1999).
250. D. A. Fedosov, B. Caswell, G. E. Karniadakis, Wall shear stress-based model for adhesive dynamics of red blood cells in malaria. *Biophys J* **100**, 2084-2093 (2011).
251. Y. K. Jawale, U. Rapol, C. A. Athale, Open Source 3D-printed focussing mechanism for cellphone-based cellular microscopy. *J Microsc* **273**, 105-114 (2019).
252. Y. Adams, A. R. Jensen, Cerebral malaria–modelling interactions at the blood–brain barrier in vitro. *Disease Models Mechanisms* **15**, dmm049410 (2022).
253. G. A. Awandare, P. B. Nyarko, Y. Aniweh, R. Ayivor-Djanie, J. A. Stoute, Plasmodium falciparum strains spontaneously switch invasion phenotype in suspension culture. *Sci Rep* **8**, 5782 (2018).
254. S. Singh, K. Miura, H. Zhou, O. Muratova, B. Keegan, A. Miles, L. B. Martin, A. J. Saul, L. H. Miller, C. A. Long, Immunity to recombinant plasmodium falciparum merozoite surface protein 1 (MSP1): protection in Aotus nancymai monkeys strongly correlates with anti-

MSP1 antibody titer and in vitro parasite-inhibitory activity. *Infect Immun* **74**, 4573-4580 (2006).
255. R. L. Ord, M. Rodriguez, T. Yamasaki, S. Takeo, T. Tsuboi, C. A. Lobo, Targeting sialic acid dependent and independent pathways of invasion in Plasmodium falciparum. *PLoS One* **7**, e30251 (2012).
256. S. E. Silk, W. F. Kalinga, I. M. Mtaka, N. S. Lilolime, M. Mpina, F. Milando, S. Ahmed, A. Diouf, F. Mkwepu, B. Simon, Superior antibody immunogenicity of a viral-vectored RH5 blood-stage malaria vaccine in Tanzanian infants as compared to adults. *Med* **4**, 668-686. e667 (2023).